



Review

Advances in preparation, mechanism and applications of graphene quantum dots/semiconductor composite photocatalysts: A review

Chunyu Cheng¹, Qinghua Liang¹, Ming Yan^{*}, Zhifeng Liu^{*}, Qingyun He, Ting Wu, Songhao Luo, Yuan Pan, Chenhui Zhao, Yang Liu

College of Environmental Science and Engineering, Hunan University and Key Laboratory of Environmental Biology and Pollution Control (Hunan University), Ministry of Education, Changsha 410082, PR China



ARTICLE INFO

Editor: R. Debora

Keywords:

Photocatalysis mechanism
Energy storage
Environmental protection
Gas monitoring
Antibacterial
Biomedicine

ABSTRACT

Due to the low efficiency of single-component nano materials, there are more and more studies on high-efficiency composites. As zero dimensional (0D) non-metallic semiconductor material, the emergence of graphene quantum dots (GQDs) overcomes the shortcomings of traditional photocatalysts (rapid rate of electron-hole recombination and narrow range of optical response). Their uniqueness is that they can combine the advantages of quantum dots (rich functional groups at edge) and sp^2 carbon materials (large specific surface area). The inherent inert carbon stabilizes chemical and physical properties, and brings new breakthroughs to the development of benchmark photocatalysts. The photocatalytic efficiency of GQDs composite with semiconductor materials (SCs) can be improved by the following three points: (1) accelerating charge transfer, (2) extending light absorption range, (3) increasing active sites. The methods of preparation (bottom-up and top-down), types of heterojunctions, mechanisms of photocatalysis, and applications of GQDs/SCs (wastewater treatment, energy storage, gas sensing, UV detection, antibiosis and biomedicine) are comprehensively discussed. And it is hoped that this review can provide some guidance for the future research on GQDs/SCs on photocatalysis.

1. Introduction

With the acceleration of the industrialization process of modern society, the problems of environmental pollution and energy shortage have become increasingly severe, which have aroused extensive attention of people. There is an urgent need to find a green method to solve the above problems. In 1972, Fujishima and Honda first used TiO_2 as photocatalyst, then decomposed water to produce hydrogen (Fujishima and Honda, 1972). Since then, photocatalysis, as a green means with little impact on the environment, has set off an upsurge of research (Wen et al., 2017; Orooji et al., 2020; Shen et al., 2019; Pan et al., 2020). SCs have been widely used as photocatalysts because of their good stability of light response, solving the problems of environmental pollution and energy shortage (Raziq et al., 2017; Basavarajappa et al., 2020; Lee et al., 2016). For example, traditional SCs, such as titanium dioxide (TiO_2), zinc oxide (ZnO) and tungsten trioxide (WO_3) and so on, have been widely used as photocatalysts (Kumar and Rao, 2017; Ding et al., 2020; Theerthagiri et al., 2019; Karthikeyan et al., 2020;

Hernández-Carrillo et al., 2020; Jamila et al., 2020a). However, some of these traditional SCs have wide band gap and narrow optical response range, which make the photocatalytic reaction is mainly limited to UV light and is not conducive to photocatalysis (Noman et al., 2019; Meng et al., 2019). Other photocatalysts are unstable, and the recombination rate of photogenerated electron-hole is very fast, which also affect the photocatalytic activity (Liu et al., 2019; Wang et al., 2016; Nandiyanto et al., 2020). Therefore, there is an urgent need to find a stable visible light responsive photocatalyst to improve the photocatalytic efficiency (Li et al., 2018a; Yan et al., 2018).

Two-dimensional (2D) graphene is a kind of visible light responsive non-metallic photocatalyst, which has attracted the attention of researchers due to narrow band gap, high carrier mobility and fast photogenerated electron-hole pairs separation (Li et al., 2018a; Peng et al., 2020). In addition, graphene has higher carbon content than other carbon nanomaterials, which makes it become an important material for photocatalytic applications (Li et al., 2018a). However, the quantum lifetime is limited due to its band gap dependence, thus reducing the photocatalytic efficiency (Yan et al., 2018). Quantum dots (QDs) are

^{*} Corresponding authors.

E-mail addresses: ym8188@hnu.edu.cn (M. Yan), zhifengliu@hnu.edu.cn (Z. Liu).

¹ Chunyu Cheng and Qinghua Liang are contributed equally to this paper.

Nomenclature	
<i>Abbreviation</i>	
GQDs	graphene quantum dots
0D/2D	zero-dimensional/two-dimensional
SC	semiconductor
PL	photoluminescence
g-CNNR	graphitic carbon nitride nanorods
SEM	scanning electron microscope
TEM	transmission electron microscope
EDS	energy dispersed spectroscopy
PyBOP	benzotriazol-1-yl-oxytripyrrolidinophosphonium hexafluorophosphate
DIEA	N, N-diisopropylethylamine
Mn-N-TiO ₂	Mn and N Co-doped titanium dioxide
CNS	g-C ₃ N ₄ nanosheets
HRTEM	high resolution transmission electron microscope
GO	graphene oxide
P-GQDs	P-doped GQDs
CN	n-type graphitic carbon nitride
OH-GQDs	hydroxyl functionalized graphene quantum dots
mpg-C ₃ N ₄	mesoporous graphite carbon nitride
NWs	nanowires
ETLs	electron transporting layers
PECVD	plasma enhanced chemical vapor deposition
NATs	nanotube arrays
CB	conduction band
VB	valence band
XPS	x-ray photoelectron spectroscopy
UV-vis DRS	ultraviolet-visible light diffuse reflection spectrum
DFT	density functional theory
ET	electronic transfer
LUMO	lowest unoccupied molecular orbital
NRs	nanorods
EIS	electrochemical impedance spectroscopy
RhB	rhodamine B
MO	methyl orange
BPA	bisphenol A
CBZ	carbamazepine
TC	tetracycline
HPA	hydroxyapatite
PEC	photoelectrochemical
DSSCs	dye-sensitized solar cells
CC	carbon cloth
HNPs	the plasmonic hybrid nanoparticles
ox-GQDs	graphene oxide quantum dots
PCNO	oxidized nanoporous g-C ₃ N ₄
MSNs	mesoporous silica nanoparticles

new type of visible light responsive super 0D material, which have adjustable band gap and long quantum life (Aguilera-Sigalat and Bradshaw, 2016; Wu et al., 2020). When 2D graphene is transformed into 0D QDs, its horizontal size decreases to nanometers (2–10 nm), and its thickness peels off to 1–2 nm, forming GQDs (Fig. 1a and b) (Zhu et al., 2017; Pan et al., 2010). GQDs have excellent properties of graphene and QDs. They have outstanding ultraviolet-visible (UV-Vis) absorption spectrum, stable fluorescence and photoluminescence (PL) spectrum (Fig. 1c, d and e) (Yao et al., 2017a; Tuteja et al., 2016; Hu et al., 2020; Tang et al., 2012), so they are ideal candidate photocatalysts. Compared with 2D graphene, GQDs are easy to obtain adjustable band gap (0–6 eV) due to their unique quantum limitation and edge effect. And GQDs with ultra-small particle size can provide more oxygen-containing functional groups, which are used as highly active reaction sites (Kittiratanawasin and Hannongbua, 2016). Compared with carbon dots (CDs), GQDs have graphene lattice and better crystallinity, which make GQDs more effective to improve the performance of batteries or capacitors (Jegannathan et al., 2018). The biocompatibility lays a foundation for applications in the field of biomedicine. In addition, GQDs have larger specific surface area and better water solubility than QDs, leading the increased separation rate of photogenerated electron-hole pairs and the improved photocatalytic efficiency (Wang et al., 2016; Wang et al., 2016). In a word, the introduction of QDs widens the application range of graphene and provides new thinking for the research of different dimensional nanomaterials.

In order to further the photocatalytic activity of GQDs and applicability, many methods of modification have been come up, such as heteroatomic doping (Qian et al., 2018a; Zheng et al., 2018; Sharma et al., 2020), morphology control (Liu et al., 2017; Jia et al., 2018a; Zhao et al., 2020), composite construction with SCs (Rajender et al., 2018; Safardoust-Hojaghan and Salavati-Niasari, 2017a; Lei et al., 2017; Liu et al., 2017). It is found that modified GQDs have unique optical, electrical, thermodynamic and mechanical properties, which can be widely used in practical fields (biomedicine (Zheng et al., 2015; Ambrosi et al., 2014; Du and Guo, 2016), photochemical reaction (Zheng et al., 2018; Liu et al., 2017), energy storage (Jia et al., 2018a; Bonaccorso et al., 2015), etc.). Therefore, benchmark photocatalysts of GQDs have become hotspots.

In recent years, GQDs have attracted much attention in the field of photocatalysis due to their excellent optical properties (Li et al., 2016; Li et al., 2016). However, the single-phase photocatalysts tend to be enriched in aqueous solution, resulting in accelerating electron-hole recombination rate and decreasing photocatalytic efficiency (Yan et al., 2019a). Therefore, combining single-phase photocatalysts with different materials is an effective way to overcome these shortcomings. For example, benchmark photocatalysts of GQDs (Liu et al., 2017; Yuan et al., 2019a; Lin et al., 2016), especially combine with SCs, have more excellent photocatalytic properties (Tian et al., 2017; Liu et al., 2019a; Nie et al., 2018). In the past seven years, the researches on GQDs/SCs have increased significantly, which indicated that they are hot field of photocatalysis (Fig. 1f). At present, reviews on GQDs, SCs and photocatalysis have been published. However, these reviews tend to focus on a specific class of SCs and GQDs, or focus on their applications in specific fields. However, they are not comprehensive enough. For example, Huo et al. (Huo et al., 2021) selected a specific SC (TiO₂) to compound with GQDs, then summarized the catalytic mechanisms of GQDs/TiO₂ and the applications only in photocatalysis. But it didn't involve biomedical applications that prove biocompatibility. Although Bokare et al. (Bokare et al., 2021) introduced the synthesis method and catalytic mechanisms of GQDs/SCs in detail, but they only discussed the applications of GQDs/SCs in some specific fields (e.g., biomedicine and energy conversion), and there is a lack of summary on UV detection and biomedicine. So far, there has been no comprehensive and systematic review on GQDs/SCs. Therefore, this review can systematically guide future research.

Based on the above overview, this work reviews the latest research progress of GQDs/SCs photocatalyst, with emphasizing on the synthesis methods, photocatalytic mechanisms, types of heterojunctions and applications of GQDs/SCs. To be more specific, two synthesis methods of GQDs/SCs are first introduced, which are bottom-up and top-down, respectively. Then the roles of GQDs in improving photocatalytic activity are introduced, including act as electron acceptors/donors, photosensitizers, electron transfer accelerator, synergistic effect, form electric field and increase contact area. In addition, the applications of GQDs/SCs (sewage treatment, energy storage, gas sensing, UV detection, antibiosis and biomedicine) are also introduced. Finally, some new

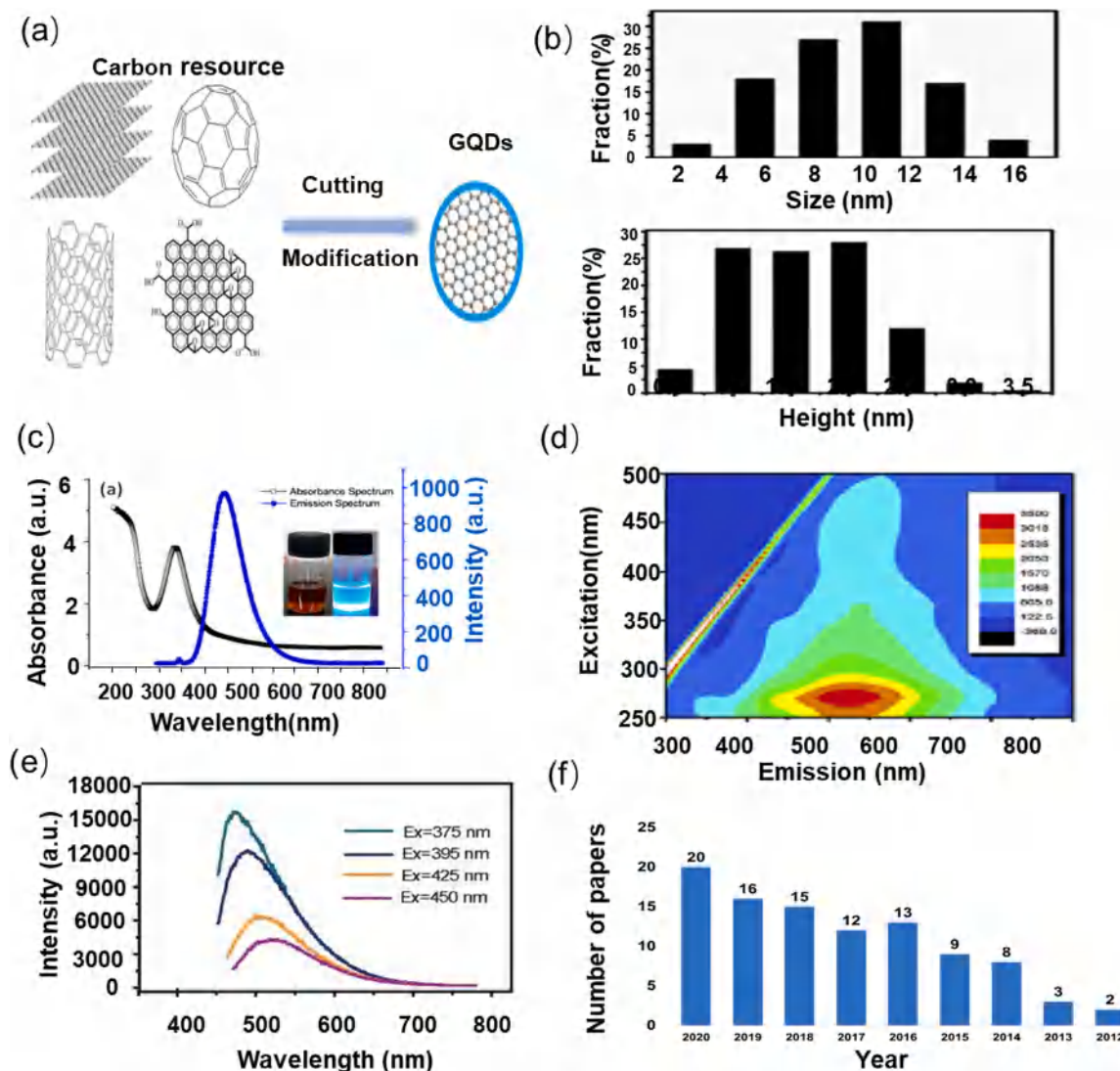


Fig. 1. (a) Preparation of GQDs from graphene. Reprinted with permission (Zhu et al., 2017; Zhu et al., 2017). Copyright 2016 Elsevier Ltd. (b) Diameter (above) and height (below) distribution of GQDs. Reprinted with permission (Pan et al., 2010). Copyright 2011 American Chemical Society. (c) The UV-vis spectrum of GQDs and photoluminescence characteristics and luminous color (inset) at 340 nm. Reprinted with permission (Tuteja et al., 2016). Copyright 2016 Elsevier B.V. (d) The fluorescence spectrum of GQDs. Reprinted with permission (Hu et al., 2020). Copyright 2019 Elsevier. (e) The PL spectrum of GQDs with different wavelengths. Reprinted with permission (Tang et al., 2012). Copyright 2012 American Chemical Society. (f) The number of publications with the keyword of “graphene quantum dots” and “semiconductor” on indexed journals from 2012 to 2020. The search results are based on the database of “Web of Science”.

ideas and insights for the study of photocatalysis of GQDs composite materials are provided.

2. Preparation of GQDs/SCs

The synthesis methods of GQDs include bottom-up and top-down (Zeng et al., 2018). These synthetic methods are very important to improve the photocatalytic efficiency by changing the morphology and structure of photocatalysts. The bottom-up generally takes small organic molecules as precursors and then forms large-sized corresponding products through relevant chemical reactions. This method can form products with controllable size and structure, which makes the experimental results accurate, but the procedures of operation are complex. Contrarily, the top-down usually cuts large reactants into corresponding small-sized nano materials through physical or chemical methods. Although this method can't control the size and structure like the bottom-up, it is simple in operation and high in yield. Similarly, the synthesis methods of GQDs/SCs can be divided into bottom-up and top-down. GQDs and SCs are closely combined to form substance with

relatively complex structure. Parts of the synthesis methods of GQDs/SCs are listed in Table 1.

2.1. Bottom-up

Bottom-up is an important method to synthesize GQDs/SCs, including traditional hydrothermal method, improved hydrothermal method and self-assembly method. The improved hydrothermal method mainly includes hydrothermal deposition method and ultrasound-assisted hydrothermal method, and self-assembly method is diverse, including electrostatic interaction, spin-coating and sequential assembly.

2.1.1. Hydrothermal method

High activity composites can be synthesized by condensed matter at the low temperature, the basic principle is dissolution and recrystallization (Pan et al., 2020). Hydrothermal method is a traditional method for preparing photocatalysts, which usually uses water as solvent, then puts the precursor to be reacted into the closed high-temperature

Table 1
Preparation of GQDs/SCs.

Photocatalysts	Synthetic methods	Reactant	Conditions	Product	Ref.
1 GQDs/g-CNNR	hydrothermal (bottom-up)	TNP, Na ₂ HPO ₄ ·12 H ₂ O, NaOH g-C ₃ N ₄ powder, GQDs solution	ultrasonic treatment for 0.5 h, heat for 6 h (160 °C), 6000 rpm for 30 min stir for 30 min, heat for 4 h (150 °C), dry for 12 h (60 °C)	GQDs solution GQDs/g-CNNR	(Yuan et al., 2019b)
2 GQDs/TCN	hydrothermal	Mn(C ₂ H ₃ O ₂) ₂ ·4 H ₂ O, HDA, ethanol, KCl melamine powder GQDs, Mn-N- TiO ₂ , CNS	stir for 20 min, dried for 16 h (160 °C), heat for 2 h (180 °C) keep for 4 h (550 °C), heat for 2 h (793 K) keep for 1 h (400 °C), stir for 24 h, dry for 3 h	Mn-N- TiO ₂ microspheres CNS GQDs/TCN-0.4	(Nie et al., 2018)
3 g-C ₃ N ₄ / ZnTcPc/GQDs	hydrothermal	urea, DMF ZnTcPc, PyBOP, DIEA g-C ₃ N ₄ /ZnTcPc, GQDs, ethanol	550 °C for 3 h (2.5 °C /min), ultrasound for 20 h ultrasound for 5 h ultrasonicate for 1 h, mix and heat for 3 h (725.15 °C), freeze for 18 h	g-C ₃ N ₄ solution g-C ₃ N ₄ /ZnTcPc g-C ₃ N ₄ /ZnTcPc/ GQDs	(Xu et al., 2019; Xu et al., 2019)
4 CdS/GQDs	hydrothermal deposition (bottom-up)	TNP, hydrazine hydrate Na ₂ S, Cd(CH ₃ COO) ₂ CdS, GQDs	ultrasonicate for 5 h, heat for 4 h (160 °C) stir for 24 h, dry for 24 h (40 °C) stir for 1 h, heat for 4 h (180 °C)	GQDs CdS CdS/GQDs	(Lei et al., 2017)
5 NH ₂ -GQDs/ TiO ₂	hydrothermal deposition	TNP, DI water TiO ₂ , GQDs solution	ultrasonicate for 5 h, heat for 10 h (150 °C) heat for 4 h (150 °C), dry at 80 °C	NH ₂ -GQDs NH ₂ -GQDs/TiO ₂	(Pan et al., 2015)
6 TiO ₂ /GQDs	ultrasonication (bottom-up)	GO, DMF ZrO ₂ GQDs, TiO ₂ powder	350 rpm for 16 h ultrasonicate for 1 h	GQDs TiO ₂ powder TiO ₂ /GQDs	(Rajender et al., 2018)
7 P-GQDs/CN	ultrasonication	TN, Na ₂ HPO ₄ ·12 H ₂ O, NaOH CN powder, P-GQDs solution	ultrasonicate for 0.5 h, heat for 4 h (200 °C) ultrasonicate for 0.5 h, dry at 60 °C	P-GQDs solution P-GQDs/CN	(Qian et al., 2018a)
8 OH-GQDs/mpg-C ₃ N ₄	electrostatic interaction (bottom-up)	mpg-C ₃ N ₄ , ethanol black GQDs	sonicate for 30 min mix and stir 12 h, dry at 80 °C	mpg-C ₃ N ₄ suspension OH-GQDs/mpg-C ₃ N ₄	(Liu et al., 2017; Liu et al., 2017; Liu et al., 2017; Liu et al., 2017)
9 DOX-MMSN/ GQDs	electrostatic interaction	Fe ₃ O ₄ , mesoporous silica DOX-MMSN, PBS, EDC, NSH	ultrasonicate for 30 min, stir for 90 °C, mix for 2 h, dry for 12 h (60 °C) stir for 24 h under dark, mix for 4 h	MMSN DOX-MMSN/ GQDs	(Yao et al., 2017a)
10 GQDs/PANI/ g-C ₃ N ₄	electrostatic interaction	urea aniline, HCl, APS, g-C ₃ N ₄ PANI/g-C ₃ N ₄ , GQDs solution	ultrasonicate for 16 h stir for 1 h ultrasonicate for 2 h	g-C ₃ N ₄ PANI/g-C ₃ N ₄ GQDs/PANI/g-C ₃ N ₄	(Liu et al., 2017; Liu et al., 2017; Liu et al., 2017; Liu et al., 2017)
11 GQDs/ZnO NWs	spin coating method (bottom-up)	graphite rods, NaOH Zinc foil, ethanol GQDs, ZnO NWs	apply 25 V, 20 000 rpm for 30 min electropolish for 3 min, anneal for 60 min 500 rpm for 30 s, anneal for 60 min (250 °C)	GQDs ZnO NWs GQDs/ZnO NWs	(Ebrahimi et al., 2017)
12 GQDs/MnO ₂	sequential assembly (bottom-up)	GO, ammonia solution ethanol, H ₂ SO ₄ , SDBS, KMnO ₄ GQDs, MnO ₂ Nanosheets	heat for 12 h (180 °C) mix, stir for 30 min mix	GQDs MnO ₂ nanosheets GQDs/MnO ₂	(Yan et al., 2016)
13 N-GQDs/TiO ₂	stirring method (bottom-up)	citric acid, ethylene diamine TiO ₂ , N-GQDs	stir, heat at 180 °C, 10000 rpm for 15 min stir for 24 h, dry for 10 h (60 °C)	N-GQDs N-GQDs/TiO ₂	(Safardoust-Hojaghan and Salavati-Niasari, 2017b)
14 SN-GQDs/ TiO ₂	impregnation (top-down)	citric, thiourea SN-GQDs, TiO ₂	stir for 3 h, heat for 4 h (160 °C), 6000 rpm for 20 min mix, 60 °C for 24 h	SN-GQDs solution SN-GQDs/TiO ₂	(Zheng et al., 2018)
15 GQDs/SrRuO ₃	impregnation	RuCl ₃ ·xH ₂ O, SrCl ₂ ·xH ₂ O citric acid, thiourea SrRuO ₃ , GQDs	heat for 48 h (200 °C), dry at 60 °C keep for 12 h (180 °C), 8000 rpm for 20 min stir for 2 h, dry at 45 °C, anneal for 0.5 h	SrRuO ₃ GQDs GQDs/SrRuO ₃	(Liu et al., 2017; Liu et al., 2017; Liu et al., 2017; Liu et al., 2017)
16 GQDs/TiO ₂ NTAs	impregnation	Ti and platinum sheet carbon fibers, H ₂ SO ₄ , Na ₂ CO ₃ GQDs, ethanol, TiO ₂ NTAs	anodized Ti sheet 4 h (40 V), anneal for 2 h ultrasonicate for 2 h, stir for 24 h drop casting with micro-syringe (40 V, 4 h)	TiO ₂ NTAs GQDs GQDs/TiO ₂ NTAs	(Gupta et al., 2015)
17 GQDs/CoP NPs	in-situ growth (top-down)	carbon black, HNO ₃ GQDs, Co(NO ₃) ₂ ·6 H ₂ O	reflux for 24 h, 8000 rpm for 10 min, heat for 200 °C heat for 12 h (120 °C), dry for 5 h (70 °C)	GQDs CoP/ GQDs	(Wang et al., 2017; Wang et al., 2017)
18 GQDs/MnO ₂	PECVD (top-down)	HCl, KMnO ₄ , Ni GO, H ₂ O ₂ MnO ₂ , GQDs	dry for 8 h (80 °C) heat at 90 °C, stir for 12 h	MnO ₂ GQDs GQDs/MnO ₂	(Jia et al., 2018b)

(continued on next page)

Table 1 (continued)

Photocatalysts	Synthetic methods	Reactant	Conditions	Product	Ref.
19 MoS ₂ /GQDs	CVD (top-down)	MoS ₂ powder, SiO ₂ , Ar carbon NFS, H ₂ SO ₄ , HNO ₃ MoS ₂ , GQD solution	treat to 350 °C (400 Pa, 200 W, 0–10 min) heat for 900 °C (10 °C/min), keep for 20 – 24 min ultrasonicate for 24 h (100 °C) dry at 40 °C	Coral MoS ₂ GQDs solution MoS ₂ /GQDs	(Guo et al., 2017)
20 P-TCN/GQDs	freeze-drying (top-down)	CA, NaOH melamine, H ₃ PO ₃ GQDs solution, P-TCN	oil bath for 30 min (473 K), filter stir for 1 h, heat for 10 h (473 K), dry at 333 K stir for 30 min, freeze-dry for 24 h	GQD solution P-TCN P-TCN/GQDs	(Gao et al., 2018a)

g-CNNR: graphitic carbon nitride nanorods; TNP: 1,3,6-trinitropyrene; g-C₃N₄: graphite carbon nitride; ZnTcPc: zinc tetracarboxyphthalocyanine; DMF: dimethyl formamide; TCN: Mn-N-TiO₂/g-C₃N₄; PyBOP: benzotriazol-1-yl-oxypyrrolidinophosphonium hexafluorophosphate; DIEA: N, N-diisopropylethylamine; CdS: cadmium sulfide; HDA: hexadecylamine; CNS: g-C₃N₄ nanosheets; NaS₂: sodium sulphide; Cd(CH₃COO)₂: cadmium acetate; DI water: deionized water; NH₂-GQDs: amine-functionalized graphene quantum dots;

CN: n-type graphitic carbon nitride; OH-GQDs: hydroxyl functionalized graphene quantum dots; mpg-C₃N₄: mesoporous graphite carbon nitride; NTAs: nanotube arrays; DOX-MMSN: doxorubicin loaded magnetic mesoporous silica nanoparticles; PBS: phosphate buffer saline; EDC:1-ethyl-3-(3-dimethylaminopropyl) carbodiimide hydrochloride; NSH: N-Hydroxysuccinimide; APS: ammonium persulfate; PANI: Polyaniline; ZnO NWs: Zinc Oxide Nanowires; GO: graphene oxide; SDBS: sodium dodecyl benzenesulfonate; SN-GQDs: sulfur and nitrogen co-doped graphene quantum dots;

SN-GQDs: sulfur and nitrogen co-doped graphene quantum dots; RuCl₃·xH₂O: Ruthenium chloride hydrate SrCl₂·xH₂O: Strontium chloride hydrate; TiO₂ NTAs: TiO₂ nanotube arrays; CoP NPs: cobalt phosphide nanoparticle; PECVD: plasma enhanced chemical vapor deposition; NFS: nanofibers; CN: n-type graphitic carbon nitride; CA: citric acid; P-TCN: phosphorus-doped tubular carbon nitride;

reaction vessel (like autoclave), and finally synthesizes the reaction products (Rajender et al., 2018). It is widely used because of simple operation and easy control of reaction conditions. Therefore, GQDs/SCs with high crystallinity can be obtained by hydrothermal method. Yuan et al. (Yuan et al., 2019b) prepared GQDs and graphitic carbon nitride (g-C₃N₄) with 1,3,6-nitropyrene and melamine as precursors respectively, and then synthesized binary GQDs/graphitic carbon nitride

nanorods (g-CNNR) composite photocatalyst by one-step hydrothermal method (Fig. 2a). Through scanning electron microscope (SEM), it could be seen that GQDs/g-CNNR presented the shape of porous nanorod. And these nanorods were intertwined to form three-dimensional porous framework, which were conducive to rapid mass diffusion in photocatalysis. Moreover, the high-resolution transmission electron microscopy (HRTEM), X-ray diffraction (XRD) and energy dispersed

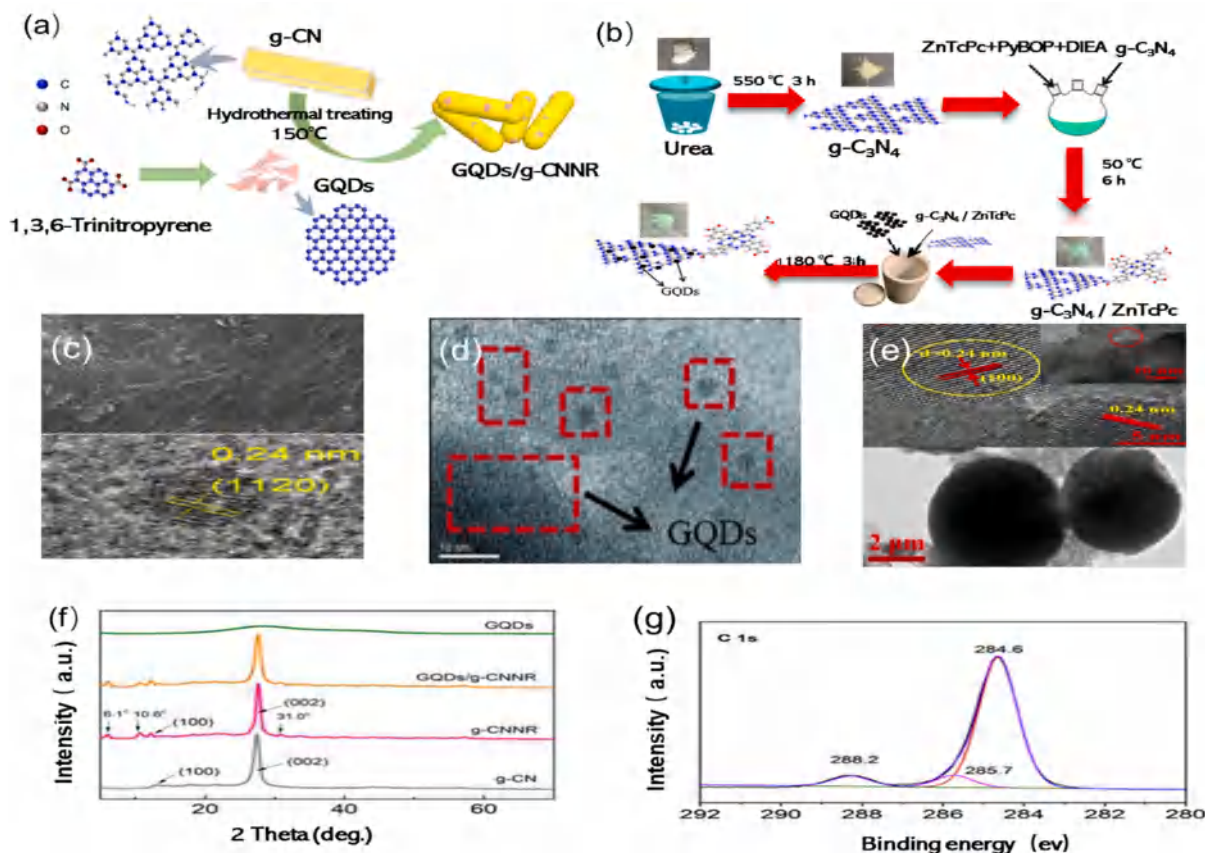


Fig. 2. (a) Preparation of GQDs/g-CNNR. (c) SEM (above) and HRTEM (below) images of GQDs/g-CNNR. (f) XRD images of GQDs/g-CNNR. Reprinted with permission (Yuan et al., 2019b). Copyright 2019 Elsevier Inc. (b) Preparation of g-C₃N₄/ZnTcPc/GQDs. (d) TEM of g-C₃N₄/ZnTcPc/GQDs. (g) XPS images of g-C₃N₄/ZnTcPc/1.0 wt% GQDs. Reprinted with permission (Xu et al., 2019; Xu et al., 2019). Copyright 2019 Elsevier. (e) HRTEM (above) and TEM (below) images of GQDs/TCN. Reprinted with permission (Nie et al., 2018). Copyright 2019 Elsevier.

spectroscopy (EDS) showed that the size of GQDs/g-C₃N₄ was 300–400 nm and had clear lattice. And the (100) peak was sharper, showing dispersion uniformly and stably of GQDs on the surface of g-C₃N₄ as well as indicating high crystallinity of complex (Fig. 2c and f). However, in the binary photocatalytic system, the biggest obstacle is to realize the expansion of visible light response and effective charge separation at the same time (Xu et al., 2019; Xu et al., 2019). The ternary photocatalyst can solve the above problems. Xu et al. (Xu et al., 2019; Xu et al., 2019) first prepared g-C₃N₄ with urea as precursor, and then synthesized ternary photocatalyst [g-C₃N₄/zinc tetracarboxyphthalocyanine (ZnTcPc)/GQDs] with thin layer structure by hydrothermal method (Fig. 2b). This thin layer structure enabled effective electron transfer. TEM and X-ray photoelectron spectroscopy (XPS) confirmed that the existence of nano film structure, and ZnTcPc in the form of small molecules didn't exist in the crystal. C–COOH and C–C bonds made the three substances coexist well, so that GQDs could be evenly distributed on the surface of g-C₃N₄/ZnTcPc (Fig. 2d and e). Similarly, Nie et al. (Nie et al., 2018) also came to similar conclusion that GQDs were evenly dispersed on the surface of Mn-N-TiO₂/g-C₃N₄ (TCN) and GQDs/TCN had high crystallinity (Fig. 2g).

From the above examples, the materials obtained by hydrothermal method have good crystal structure, complete grains and uniform distribution. At present, hydrothermal method is an important method to prepare GQDs/SCs, which has broad application prospects. However, due to the high requirement of equipment and long time, this method is not widely used in industrial production. Therefore, it is necessary to put forward some reasonable scheme to shorten the production cycle, improve work efficiency and expand its application scope.

2.1.2. Improved hydrothermal method

The improved hydrothermal method mainly includes hydrothermal deposition and ultrasound-assisted hydrothermal method. The improved hydrothermal method overcomes the shortcomings of traditional hydrothermal method (not suitable for substances which easy to react with water) and shows great application potential in industry (Xie et al., 2014; Wang et al., 2018; Chen et al., 2018).

Hydrothermal deposition is an improved hydrothermal method. Its reaction product is chemical precipitation, and the crystals separate out in the form of precipitation, which simplifies the experimental steps and overcomes the disadvantage of long impurity removal time of traditional

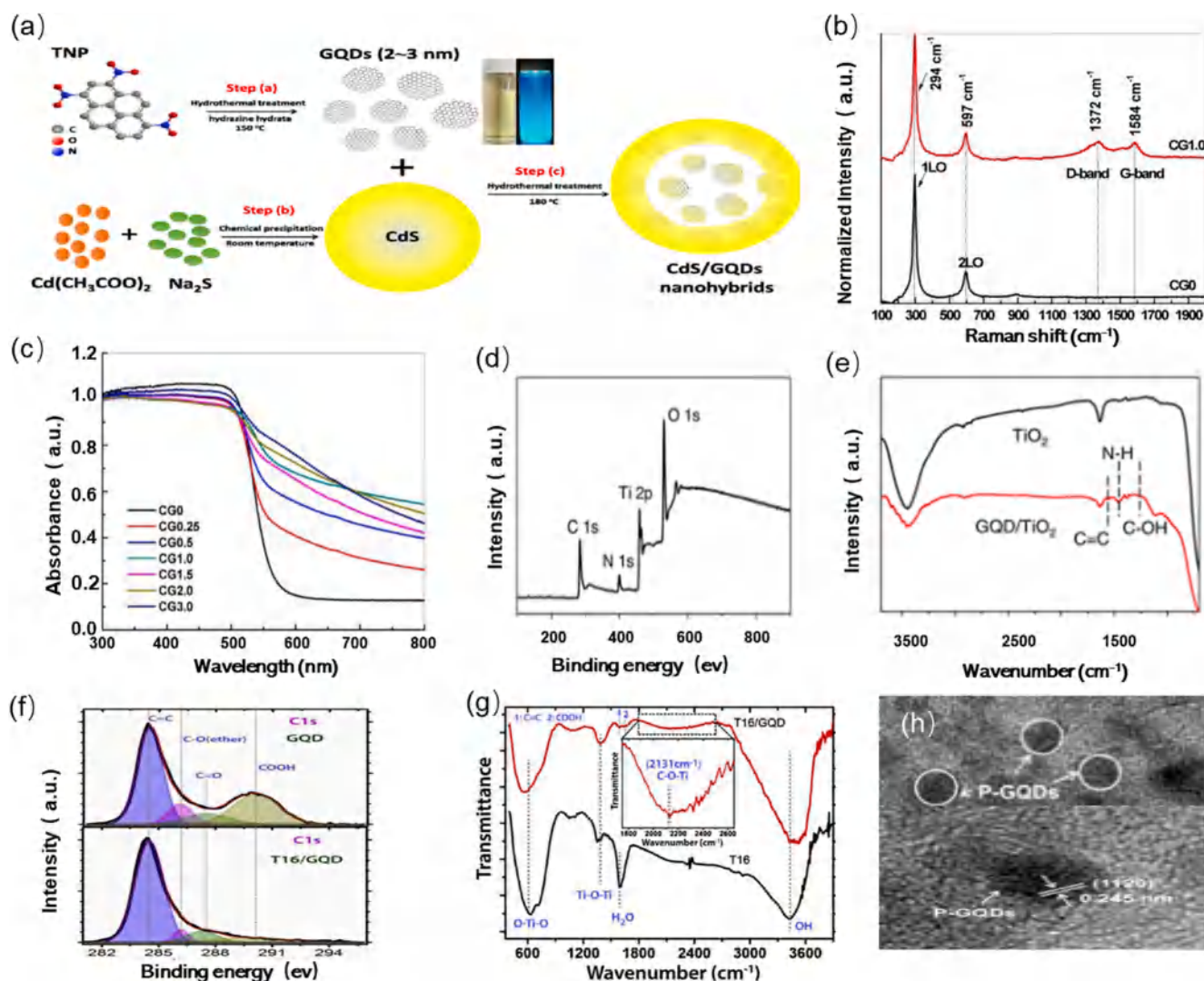


Fig. 3. (a) Preparation of CdS/GQDs. (b) Raman spectra image of CdS/GQDs. (c) UV-Vis DRS Reprinted image of CdS/GQDs. Reprinted with permission (Lei et al., 2017). Copyright 2017 Elsevier B.V. (d) XPS images of NH₂-GQDs/TiO₂. (e) FTIR images of NH₂-GQDs/TiO₂. Reprinted with permission (Pan et al., 2015). Copyright 2015 American Chemical Society. (f) XPS images of GQDs (above) and GQDs/TiO₂ (below). Reprinted with permission (Rajender et al., 2018). Copyright 2017 Elsevier B.V. (h) TEM (above) and HRTEM (below) images of p-GQDs/CN. Reprinted with permission (Qian et al., 2018a). Copyright 2017 American Chemical Society.

hydrothermal method. And it can be widely used in industrial production. Lei et al. (Lei et al., 2017) used 1,3,6-trinitropyran, Na_2S and Cd (CH_3COO)₂ as reactants, and then prepared CdS/GQDs by hydrothermal deposition (Fig. 3a). From Raman spectra and UV–vis diffuse reflectance spectra (DRS), it could be seen that GQDs/CdS had typical vibration peaks of GQDs and CdS. At the same time, the peaks and intrinsic band gap absorption were similar to pure CdS. It indicated that GQDs were well coupled on the surface of CdS, which had no effect on the good crystal structure of CdS, but enhanced the absorption of visible light (Fig. 3b and c). Doping can change the electron density of SCs and adjust the photoelectric properties effectively (Khaki et al., 2017). Pan et al. (Pan et al., 2015) added N-dopant to GQDs to obtain amine-functional GQDs (NH_2 -GQDs), which were conducive to improving the degradation rate of pollutants. Then NH_2 -GQDs/ TiO_2 was prepared by hydrothermal deposition. It could be seen from XPS and Fourier Transform Infra-Red (FTIR) that NH_2 -GQDs/ TiO_2 had diffraction peaks of Ti 2p, C 1 s, O 1 s and N 1 s, and also had the same diffraction peaks as anatase TiO_2 . It indicated that GQDs/ TiO_2 didn't change the crystal structure of pure TiO_2 , so that the crystal was stable and had high purity (Fig. 3d and e). In addition, the strong sp^2 bond at the interface of NH_2 -GQDs/ TiO_2 was conducive to interfacial electron transfer.

The hydrothermal deposition can be used to prepare GQDs/SCs, and SCs are precipitated on the surface of GQDs rather than doped. The coupling of GQDs doesn't change the crystal structure of SCs. In addition, the crystal purity of GQDs/SCs is high, but impurities are easy to be generated in the experimental process of depositing crystals. Therefore, the reasonable removal of impurities is needed to improve the precipitation method, such as filtration method, absorption method and impurity conversion method.

Ultrasound-assisted method is also used to improve crystal purity. And ultrasound can produce the effect of cavitation (high-speed and strong) and the effect of stirring (Shamaila et al., 2016). In the process of hydrothermal method of nano materials, the crystals are separated from impurities by ultrasound so as to prepare high-purity composites. Moreover, ultrasound-assisted method includes stirring method and ultrasonic method (Teh et al., 2017). And it overcomes the disadvantage of uneven heating by hydrothermal method and makes the material easy to prepare (Muthoosamy and Manickam, 2017). Rajender et al. (Rajender et al., 2018) obtained GQDs with graphene oxide (GO) as precursor by hydrothermal method, and then processed GQDs/ TiO_2 by ultrasonic treatment. XPS and FTIR showed that GQDs and TiO_2 were hybridized into complex with stable crystalline phase to promote charge separation. Meanwhile, the existence of Ti-O-C bond and the significant reduction of C-O and COOH functional groups in the complex could confirm this (Fig. 3f and g). Changing the semiconductor type of GQDs and forming effective heterojunction are also can improve the photocatalytic efficiency of GQDs/SCs. Qian et al. (Qian et al., 2018a) doped P into GQDs (p-GQDs) to change n-type semiconductor into p-type. P-GQDs/n-type graphitic carbon nitride (CN) was also prepared by ultrasonic-assisted hydrothermal method. And the morphological results of GQDs/ TiO_2 were similar to the report by rajender et al. (Rajender et al., 2018) P-GQDs/CN was stable and had clear lattice, reflecting high crystallinity (Fig. 3d).

With the aid of ultrasound, the crystal of GQDs/SCs has high crystallinity and high stability. Different synthesis experiments can be carried out by setting the ultrasonic system. However, the research on the preparation of GQDs/SCs by this method is not perfect, and the high-temperature reaction conditions are difficult to achieve, not resulting in maximizing the yield. Therefore, it is necessary to standardize the control parameters. In addition, it is found that ultrasonic-assistance in liquid is more stable and effective than in solid (Liao et al., 2019). Liquid phase solutions (water, alcohol etc.) can be used to improve the yield of photocatalysts.

2.1.3. Self-assembly method

Self-assembly is an important method to form stable structures,

including electrostatic interaction, spin-coating and sequential assembly. And under the action of hydrogen bond, van der Waals force and electrostatic force, nano materials can be stripped and aggregated from large objects to form stable heterojunctions (Su et al., 2019a; Liang et al., 2021). The interlayer distance and superimposed lattice of heterojunctions affect the photocatalysis, and the interface interaction can be adjusted by changing the number of layers (Fang et al., 2014). The composites formed by self-assembly have uniformity and stability, and can be used for preparing GQDs/SCs.

Electrostatic interaction is the main self-assembly and it is a potential method to solve the problems of aggregation and contact. It combines two substances with different charges through static electricity, and balances the charges through electronic gain and loss, so as to self-assembly into corresponding nano materials (Yu et al., 2021). Due to the strong electrostatic force, GQDs/SCs are very stable. Liu et al. (Liu et al., 2017; Liu et al., 2017; Liu et al., 2017; Liu et al., 2017) synthesized hydroxyl functionalized graphene quantum dots (OH-GQDs)/mesoporous graphitic carbon nitride (mpg- C_3N_4) through electrostatic interaction, and realized the self-assembly of negative charge GQDs and positive charge mpg- C_3N_4 (Fig. 4a). Fast Fourier Transform (FFT) showed that GQDs were closely contact with mpg- C_3N_4 and well dispersed by electrostatic attraction (Fig. 4b). And they successfully constructed stable 0D/2D heterojunction to improve the light collection and adsorption capacity.

Spin-coating is a solution-based self-assembly method, which is mostly used for preparing porous materials (nanowires, films, coatings, etc.) (Nisticò et al., 2017). The research on spin-coating mainly focuses on oxides (SiO_2 , TiO_2 , ZnO, etc.) (Ciriminna et al., 2013; Wan et al., 2006). Moreover, spin-coating generally requires the use of templates. And templates can be self-assembled into colloidal crystals with clear size and geometry or form nanospheres by lithography (Chtouki et al., 2021). The method is simple, rapid, and it also can apply in depositing uniform thin film coatings, but it is only suitable for small molecular materials. Ebrahimi et al. (Ebrahimi et al., 2017) successfully prepared GQDs/ZnO nanowires (ZnO NWs) by depositing GQDs on ZnO NWs (Fig. 4c). The structure and chemical composition of the samples were analyzed by TEM and XPS, which confirmed that GQDs were stably and deposited on the surface of ZnO NWs uniformly. In addition, Zn-O-C bond was formed at the interface of GQDs/ZnO NWs, which was conducive to the improvement of catalytic activity (Fig. 4d). Similarly, Xie et al. (Xie et al., 2017; Xie et al., 2017) synthesized electron transporting layers (ETLs) of SnO_2 /GQDs by spin-coating method.

Sequential assembly solves the problem of small application range of spin-coating, which is suitable for nano materials of any size, and well controls the composition and thickness of the layer (bin Zhang et al., 2014; Zhang and Shen, 2001). As the name suggests, sequential assembly is a continuous system. Firstly, a self-assembly system is synthesized, and then it is used as the initial template for subsequent self-assembly (Burnett and Choe, 2012). In addition, sequential self-assembly is a common method to prepare ultra-thin films (layered nanostructures and functional components) and construct nano materials with highly complex structures (Moxon et al., 2017). Yan et al. (Yan et al., 2016) synthesized GQDs/ MnO_2 by sequential assembly (Fig. 4e). TEM confirmed that MnO_2 nanosheets were ultra-thin layers with folds, GQDs adsorbed on MnO_2 nanosheets tightly and uniformly (Fig. 4f). The prepared GQDs/ MnO_2 could be used as the nano probe to evaluate the redox state of cells.

The biggest feature of the prepared GQDs/SCs by self-assembly is that it has stable lattice structure. At the same time, composites are synthesized through self-assembly (adsorption or deposition), which are not easy to agglomerate. However, the stacking structure and reaction conditions of synthetic materials are difficult to control. Therefore, when preparing GQDs/SCs by this method, it is necessary to avoid agglomeration of synthetic substances and pay attention to the influence of reaction conditions.

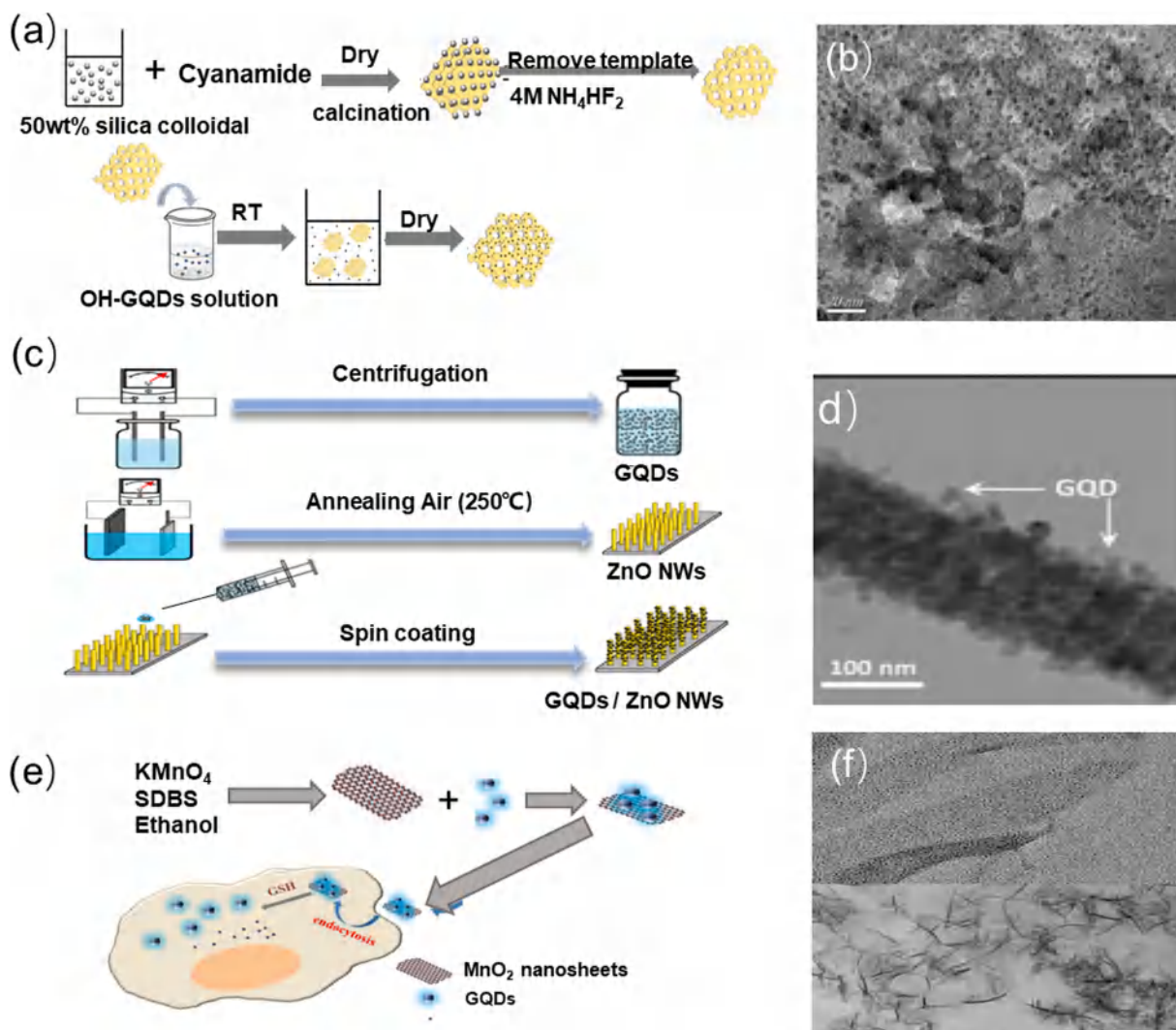


Fig. 4. (a) Preparation of OH-GQDs/mpg-C₃N₄. (b) FFT image of 0.5 wt% GQDs/mpg-C₃N₄. Reprinted with permission (Liu et al., 2017; Liu et al., 2017; Liu et al., 2017; Liu et al., 2017). Copyright 2017 Elsevier B.V. (c) Preparation of GQDs/ZnO NWs. (d) TEM (left) and FESEM (right) of GQDs/ZnO NWs. Reprinted with permission (Ebrahimi et al., 2017). Copyright 2017 American Chemical Society. (e) Preparation of GQDs/MnO₂. (f) TEM image of GQDs/MnO₂ and MnO₂. Reprinted with permission (Yan et al., 2016). Copyright 2016 American Chemical Society.

2.2. Top-down

Top-down is another kind of synthesis method of GQDs/SCs, including chemical method (chemical vapor deposition), physical method (impregnation method and freeze-drying). And the top-down is considered to be a potential method for the synthesis of GQDs/SCs.

2.2.1. Chemical vapor method

In-situ synthesis is a method to prepare nano materials by in-situ crystallization or in-situ polymerization (Wang et al., 2017; Wang et al., 2017). It avoids SCs agglomerating on GQDs. Chemical vapor deposition (CVD) is an in-situ growth method, which solves the problem that the self-assembled structure is difficult to control. And it usually deposits gaseous substances onto the solid surface at moderate/high temperatures. In addition, the flow rate (H₂ and carbon source), growth time, temperature and the surface morphology (substrate) are the key parameters to determine the size of final products (Younis et al., 2020). By adjusting these parameters, the size of GQDs/SCs can be changed, so as to improve the photocatalytic properties. Guo et al. (Guo et al., 2017) deposited the evaporated GQDs solution on coral MoS₂ by CVD. HRTEM and Raman showed that coral MoS₂/GQDs had a large number of reaction sites, which could effectively modify energy band structure of

MoS₂/GQDs (Fig. 5a). In addition, the band gap of MoS₂/GQDs obviously reduced to zero, which was conducive to electron-hole separation. Compared with CVD, plasma enhanced chemical vapor deposition (PECVD) can significantly improve the chemical reaction, so that the deposition can be carried out at a lower temperature. The interaction between plasma and deposited substrate usually involves a large number of simultaneous interleaving processes, which is easy to form network GQDs/SCs. In addition, PECVD generally uses hydrocarbon gas and other functional gases (H₂, N₂, NH₃, Ar and He) as carbon source (Gordillo-Vázquez et al., 2007). Jia et al. (Jia et al., 2018c) creatively used CO₂ instead of traditional hydrocarbons as carbon source, and in-situ deposited GQDs on the surface of MnO₂ nano arrays by PECVD (Fig. 5b). XPS and SEM confirmed that the formation of Mn-O-C covalent bond at the interface of GQDs/MnO₂, and would interconnect to form stable network structure so as to improve catalytic performance (Fig. 5c).

CVD makes the synthesis of super large surface easier. This method is suitable for the preparation of large-area GQDs/SCs. Plasma enhanced method can improve the properties of the crystal and make the crystal have higher crystallinity than CVD (Papageorgiou et al., 2017). Moreover, CVD maintains the integrity and stability of nano materials. The good catalytic properties of the synthesized GQDs/SCs are attributed to

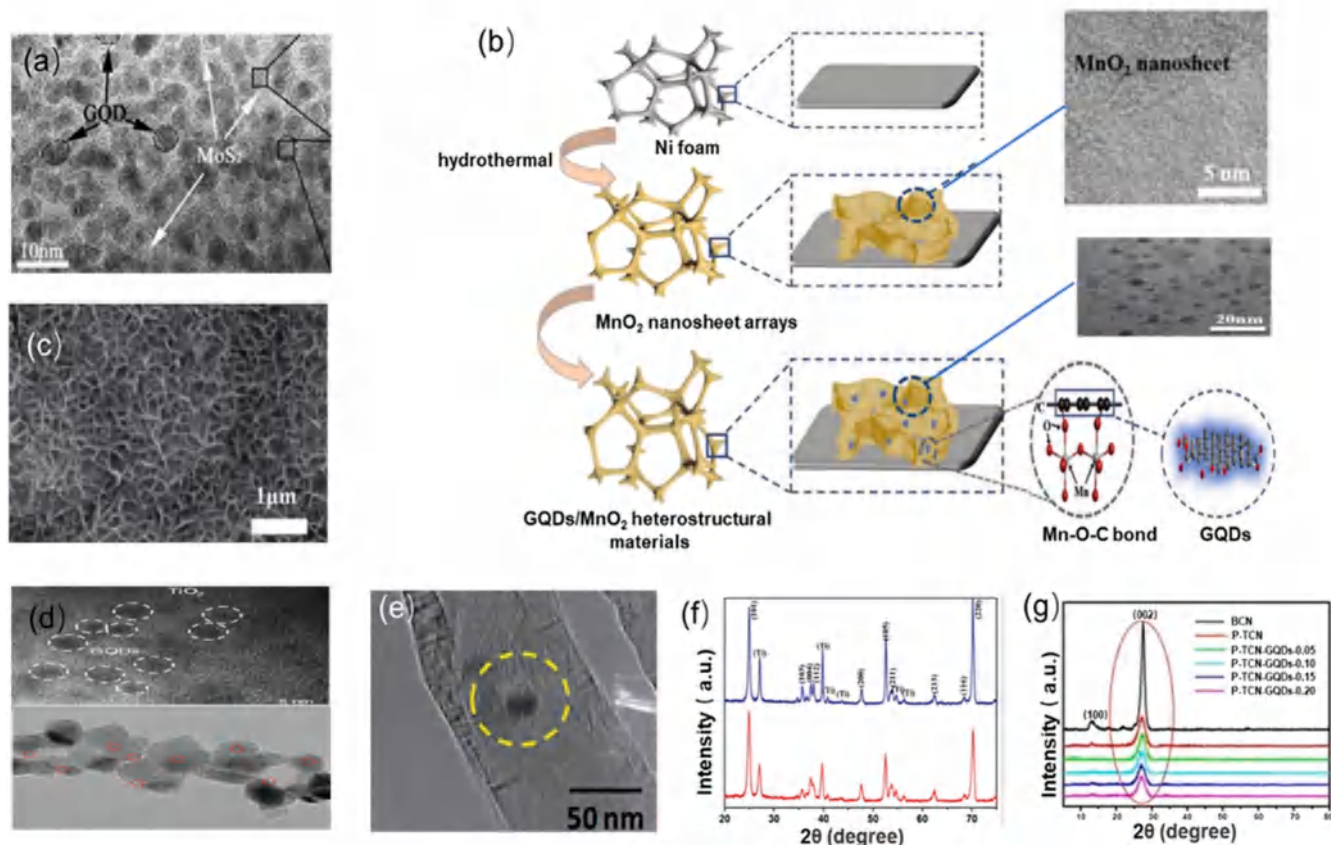


Fig. 5. (a) HRTEM image of GQDs/MoS₂. Reprinted with permission (Guo et al., 2017). Copyright 2017 American Chemical Society. (b) Preparation of GQD/MnO₂. (c) SEM image of GQD/MnO₂. Reprinted with permission (Jia et al., 2018c). Copyright 2018 WILEY-VCH Verlag GmbH & Co. KGaA, Weinheim. (d) (above) TEM image of NH₂-GQDs/TiO₂ Reprinted with permission (Pan et al., 2015). Copyright 2015 American Chemical Society. (below) TEM image of SN-GQDs/TiO₂. Reprinted with permission (Zheng et al., 2018). Copyright 2018 Elsevier B.V. (e) TEM image of GQDs/ TiO₂ NTAs. Reprinted with permission (Gupta et al., 2015). Copyright 2015 Royal Society of Chemistry. (f) XPS image of GQDs/ TiO₂ NTAs. Reprinted with permission (Gao et al., 2018a). Copyright 2017 Wiley. (g) XRD patterns of BCN, P-TCN and P-TCN/GQDs. Reprinted with permission (Gao et al., 2018a). Copyright 2017 Wiley.

the good lattice orientation and strong interface coupling of heterojunctions (Su et al., 2019b). Compared with CVD, physical vapor deposition (PVD) is also effective due to simple operation and low cost. So far, there is few literatures on the synthesis of GQDs/SCs by PVD. In the future, PVD should be paid more attention.

2.2.2. Impregnation method

The impregnation is one of the common methods for manufacturing solid-phase catalysts (Munnik et al., 2015). Generally, the solid carrier is impregnated with the solution containing appropriate catalytic components (Aris, 1985). It can immerse solid powder SCs into GQDs solution to make GQDs penetrate into the inner surface of SCs. In this method, GQDs are evenly dispersed in the pores of SCs to obtain highly dispersed GQDs/SCs. Zheng et al. (Zheng et al., 2018) added TiO₂ powder to S and N co-doped GQDs (SN-GQDs) solution by impregnation and finally synthesized SN-GQDs/TiO₂. The results of HRTEM image of SN-GQDs/TiO₂ were consistent with amine functionalized GQDs (NH₂-GQDs)/TiO₂ prepared by hydrothermal deposition, but the molecular size was smaller, only 20–30 nm (Fig. 5d). The highly dispersed SN-GQDs/TiO₂ could realize highly selective double electron redox reaction and improved the catalytic efficiency greatly. Gupta et al. (Gupta et al., 2015) also confirmed that GQDs/SCs prepared by impregnation had small size and high dispersion. They instilled GQDs into the pores of vertically aligned TiO₂ nanotube arrays (TiO₂ NTAs) and finally formed GQDs/TiO₂ NTAs. TEM showed narrow size distribution and GQDs were evenly dispersed in the pores of TiO₂ NTAs (Fig. 5e). XPS and Raman confirmed that the crystal of GQDs/TiO₂ NTAs had high purity and

crystallinity (Fig. 5f).

Impregnation is simple to operate, and it is suitable for the preparation of GQDs/SCs of porous heterogeneous catalysts. In addition, it usually prepared in the form of immersion (drip). The synthesized products have smaller size, larger area and higher dispersion, which show the great potential of impregnation in the preparation of high-performance photocatalysis, and the mechanism can be summarized adsorption of porous matrix and photocatalytic decomposition of composites. However, GQDs/SCs prepared by impregnation don't have good long-term stability. Because the morphological characteristics (particle size, surface area and crystal phase) of synthesized products depend on the experimental conditions in the synthesis process (Zhang et al., 2009), the stability of GQDs/SCs can be improved by changing the synthesis conditions.

2.2.3. Freeze-drying method

Freeze-drying and impregnation are physical methods. Compared with chemical methods, the operation is simpler and can better maintain the original physical structure of materials (Kasper and Friess, 2011). Lyophilization can turn nano materials into solids after freezing, primary drying and secondary drying. Compared with impregnation, solid material is easy to transport, and freezing is generally carried out at the low temperature, so as to improve the stability of the composite (Tang and Pikal, 2004). Gao et al. (Gao et al., 2018a) modified GQDs (citric acid as precursor) on phosphorus-doped tubular carbon nitride (P-TCN) (melamine as a precursor) to form composite photocatalyst. XRD showed that similar crystal structures were observed in P-TCN and

P-TCN/GQDs, and indicated that the doping of GQDs didn't change the structure of the original P-TCN. In addition, (002) peaks of them widened and weakened, it indicated that carbon nitride formed hollow structure to avoid the agglomeration of GQDs (Fig. 5g).

Freeze-drying is generally used to construct 3D GQDs/SCs (tubular, etc.). 3D structure increases the surface area of GQDs/SCs and effectively improves the catalytic performance. However, due to the high cost of freeze-drying method, there are few studies on the preparation of GQDs/SCs by freeze-drying. In addition, the materials of 3D structure are fragile and vulnerable. Therefore, the effects of experimental conditions (temperature, oxygen, time, pressure, etc.) and product quality (form, moisture, etc.) on freeze-drying should be pay more attention.

A large number of studies have found that the bottom-up is the main method for the synthesis of GQDs/SCs. It uses organic precursors to make nano materials. However, it is difficult to synthesize complex organic precursors, which increases the difficulty of experiment. Although the top-down is more convenient and can form GQDs/SCs by decomposing carbon materials, there are few studies on the preparation of GQDs/SCs by this method. Moreover, the surface of GQDs/SCs contains oxygen functional groups, which are conducive to the improvement of photocatalytic activity. In the future, we can develop more top-down to synthesize GQDs/SCs.

3. Photocatalytic mechanisms of GQDs/SCs

The band gap of GQDs is the distance between π and π^* orbitals, and it can be narrowed by adjusting the particle size and expanding the π conjugated sp^2 carbon network (Colherinhas et al., 2015; Yan et al., 2019b; Choi, 2017). Therefore, different kinds of heterojunctions can be formed to reduce the band gap, accelerate charge transport and increase

catalytic efficiency. Two kinds of semiconductor materials with different bandgap may combine to form heterojunction (Shao et al., 2021; Zheng et al., 2011). GQDs/SCs can form different kinds of heterojunctions. For example, the traditional type-II heterojunction formed by the staggered band gap arrangement of two SCs (the conduction band and valence band energy of semiconductor A are relatively higher than that of semiconductor B) (Xu et al., 2019; Xu et al., 2019), p-n heterojunction formed by the interface of n-type and p-type semiconductors (Low et al., 2017a; Zarezadeh et al., 2019), Z-scheme heterojunction with the same energy band arrangement as type-II heterojunction but electron migration path looks as a "Z" shape (Zhang et al., 2020; Low et al., 2017b), shell-core structure formed by a semiconductor as a core and the other semiconductor as an outer close contact layer (Gawande et al., 2015; Lu et al., 2020; Li et al., 2019; Wang et al., 2018a). The energy band structure of the above heterojunctions leads to the arrangement of energy bands and control the transport behavior of carriers accurately (Low et al., 2017a; Fang et al., 2020). Heterojunction has been proved to be one of the most promising structures for the preparation of advanced photocatalysts. And it can accelerate separation of electron-hole and effectively improve the optical conversion efficiency.

The photocatalytic efficiency of GQDs is enhanced when it is combined with SCs. Photocatalysis refers to the process of nanomaterials with photocatalytic properties (mostly semiconductors) to speed up the rate of chemical reaction in sunlight. And it begins the photoinduced production of carriers (electrons and holes) (Han et al., 2018; Buzzetti et al., 2019; Li et al., 2018b), electron (e^-) rises from the valence band (VB) to the conduction band (CB), leaving holes (h^+) in the VB. Then the electron reacts with oxidant to form superoxide anion radical ($\cdot O_2^-$) and the hole reacts with reductant to form hydroxyl radical ($\cdot OH$), $\cdot O_2^-$ and $\cdot OH$ act as active substances can make pollutants harmless (Fig. 6a).

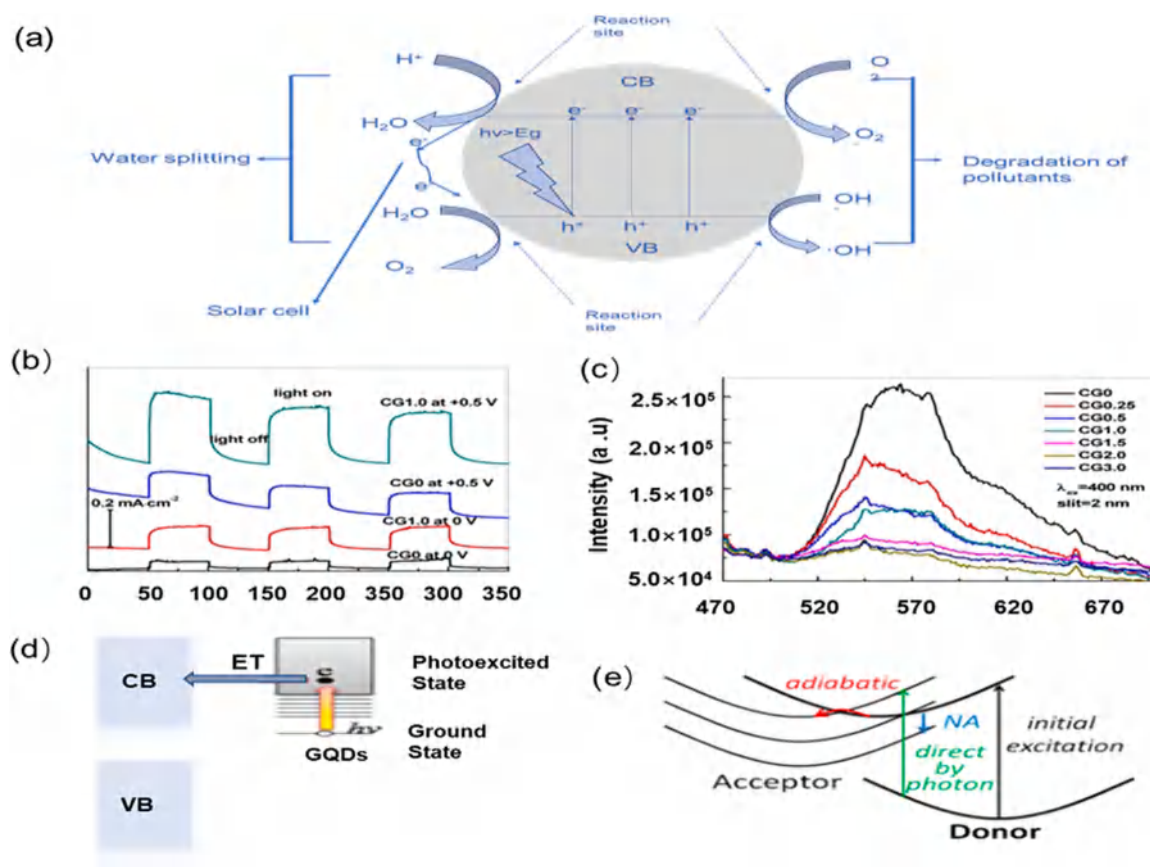


Fig. 6. (a) The schematic diagram of photocatalysis. (b) The photocurrent spectra of CdS/GQDs (c) The PL spectra image of CdS/GQDs. Reprinted with permission (Lei et al., 2017). Copyright 2017 Elsevier B.V. (d) Schematic of photoinduced electron injection. (e) The path of Electron transfer. Reprinted with permission (Long et al., 2017). Copyright 2017 American Chemical Society.

Therefore, to improve the photocatalytic efficiency of GQDs/SCs, important factors (light capture ability, photogenerated carrier mobility, electron-hole separation efficiency, etc.) need to be considered (Bokare et al., 2021). In the previous paragraph, we briefly introduce the band structure and corresponding optical properties of GQDs. According to the corresponding theoretical knowledge, we know that GQDs play important roles in improving the photocatalytic performance of GQDs/SCs.

In this chapter, the photocatalytic mechanisms are analyzed by explaining the roles of GQDs in photocatalytic reaction. They include electron acceptor or donor, photosensitizer, electron transfer accelerator, increasing contact surface and forming electric field. Specifically, (1) GQDs acts as electron acceptor (donor) to induce effective charge separation. (2) GQDs acts as photosensitizer to expand the absorption range of light. (3) GQDs acts as electron accelerator to accelerate electron transfer. (4) The local electron transfer of GQDs/SCs can form electric field. (5) The porous structure of GQDs/SCs increases the contact area and reaction site. Moreover, by observing a large number of experimental data and result, the photocatalytic efficiency of GQDs/SCs was apparently higher than that of GQDs alone. The roles of GQDs in improving the photocatalytic activity of GQDs/SCs are shown in Table 2.

3.1. GQDs as electron acceptor/donor

Due to their easily tunable band gap, high charge carrier mobility and efficient intramolecular charge transfer, donor-receptor complexes are feasible in the preparation of high-performance photocatalysts. In addition, electron acceptor/donor refers to the substance receiving/providing electron (Cao and Yu, 2016; Ou et al., 2018; Sheng et al., 2021). In GQDs/SCs, when SCs are excited by light, the VB electrons rise to the CB, and then the electrons transfer to GQDs, which act as electron acceptors. On the contrary, GQDs, as electron donors, transfer electrons to SCs under light excitation. Whether GQDs are electron acceptors or donors, they can induce effective charge separation and inhibit the recombination of electron-hole pairs. Lie et al. (Lei et al., 2017) demonstrated that GQDs as electron acceptor could lead to effective charge separation. Photoluminescence (PL) and photocurrent spectra showed that the presence of GQDs enhanced the photocurrent intensity of GQDs/CdS greatly, but reduced PL emission significantly (Fig. 6b and c). The existence of GQDs provided a fast electron transfer pathway, which greatly delayed the charge recombination of CdS and realized effective charge separation. The experiment (characterization) proves crystal structure and intermolecular interaction. Besides, density functional theory (DFT) (calculation) is also very effective (Beran, 2016). It overcomes the limitation of wave mechanics and reduces the complexity (degree of freedom) of the problem by dealing with electron density functional (wave function including electrons) (Parr and Pearson, 1983; Obot et al., 2015). In addition to being electron acceptors, GQDs can also be electron donors to induce effective charge separation and improve photocatalytic performance. Long et al. (Long et al., 2017) proved this by using real-time DFT and diabatic molecular dynamics hybrid quantum method. GQDs and TiO₂ were coupled in the form of electron donor-acceptor, the energy gap was reduced, allowing more excited states and hot electron injection. Therefore, the separation of electrons and holes was effectively realized. The electron transfer (ET) images also confirmed this effective charge separation, the donor containing material moved faster, the charge separation was much faster than the energy relaxation, and accelerated the electron transfer from GQDs to TiO₂ (Fig. 6d and e).

Electron donor-acceptor polymers can be constructed by covalent binding or π -bond spatial binding (Stergiou et al., 2014). GQDs/SCs in the form of electron donor-acceptor have significant advantages in improving photocatalytic efficiency. The reasons are as follows: (1) the electron donor-acceptor polymers have unique stacked crystal structure, which can produce tunable energy band structure. (2) When GQDs are used as electron donor, the VB of SCs is lower than the reduction

potential of GQDs, and the photogenerated electrons can be easily transferred from the CB of GQDs to SCs. (3) When GQDs are used as electron acceptor, the electron transfer path is opposite. The ideal donor SCs can have relatively lowest unoccupied molecular orbital (LUMO) energy level and narrow band gap. (4) Electron donors and acceptors are coupled to form GQDs/SCs, which provide the platform for carrier transport and have better performance than single component GQDs.

3.2. GQDs as photosensitizer

Photoinduced electron injection from excited state photosensitizer to CB is an important step in the photosensitization of wide gap SCs (Buchalska et al., 2013). Therefore, adjustable band gap GQDs are suitable to be photosensitizers. Due to the multiphoton activity of carbon dots, GQDs, as photosensitizer, exhibit excellent up conversion photoluminescence (PL) under near-infrared light (Jamila et al., 2020b). Moreover, PL excite SCs to absorb energy equal to or greater than the band gap, and then form electron-hole pairs. It is good for accelerating electron transfer and improving photoreaction activity. In addition, photoinduced electrons injection involves the charge transfer of surface bound photosensitizer. It usually transfers electron to the CB of photosensitizer, and then forms the reactive oxygen species by residual holes on the surface, improving the catalytic efficiency (Buchalska et al., 2013). Tang et al. (Tang et al., 2017) confirmed that GQDs as a photosensitizer extended the light absorption wavelength to the visible region (Fig. 7a). And adjustable band gap GQDs sensitized BiVO₄ to form heterojunction. Heterojunction was conducive to electrons transfer from BiVO₄ and electrons injected into the LUMO of GQDs, while the left holes and oxidized H₂O to form ·OH. Moreover, the stable crystal structure of GQDs could also promote the photocatalytic reaction. And GQDs had the lowest density of trap states and the smallest potential energy barrier at the grain boundary. These advantages proved that the promotion of electron transport. Ghosh et al. (Ghosh et al., 2016) also confirmed this. Furthermore, the LUMO of GQDs was located above the CB of ZnO and had good absorption of visible light, so as to better promote the transfer of electrons to the CB of ZnO nanorods (NRs) (Fig. 7b and c).

When GQDs are used as photosensitizers, photoexcitation and photoinduced electron injection are the main reaction mechanisms. The specific catalytic process has been introduced in the previous paragraph. GQDs, as photosensitizer, improve the photocatalytic efficiency, and the efficiency strongly depends on composition. The structure should ensure that the CB of SCs inject electrons quickly and effectively. However, GQDs/SCs involving holes injection photosensitization system has not been studied. Hole injection related researches mainly focuses on p-type SCs (NiO, CuO, etc.) (Buchalska et al., 2013), which provide guidance for the study of photocatalytic mechanisms of GQDs/(p-type SCs).

3.3. GQDs as electron transfer accelerator

Rapid interfacial charge transfer and interfacial photocatalytic reaction are important ways to improve photocatalytic performance (Xu et al., 2018; Xu et al., 2018). In addition to being photosensitizer to accelerate electron transfer, GQDs can act as electron transfer accelerator to accelerate electron transfer itself. As electron transfer medium, GQDs should follow the mechanism of interfacial charge carrier transfer to effectively separate charge carriers (Natarajan et al., 2018). When the Fermi level of GQDs is lower than the CB of SCs, electrons can be transferred from CB of SCs to GQDs (Hu et al., 2021; Hu et al., 2021; Hu et al., 2021). Therefore, increasing the CB of GQDs or reducing the CB of SCs can accelerate the interfacial electron transfer and ensure the stability of photoreaction. Wang et al. (Wang et al., 2017; Wang et al., 2017) confirmed that GQDs could be used as electron accelerator and facilitated the transfer of electrons from Fe₂O₃ to TiO₂. Meanwhile, the great photocurrent response of Fe₂O₃-GQDs/NF-TiO₂ promoted interfacial electron transfer (Fig. 8a). Furthermore, the electrochemical

Table 2

The roles of GQDs in improving the photocatalytic activity of GQDs/SCs and applications of GQDs/SCs.

Photocatalysts	Mechanism	Light source	Times	Efficiency	Applications	Ref.
1 CdS/GQDs	as electron acceptor	300 W Xe lamp (> 420 nm)	2.7(CdS)	95.4 $\mu\text{mol h}^{-1}$	generation of H ₂	(Lei et al., 2017)
2 GQDs/TiO ₂	as electron acceptor	—	—	—	synthesis of DSSCs	(Kumar et al., 2019)
3 N-GQDs/In ₂ O ₃	as electron acceptor	—	—	—	synthesis of gas sensor	(Lv et al., 2020)
4 GQDs/TiO ₂	as electron donor	—	—	—	synthesis of solar cells	(Long et al., 2017)
5 SN-GQDs/RGO/TiO ₂ NA	as electron donor	300 W Xe lamp (> 400 nm)	16.3(TiO ₂ NA)	—	degradation of MO	(Zhang et al., 2012)
6 GQDs/ZnO NWs	as photosensitizer	solar light	3(ZnO NWs)	—	degradation of MB	(Ebrahimi et al., 2017)
7 GQDs/BiVO ₄	as photosensitizer	350 W Xe lamp	1.8(BiVO ₄)	—	degradation of CBZ	(Tang et al., 2017)
8 N-GQDs/g-C ₃ N ₄	as photosensitizer	visible light irradiation ($\lambda \geq 420 \text{ nm}$)	7.7 (g-C ₃ N ₄)	139.6 $\mu\text{mol h}^{-1}$	generation of H ₂	(Mou et al., 2019)
9 N-GQDs/CN-U	as photosensitizer	300 W Xe lamp (> 420 nm)	2.16(CN-U)	2.18 $\text{mmol h}^{-1}\text{g}^{-1}$	generation of H ₂	(Zou et al., 2016)
10 GQDs/ZnO NRs	as photosensitizer	a Xe lamp (309 nm)	—	—	synthesis of ultraviolet detector	(Ghosh et al., 2016)
11 ZnO/GQDs	as photosensitizer	—	—	—	synthesis of DSSCs	(Zamiri and Bagheri, 2018)
12 OH-GQDs/Ni ₂ P	as photosensitizer	300 W Xe lamp (> 420 nm)	94(OH-GQDs)	1567 $\mu\text{mol h}^{-1}\text{g}^{-1}$	generation of H ₂	(Zhu et al., 2018)
13 GQDs/TiO ₂ /HNPs	as photosensitizer	solar light	95(TiO ₂)	—	synthesis of UV detector	(Kunwar et al., 2021)
14 TiO ₂ /Sb ₂ S ₃ /GQDs	as photosensitizer	—	—	—	removal of bacteria	(Teymourinia et al., 2019a)
15 Fe ₂ O ₃ -GQDs/NF-TiO ₂	as electron transfer accelerator	—	—	7(Fe ₂ O ₃ /TiO ₂)	removal of Cr ⁶⁺	(Wang et al., 2017; Wang et al., 2017)
16 NP-GQDs/g-C ₃ N ₄	as electron transfer accelerator	300 W Xe lamp (> 420 nm)	1.85(g-C ₃ N ₄)	—	degradation of MO	(Guo et al., 2021)
17 TiO ₂ /GQDs	as electron acceptor and photosensitizer	—	7(TiO ₂)	2.2 $\mu\text{mol h}^{-1}$	generation of H ₂	(Min et al., 2017)
18 TNT/GQDs	as electron acceptor and photosensitizer	100 W Xe lamp (> 430 nm)	5.6(TNT)	1.98 $\text{ppm cm}^{-2}\text{h}^{-1}$	CO ₂ conversion	(Zubair et al., 2018)
19 N-GQDs/I-BiOCl	as electron acceptor and photosensitizer	—	—	—	synthesis of PEC sensor	(Wang et al., 2018b)
20 N-GQDs/BiO _{2-x}	as electron acceptor and photosensitizer	300 W Xe lamp (> 420 nm)	2.9(BiO _{2-x})	—	degradation of TC	(Chen et al., 2020; Chen et al., 2020)
21 TiO ₂ /GQDs	as electron donor and photosensitizer	Xe lamp	5.2(TiO ₂)	—	degradation of MB	(Rajender et al., 2018)
22 GQDs/P-TCN	as electron donor and photosensitizer	Visible light (> 420 nm)	9(P-TCN)	112.1 $\mu\text{mol h}^{-1}$	generation of H ₂	(Gao et al., 2018b)
23 S, N-GQDs/TiO ₂	as electron donor and photosensitizer	300 W Xe lamp (> 400 nm)	3.6(TiO ₂)	5.7 $\mu\text{mol h}^{-1}$	generation of H ₂	(Xie et al., 2017; Xie et al., 2017)
24 SN-GQDs/TiO ₂	as photosensitizer and electron transfer accelerator	500 W Xe lamp (> 420 nm)	3.2(TiO ₂)	451 $\mu\text{mol L}^{-1}$	generation of H ₂ O ₂	(Zheng et al., 2018)
25 N-GQDs/ BiOBr	as photosensitizer and electron transfer accelerator	300 W Xe lamp (> 400 nm)	—	—	degradation of RhB	(Yin et al., 2016)
26 SnO ₂ /GQDs	as photosensitizer and electron transfer accelerator	Xe lamp	3.2(SnO ₂)	—	removal of NO	(Xie et al., 2018)
27 N-BOC/GQDs	as photosensitizer and electron transfer accelerator	Xe lamp	2.5(N-Bi ₂ O ₂ CO ₃)	—	removal of NO	(Liu et al., 2017; Liu et al., 2017; Liu et al., 2017)
28 ox-GQDs/PCNO	as photosensitizer and electron transfer accelerator	solar light	3.1(PCNO)	0.656 h^{-1}	removal of bacteria	(Xu et al., 2020)
29 N-GQDs/In ₂ O ₃	as electron acceptor and electron transfer accelerator	—	—	—	synthesis of gas sensor	(Lv et al., 2020)
30 GQDs/ZnS	as electron donor, photosensitizer and electron transfer accelerator	300 W Xe lamp	14(ZnS)	0.0046 min^{-1}	degradation of RhB	(Ham et al., 2016)
31 GQDs/MnO ₂	formation of electric field	—	—	—	synthesis of supercapacitor	(Jia et al., 2018b)
32 p-GQDs/CN	formation of electric field	300 W Xe lamp (> 420 nm)	5.9(CN)	0.030 25 min^{-1}	degradation of RhB	(Qian et al., 2018b)
33 MoS ₂ /GQDs	formation of electric field	—	—	—	—	(Li et al., 2019; Li et al., 2019)
34 BiOCl/BiVO ₄ /N-GQDs	formation of electric field	250 W Xe lamp (> 400 nm)	1.8(BiOCl/BiV ₄)	—	degradation of BPA	(Zhu et al., 2017; Zhu et al., 2017)
35 ZnO/S, N: GQDs/PAIN	formation of electric field	—	—	—	synthesis of gas sensor	(Zhang et al., 2019)
36 ZnO/GQDs	formation of electric field	solar light	—	—	synthesis of UV detector	(Wu et al., 2020; Wu et al., 2020)
37 OH-GQDs/mpg-C ₃ N ₄	increase contact area	300 W Xe lamp (> 400 nm)	1.42(mpg-C ₃ N ₄)	—	degradation of RhB	(Liu et al., 2017; Liu et al., 2017; Liu et al., 2017)
38 GQDs/g-CNNR	increase contact area	—	—	—	remove of antibiotics	(Yuan et al., 2019b)

(continued on next page)

Table 2 (continued)

Photocatalysts	Mechanism	Light source	Times	Efficiency	Applications	Ref.
39 Ag ₂ CrO ₄ /N-GQDs @g-C ₃ N ₄	increase contact area	300 W Xe lamp (> 420 nm) 300 W Xe lamp	2.03(g-CNNR)	—	degradation of DC	(Feng et al., 2018)
40 GQDs/NiCo ₂ S ₄ NWs	increase contact area	—	—	—	synthesis of supercapacitor	(Huang et al., 2018)
41 GQDs/Bi ₂ MoO ₆	increase contact area	300 W Xe lamp	2.3 (Bi ₂ MoO ₆)	—	degradation of BPA	(Hao et al., 2016)
42 NiO/GQDs	increase contact area	—	—	—	synthesis of lithium battery	(Yin et al., 2018)
43 N-GQDs/NiCo ₂ S ₄ /CC	increase contact area	—	—	—	synthesis of flexible zinc air batteries	(Liu et al., 2019b)
44 NiCo ₂ O ₄ /GQDs	increase contact area	—	—	—	synthesis of supercapacitor	(Luo et al., 2019)
45 N-GQDs/SnO ₂	increase contact area	—	—	—	synthesis of gas sensor	(Chen et al., 2020; Chen et al., 2020)
46 Cu ₂ O/GQDs	increase contact area	—	—	—	removal of bacteria	(Teymourinia et al., 2019b)
47 NiFe ₂ O ₄ /HAP/GQDs	—	—	—	—	removal of Cd ²⁺	(Kahrizi et al., 2018)
48 N-GQDs/V ₂ O ₅	—	—	—	—	synthesis of biosensor	(Ganganboina et al., 2018)
49 GQDs/ MoS ₂	—	—	—	—	synthesis of biosensor	(Shi et al., 2017)
50 MnO ₂ /GQDs	—	—	—	—	formation of bioimage	(Song et al., 2018)
51 GQD@Fe ₃ O ₄ @SiO ₂	—	—	—	—	deliver of drug	(Su et al., 2017)
52 TiO ₂ NPs/N-GQDs/g-C ₃ N ₄ QDs	—	—	—	—	synthesis of biosensor	(Pang et al., 2017)

RhB: rhodamine B; CN-U: graphite carbon nitride prepared from urea; DSSCs: dye-sensitized solar cells; RGO: reduced graphene oxide; TiO₂ NA:TiO₂ nanotubes ; MO: methyl orange ZnO NWs: Zinc Oxide Nanowires; NRs: nanorods; PEC: Photoelectrochemistry; CBZ: carbamazepine; MB: methylene blue; TC: tetracycline; HNPs: the plasmonic hybrid nanoparticles; NF-TiO₂: N and F doped TiO₂;

NP-GQDs: nitrogen and phosphorus co-doped GQDs; TNT: TiO₂ nanotube arrays; I-BiOCl: I doped bismuth oxychloride; TC: tetracycline; BPA : Bisphenol A; P-TCN: phosphorus-doped hexagonal tubular carbon nitride;

N-BOC: N-doped bismuth dioxide; ox-GQDs: graphene oxide quantum dots; PCNO: oxidized nanoporous g-C₃N₄; DC: doxycycline; CN: n-type graphitic carbon nitride; PIAN: polyaniline;

mpg-C₃N₄: mesoporous graphite carbon nitride; OH-GQDs: Hydroxyl functionalization GQDs; mpg-C₃N₄: mesoporous graphite carbon nitride; g-CNNR : graphite nitride carbon nanorods; CC: carbon cloth; HAP: hydroxyapatite; NPs: nanoparticles;

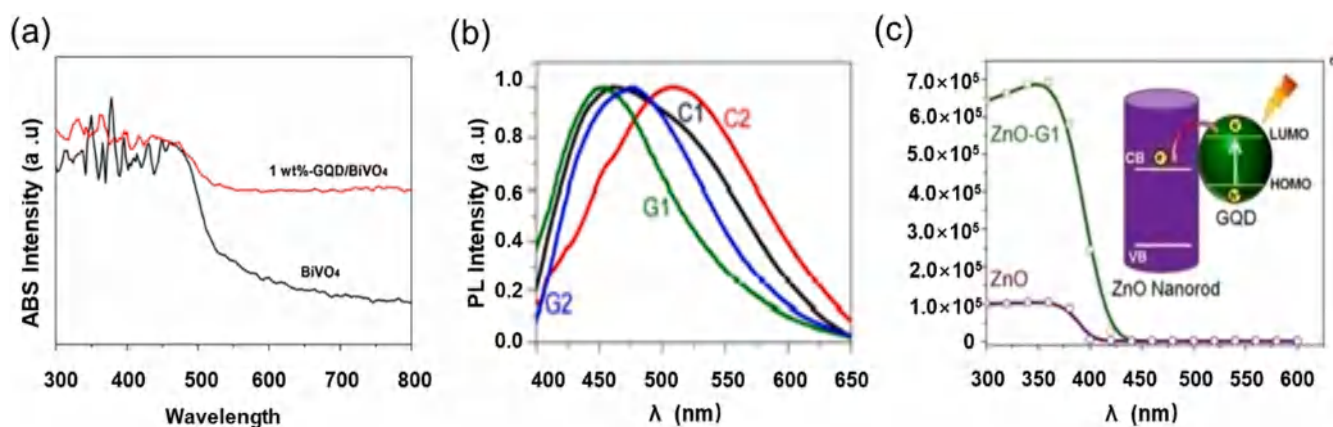


Fig. 7. (a) The UV-vis absorption spectra of BiVO₄ and GQDs/BiVO₄. Reprinted with permission (Tang et al., 2017). Copyright 2016 Elsevier B.V. (b) The PL spectra of GQDs/ZnO NRs. (c) Selectivity of ZnO and ZnO/GQDs at different wavelengths, inset: electron transfer image. Reprinted with permission (Ghosh et al., 2016). Copyright 2016 American Chemical Society.

impedance spectroscopy (EIS) showed that small charge transfer resistance and also confirmed that GQDs were used as electron accelerator to accelerate electron transfer (Fig. 8b).

When GQDs are used as electron transfer medium, it is very important to control the electron transfer between redox molecules at the interface (Cho et al., 2018). Because carriers can extend beyond the GQDs boundary, the quantum confinement effect in GQDs makes them possible to become electron transfer accelerator (Cho et al., 2018; Yang

et al., 2012). When GQDs and SCs have strong interfacial electron coupling, the interfacial charge transfer is accelerated (Wu and Lian, 2016). At present, there are few studies on GQDs as electron accelerator alone. GQDs/SCs mainly promote electron transfer by synergistic effect. Generally, GQDs are used as electron accelerator and donor (acceptor), or GQDs are used as electron accelerator and photosensitizer to synergistically improve the rate of photoreaction. The synergistic effects are introduced in detail in the next section.

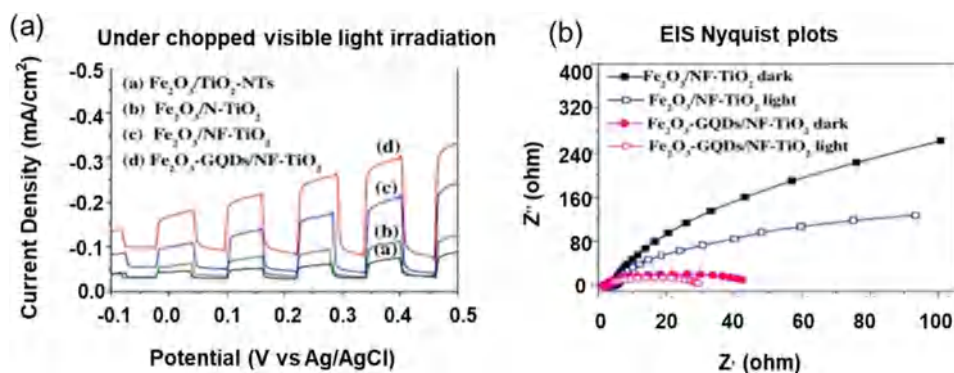


Fig. 8. (a) Photocurrent response of different films under the irradiation of $\lambda > 420$ nm. (b) EIS Nyquist plots measured in 0.5 M Na_2SO_4 aqueous solution. Reprinted with permission (Wang et al., 2017; Wang et al., 2017). Copyright 2016 Elsevier B.V.

3.4. Synergistic effect

In addition to the above-mentioned GQDs acting as electron acceptor/donor, photosensitizer or electron transfer accelerator, more GQDs/SCs can improve the photocatalytic efficiency through two or more synergistic effects. The synergistic effect is better than the single effect. Photocatalysts with synergistic effect have better photocatalytic performance, more sufficient light absorption (from UV to visible light), more charge carriers and better conductivity (Cheng et al., 2017; Xiang et al., 2016). Min et al. (Min et al., 2017) found that GQDs could be used as photosensitizer and electron acceptor to improve photocatalytic activity. Energy shift could absorb more light energy, which made more charge carriers form and promoted charge transfer from TiO_2 to GQDs. Besides, the interaction of functional bonds can produce synergistic effect (Cheng et al., 2021). Because it can form local occupied state and narrow the band gap. Rajender et al. (Rajender et al., 2018) found that TiO_2 induced the generation of oxygen vacancies and the rearrangement of in-plane epoxy functional group GQDs, resulting in the production of C-O-Ti. C-O-Ti promoted the formation of heterojunction. Because the band rearrangement of heterojunction reduced the local potential barrier of intramolecular carrier transfer, GQDs could be used as electron donor and photosensitizer, which sped up the electron transfer from GQDs to TiO_2 , and made the absorption edge of GQDs/ TiO_2 red shift. In addition, optimizing the charge transfer path can also produce synergy, such as changing the two-electron redox reaction (ORR) path and activating multi-path charge carriers to improve the catalytic efficiency. Zheng et al. (Zheng et al., 2018) found that SN-GQDs, as photosensitizers and electron transfer accelerators, induced visible light absorption, provided adsorption sites for $^*\text{OOH}$ formation and proton transform, significantly promoting the selective double electron ORR and accelerating electron transfer. Moreover, adjusting the energy band structure can also effectively produce synergy. The energy band bending may change the space charge region, which near the interface contact surface. Ham et al. (Ham et al., 2016) found that the energy band could bend upward in the equilibrium state to form metal-semiconductor Schottky junction. GQDs doping could narrow the band gap. The charge of ZnS nanobelts were excited and transferred to GQDs, and there were residual holes on the surface of ZnS. Residual holes inhibited charge transfer to GQDs and brought new visible light absorption. Meanwhile, due to the energy barrier between them, charge separation was promoted. The excellent photocatalytic effects of GQDs as electron acceptor, photosensitizer and electron transfer accelerator are confirmed.

The transfer of energy, construction of stable chemical bonds, optimization of charge transfer path and adjustment of energy band structure can produce excellent synergy. And synergistic effect is better than single effect. Furthermore, GQDs as electron acceptor/donor and photosensitizer are the main synergistic effect, which have become the main trend of photocatalytic mechanism research.

3.5. Formation of electric field

Using the formation of electric field to separate electron-hole has attracted extensive attention as a new direction. Local charge transfer leads to charge redistribution, and the band bends when the charge is redistributed to equilibrium. Upward/downward bending can drive holes/electrons to carry out oxidation/reduction reaction respectively, and promote charge separation (Liu et al., 2020; Liu et al., 2020).

GQDs/SCs form built-in electric field at the interface, which drive the carrier space separation in the opposite direction, and effectively promotes the development of type-II heterojunction. Fundamentally speaking, piezoelectric photoelectric effect is the key to the construction of built-in electric field. MoS_2 is a typical piezoelectric material. The methods of applying mechanical stress and deformation are the basic requirement for piezoelectric SCs to generate the built-in electric field (Wang, 2010; Zhao et al., 2019). Li et al. (Li et al., 2019; Li et al., 2019) found that the LUMO/ highest occupied molecular orbital (HOMO) of GQDs was higher than conduction band maximum/valence band maximum (CBM/VBM) of MoS_2 , type-II energy band arrangement could be formed, and built-in electric field could promote carrier separation. However, in the redox process, the electron hole separation efficiency of type-II heterojunction is not high. Therefore, it is necessary to develop more effective heterojunctions to accelerate the improvement of photocatalytic efficiency. p-n heterojunction overcomes the inhibition of type-II heterojunction on photocatalyst redox reaction.

Although the built-in electric field can promote carrier separation, it is fixed and saturate easily, its ability to promote photocatalysis is still limited (Kubacka et al., 2012). The introduction of applied electric field can significantly improve the photocatalytic performance of GQDs/SCs from the inside out (Hu et al., 2021; Hu et al., 2021; Hu et al., 2021). Moreover, the polarization effect and band bending caused by applied electric field are used to promote charge carrier transfer. And p-n heterojunction is beneficial to the generation of applied electric field. Due to the acceleration of electron-hole separation in heterojunction by applied electric field, Qian et al. (Qian et al., 2018a) confirmed that the efficient photocatalytic activity of p-GQDs (p-type)/g- C_3N_4 (n-type). Furthermore, the band arrangement of the heterojunction made it present cross-border band junction, which promoted the transfer of electrons in the electric field from the CB of p-GQDs to the CB of g- C_3N_4 .

The Z-scheme heterojunction catalyst has strong redox ability, and optimizes the electron transfer path of type-II heterojunction to improve the photocatalytic efficiency. Because the Fermi levels of GQDs and SCs are different, band bending occurs and it induces potential barrier (Di et al., 2019). Zhu et al. (Zhu et al., 2017; Zhu et al., 2017) confirmed that built-in electric field was formed at the interface with N-GQDs, after $\text{BiOCl}/\text{BiVO}_4$ formed p-n heterojunction. And it promoted the "Z" type charge transfer. Ternary heterojunctions generally possess effective electron-hole separation and prolong charge life.

At the interface of GQDs/SCs heterojunctions, the built-in electric

field forms the curved interface band, which effectively promotes carrier separation. In addition, the polarization effect excited by the applied field provides a driving force for the introduction of the applied field, which can improve the photocatalytic activity without changing the properties of GQDs/SCs.

3.6. Increasing contact area

The increase of contact area provides more active centers for photocatalysis and drives the photocatalytic reaction. Porous materials are desirable in the catalytic process, but the region of diffusion and confinement need to be optimized (Hu et al., 2010). Hierarchically microporous materials can effectively increase the contact area on the surface because of their good pore structure and high specific surface area. Yuan et al. (Yuan et al., 2019b) prepared 1D nanorods with layered microporous structure by controlling the morphology of g-C₃N₄. GQDs/graphitic carbon nitride nanorods (g-CNNR) with high crystallinity had large contact area. In addition, a new mesoporous structure appeared, showing larger specific surface area than the porous structure (Cherevan et al., 2018). Because more internal active sites are obtained, the structure are greatly popularized. Liu et al. (Liu et al., 2017; Liu et al., 2017; Liu et al., 2017) confirmed that mesoporous structure was conducive to photocatalytic activity. An appropriate amount of GQDs covered mpg-C₃N₄ to form the mesoporous structure, which had large contact area inside. Furthermore, the active center of shell-core structure can be designed not only inside the catalyst, but also on the surface of the shell (Li et al., 2016; Li et al., 2016). For the active sites locate in the core and embedded in the shell, the charge transfer can be maximized. Feng et al. (Feng et al., 2018) confirmed that Ag₂CrO₄/N-GQDs@g-C₃N₄ formed shell-core structure and provided active sites on both inside and outside. It paved the way for improving the activity of nano catalysts.

Microporous, mesoporous and shell-core structures can increase the contact area of GQDs/SCs. Adjusting their pore size distribution can change their size and shape. Large contact area is conducive to the separation of electrons and holes. Besides, the existence of large channels is more prone to form active sites, avoiding pore blockage (Osterloh, 2015). Therefore, large channel nano materials can be constructed to increase the contact area, such as the composite of GQDs and 1D nano materials (nanotubes, nanorods, etc.), which are conducive to improve

the characteristics of charge transfer.

4. Applications of GQDs/SCs

The practical value of GQDs/SCs has been confirmed because of their good biocompatibility and photocatalytic performance. At present, GQDs/SCs can be used in wastewater treatment, energy storage, gas sensing, UV detection, antibiosis, and biomedicine, having wide application prospect (Fig. 9). Parts of applications of GQDs/SCs can be seen in Table 2.

4.1. Sewage treatment

With the development of industrial society, there are more and more pollutants in water, and the problems of water pollution are more and more serious (Boyce, 2016; Liu et al., 2019; Zhao et al., 2021). The system of traditional wastewater treatment includes the combination of physical, chemical and biological processes (Feng et al., 2013). Generally speaking, there are three removal stages: (1) the primary treatment (screening or sedimentation) can remove stones and fat contained in sewage through mechanical treatment. (2) The secondary treatment is biological treatment, which can greatly degrade organic matter in water. (3) Tertiary treatment is the advanced treatment of sewage, which can remove refractory pollutants in water by biological, membrane filtration, chemical precipitation and photocatalytic method (Zhou et al., 2021). Photocatalysis has the advantages of environmental protection, low cost and easy control of catalyst dosage (Herrmann, 2010). Therefore, compared with other technologies, photocatalysis technology is widely used to remove pollutants in water, such as organic pollutants and heavy metal pollutants (Cheng and Dong, 2020; Jamila et al., 2020c; Hatefi et al., 2021) (Fig. 6a). GQDs/SCs have great application prospect in wastewater treatment technology because of their strong degradation ability.

Organic pollutants can be divided into two categories, one is organic dye pollutants, such as rhodamine B (RhB), methyl orange (MO), methylene blue (MB), the other is small molecular organic compounds, such as bisphenol A (BPA), carbamazepine (CBZ). Oxidation, adsorption and degradation are the most common methods to remove organic pollutants from water (Hu et al., 2021; Liu et al., 2018; He and Zhou, 2017; Lu and Astruc, 2020) (Fig. 10), in which photocatalytic

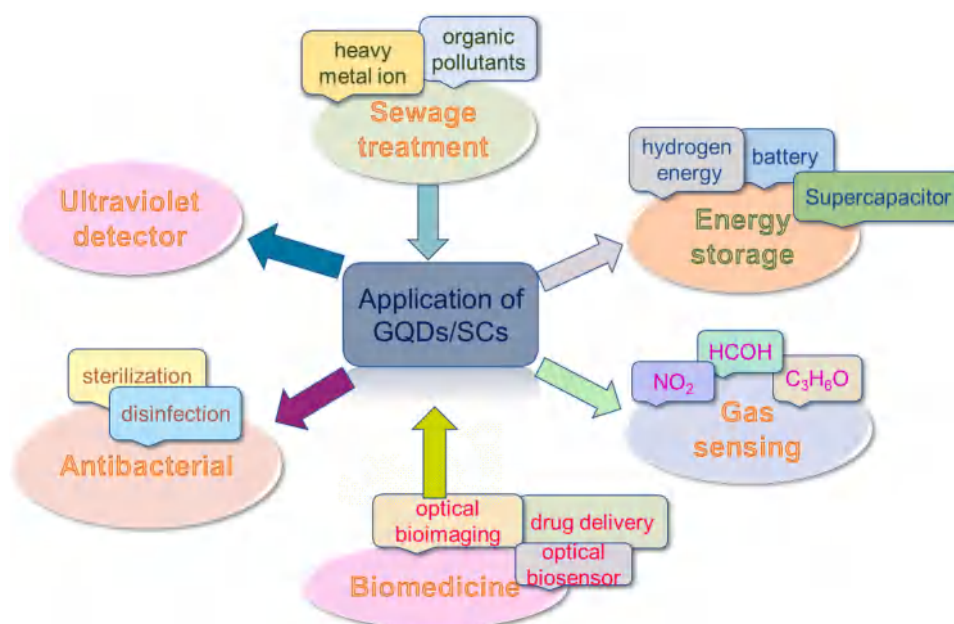


Fig. 9. Applications of GQDs/SCs.

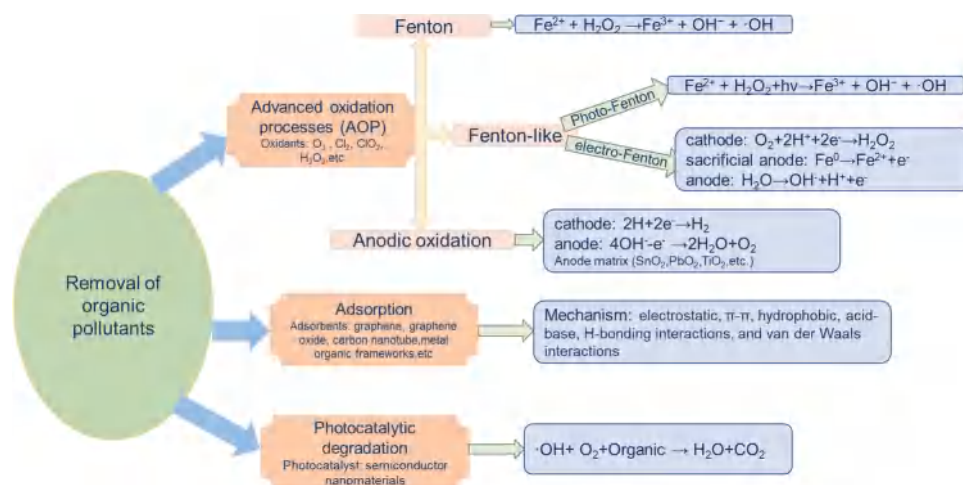


Fig. 10. The method of organic pollutant removal.

degradation of organic pollutants is most effective (Guo et al., 2021). Hao et al. (Hao et al., 2016) found that GQDs/Bi₂MoO₆ was used as mesoporous photocatalyst, degrading organic pollutants in water (BPA, MB, tetracycline (TC), phenol). They also proved photocatalysis technology had good degradation effect on organic pollutants and unique catalytic behavior.

At present, water treatment technologies that can be used to remove toxic ionic pollutants include precipitation, coagulation and liquid extraction (Yue et al., 2015). The above methods can not completely eliminate heavy metal ions. Therefore, photocatalysis can converse ionic pollutants into non-toxic substances (changing ionic valence). And it is an important progress in the removal of inorganic pollutants in water. Compared with organic pollutants, although the types of inorganic pollutants in water are less, they also play roles in harming to water. Kahrizi et al. (Kahrizi et al., 2018) synthesized NiFe₂O₄/hydroxyapatite (HPA)/GQDs as adsorbents and reacted with -COO⁻ and -OH of Cd to remove heavy metal ion Cd (II) in water. In addition to removing Cd (II)

by GQDs/SCs, Cr (VI) can also be removed. Wang et al. (Wang et al., 2017; Wang et al., 2017) found that Fe₂O₃-GQDs /NF-TiO₂ had good reduction activity and stability for Cr (VI). The technology of photo-electrochemical (PEC) could reduce Cr (VI) in water to Cr (III), and removed coexisting organic ions to reduce the harm to water and human body.

In conclusion, GQDs/SCs can be used to remove a large number of organic pollutants (RHB, Mo, MB, BPA, TC, etc.), while the removal of heavy metal ions is only limited to Cd (II) and Cr (VI). At present, the research on the removal of heavy metals by GQDs/SCs is not comprehensive. In the future, the researches on the removal of other toxic heavy metal ions (Pb (II), Hg (I), Ag (I), etc.) can be expanded, so that GQDs/SCs are used more effectively.

4.2. Energy storage

In addition to environmental pollution, the energy crisis is also a

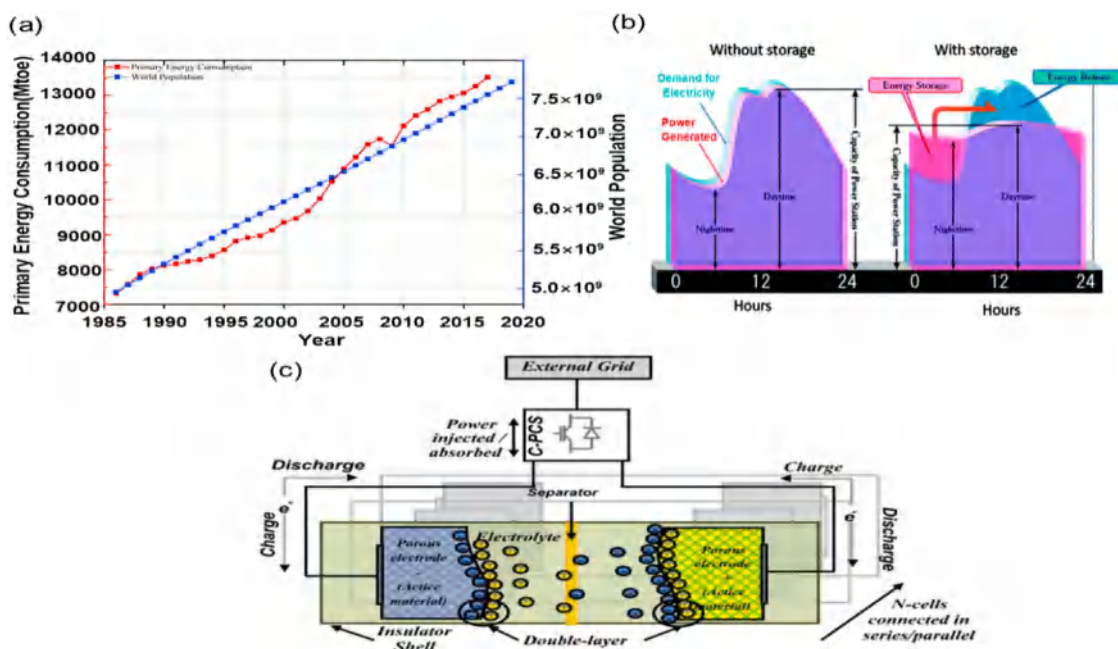


Fig. 11. (a) Year of energy consumption. Reprinted with permission (Olabi et al., 2021). Copyright 2020 Elsevier Ltd.(b) The balance system of battery energy storage. Reprinted with permission (Yang et al., 2011).Copyright 2011 American Chemical Society. (c) The system of Capacitor storage. Reprinted with permission (Kousksou et al., 2014). Copyright 2013 Elsevier B.V.

matter of public concern. Thus, reducing energy consumption and improving energy efficiency has gradually become the consensus of mankind. Moreover, existing energy sources generally include coal, oil, natural gas, coal, nuclear energy, hydropower and renewable energy. In the past decade, energy consumption has increased significantly, but due to the penetration of renewable energy system, the percentage of fossil fuels has gradually decreased (Fig. 11a) (Olabi et al., 2021). And carbon dioxide emissions from fossil fuels lead to global warming, so the reserve of renewable energy has attracted the attention of people. Photocatalytic storage of clean energy has become the research hotspot in field of energy storage (Wang and Domen, 2020; Hisatomi and Domen, 2019; Liu et al., 2020; Lin et al., 2020), and GQDs/SCs have been widely used in energy reserve.

4.2.1. Storage in the form of hydrogen energy

As a renewable energy, hydrogen energy overcomes the shortcomings of traditional fossil energy and has made great progress in generation and storage. It includes hydrogen or hydrocarbons extracted directly from the atmosphere, as well as hydrogen storage as compressed gases, cryogenic liquids and compounds. In order to convert the stored energy into work and heat, traditional internal combustion engines and turbines can be used (Züttel et al., 2010). Direct production of hydrogen by solar energy is an environmentally friendly energy storage method (Liu et al., 2020; Dawood et al., 2020; Noor et al., 2021) (Fig. 6a). GQDs/SCs show excellent performance in the photocatalytic production of hydrogen (Liu et al., 2017; Liu et al., 2017; Liu et al., 2017; Liu et al., 2017). Mou et al. (Mou et al., 2019) used N-GQDs/g-C₃N₄ as photocatalyst to generate hydrogen under sunlight and N-GQDs/g-C₃N₄ showed excellent activity and durability, which laid the foundation for photocatalytic energy storage.

4.2.2. Storage in the form of electrochemistry

In addition to the above way of generating clean energy to store energy, the storage of electric energy is also very important. Electric energy is mainly stored in the following five forms: mechanical energy, chemical energy, electrochemistry (battery, supercapacitor), superconducting magnetism and thermal energy (Aneke and Wang, 2016). Among them electrochemical energy storage is more and more widely used in electronic equipment and large-scale power grid. In addition, electrochemical storage usually involves many physical and chemical interactions on the surface and inside of electrode/electrolyte, so the energy storage mechanisms of battery and capacitor are inconsistent. The battery stores charge in the electrode through faradaic reaction, while the capacitor stores charge near the electrolyte surface (electrochemical double-layer capacitor) (Fig. 11b and c) (Liu et al., 2014).

Battery energy storage system has the advantages of rapid response and strong controllability. And it realizes the efficient utilization of electric energy through uninterrupted power supply and transmission upgrade delay (Yang et al., 2018). It includes lithium battery, solar cell, dye-sensitized solar cell (DSSC) and flexible zinc battery (Tsang et al., 2020). Lithium battery is now the most widely used battery in society, it has high energy storage and long life, but it is unsafe (Fan et al., 2020). Yin et al. (Yin et al., 2018) confirmed that NiO/GQDs could reserve energy in the modality of lithium battery. And the diffusion of Li⁺ promoted electron transfer, which made NiO/GQDs have good photoelectric properties, utilizing the photocatalytic energy storage technology effectively. Compared with traditional lithium battery, solar cell has unlimited development potential, and the raw material is environmentally friendly and widely used (Hashemi et al., 2020). Long et al. (Long et al., 2017) confirmed that GQDs/TiO₂ could be used as a raw material for the preparation of solar cell. Through the interface charge transfer, it could promote the conversion of solar energy into electric energy, which laid the foundation for the design of high-performance solar cell. However, at this stage, the cost of solar cell preparation is high, so it can not be widely used. As a new type of solar cell, DSSC can also store energy. Compared with solar cell, it has the characteristics of low cost

and non-toxic, so as to be widely used in industrial production (Sharma et al., 2018). Kumar et al. (Kumar et al., 2019) confirmed that GQDs/TiO₂ could be used to prepare DSSC, GQDs could be used as DSSC anode material. GQDs/TiO₂ had good photoelectric conversion efficiency, which could increase the absorption rate of charge and promote the development of photovoltaic field. With the increasing demand for flexible energy storage devices, flexible zinc air battery appears in the public view. It is a wearable battery with simple preparation process and good safety (Mo et al., 2020). Liu et al. (Liu et al., 2019b) studied the flexible rechargeable zinc air cell with GQDs/NiCo₂S₄/carbon cloth (CC). The composite had good conductivity and softness, excellent electrocatalytic activity and good cycle durability, which provided good prospect for the development of electronic devices.

Supercapacitor has the advantages of simple operation, high efficiency, long cycle life and fast response, but its energy is low (Olabi et al., 2021). Compared with the battery, it has long service life and environmental protection. And it can be used for short-time, high-frequency charge and discharge, high-power output and other occasions. GQDs/SCs can store energy not only in the form of battery, but also in the form of supercapacitor. Luo et al. (Luo et al., 2019) studied that GQDs/NiCo₂O₄ could be assembled into supercapacitor for energy storage. It had high specific capacitance and good stability, which promoted the energy storage by photocatalysis.

GQDs/SCs can store energy in the form of hydrogen energy and electrochemistry (batteries and supercapacitors). Although they have good energy storage efficiency and stable photoelectric performance, they are difficult to be applied in industry. Furthermore, mass load, the amount of electrolyte used, electrode manufacturing (size, shape, spatial arrangement, etc.) affect the carrier transmission efficiency (Wang and Domen, 2020; Wang et al., 2020), which limit the industrial applications of them. In order to expand the application range of GQDs/SCs, the electrochemical performance under industrial conditions should be considered.

4.3. Gas sensing

Air pollution also needs special attention. The monitoring of toxic gases is very important for the prevention and control of air pollution. Therefore, miniature gas sensors with high sensitivity, high selectivity, low cost and low energy consumption are needed to monitor gases in air. Electrochemical sensors (usually using ampere operating principle) and chemiluminescence sensors are often used in atmospheric monitoring, but both need calibration (Buckley et al., 2020). GQDs/SCs combine electricity based monitoring (strong charge transfer response) and light based monitoring (with clear spectral lines), so GQDs/SCs can be well used as gas sensors (Buckley et al., 2020; Xu et al., 2018). By detecting their sensitivity to gas, they can detect NO₂, formaldehyde, acetone and other toxic volatile gases, which can effectively prevent the diffusion of gas and reduce the harm of air pollution.

NO₂ is common pollutant in the air, usually forms combustion sources and vehicle exhaust. It is a toxic gas causing acid rain which is harmful to animals and plants. Therefore, it is necessary to detect NO₂ (Khreis et al., 2017). Besides, absorption spectroscopy and photoacoustic spectroscopy are commonly used to measure the concentration of atmospheric NO₂ (Al-Jalal et al., 2019). Lv et al. (Lv et al., 2020) modified N-GQDs into In₂O₃ to prepare NO₂ gas sensor and detected its response to NO₂. The result showed that the composite material could detect ppb-level NO₂, which had guiding significance for the construction of new gas sensors (Fig. 12a).

Formaldehyde (HCHO) is a kind of poisonous volatile gas in indoor air and easy to harm human respiratory tract (Nielsen et al., 2017). Moreover, the methods for measuring HCHO include traditional passive sampling technology and advanced remote sensing technology. GQDs/SCs can be used as gas sensor to monitor the toxic HCHO in the atmosphere, which are significant to human health (Fig. 12b). Chen et al. (Chen et al., 2020; Chen et al., 2020) confirmed that GQDs/SnO₂

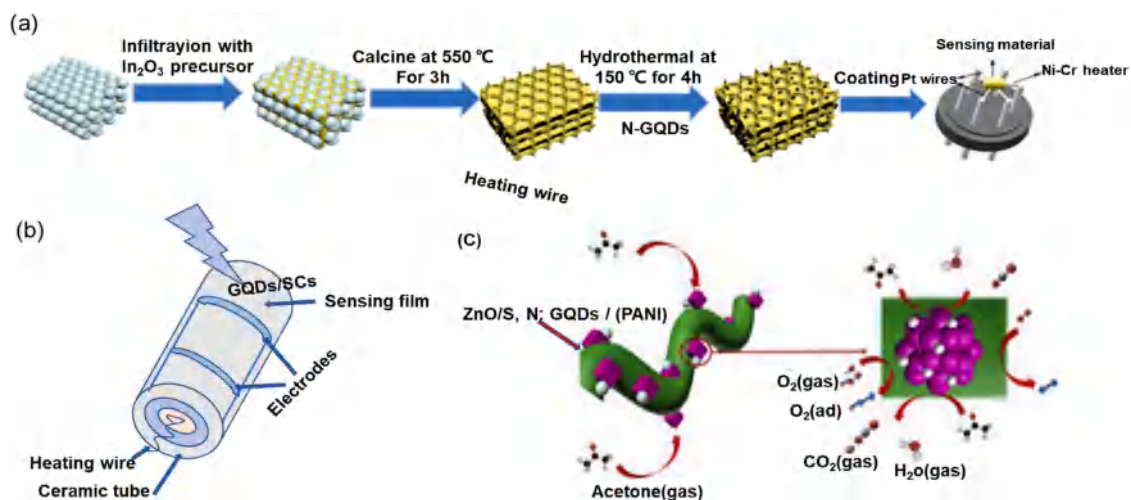


Fig. 12. (a) The synthesis of N-GQDs/In₂O₃ Sensor. Reprinted with permission (Lv et al., 2020). Copyright 2020 American Chemical Society. (b) GQDs/SC sensor of structure. (c) Mechanism diagram of the ZnO/S, N:GQDs/PANI toward acetone sensing. Reprinted with permission (Zhang et al., 2019). Copyright 2019 Elsevier B.V.

could be used as a gas sensor for HCHO detection. The composite could increase the sensitivity of the active sites of nano plates, effectively adjust the electrical properties, and increase the applications of photocatalyst in the sensing field.

Acetone (C₃H₆O) is also a volatile toxic gas, which has adverse effects on the environment and human body. And the sensor with large detection range and low detection limit can effectively monitor acetone gas and prevent toxic gas from polluting the environment and endangering health. Therefore, the monitoring of acetone is significant to environmental monitoring and disease diagnosis (Su et al., 2020). In addition, acetone in the environment can be determined by gas chromatography (Qin et al., 1997). Zhang et al. (Zhang et al., 2019) prepared ZnO/S,N:GQDs/polyaniline (PANI) thin film sensor on polyethylene terephthalate (PET) substrate, which could detect acetone at room temperature (Fig. 12c). The sensor played an important role in industrial

production, environmental monitoring and leakage of volatile toxic chemical gases.

GQDs/SCs have great application potential in sensor field. They have good stability and circulation, monitoring toxic gases in the atmosphere, and play certain roles in environmental protection. However, there is no relevant research on the removal of toxic gases by GQDs/SCs at present. In the future, we can increase the research on this aspect, so that GQDs/SCs can be effectively used.

4.4. Ultraviolet detector

There are many kinds of ultraviolet detectors. Among them solid-state UV detectors are semiconductor-based UV detectors (photoconductive UV detector and photovoltaic UV detector), which can effectively detect UV by converting optical signal into electrical signal

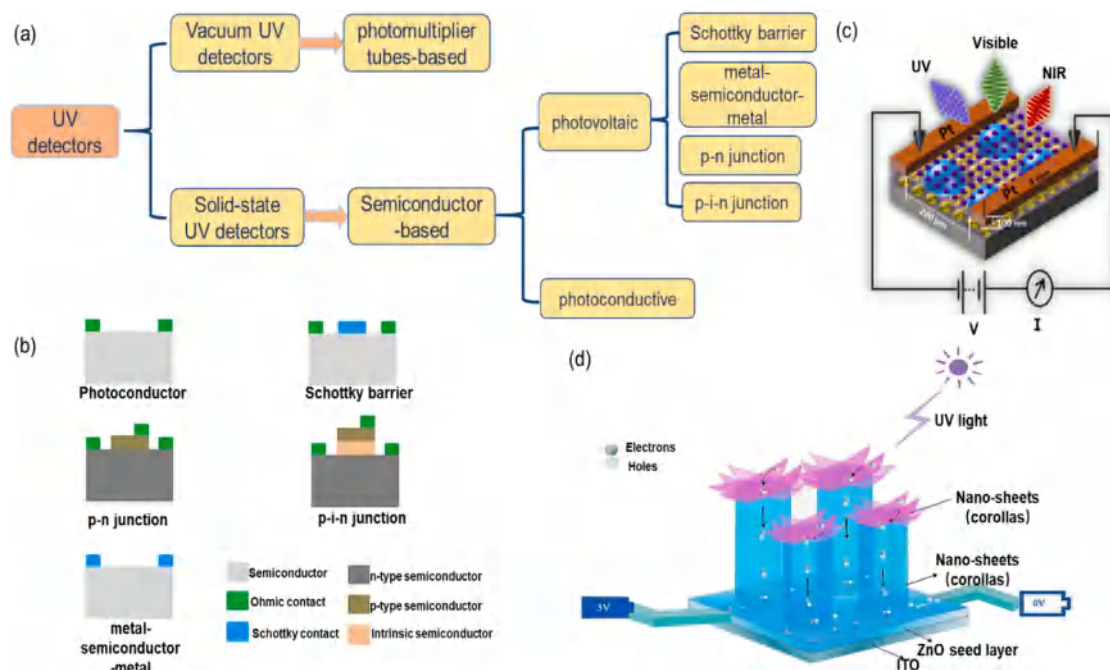


Fig. 13. (a) The classification of UV detector. (b) Schematic structure of UV photovoltaic detector. Reprinted with permission (Zou et al., 2018). Copyright 2018 MDPI. (c) Schematic of hybrid photodetector. Reprinted with permission (Kunwar et al., 2021). Copyright 2021 American Chemical Society. (d) The process of photo-generated electron-hole transmission. Reprinted with permission (Wu et al., 2020; Wu et al., 2020). Copyright 2020 Elsevier Ltd and Techna Group S.r.l.

(Fig. 13a and b). GQDs/SCs can be used to synthesize UV detectors with good stability and ultrafast response. And their structure can greatly improve the sensitivity of sensors with various quantum effects. Wu et al. (Wu et al., 2020; Wu et al., 2020) proved that ZnO/GQDs formed a weak UV photovoltaic detector. Wide bandgap ZnO could absorb weak ultraviolet radiation, and the doping of GQDs established its electron hole transmission path (Fig. 13d). At the same time, a weak UV signal acquisition and voltage conversion system were developed to realize the photoelectric conversion of weak UV signal. GQDs/SCs can prepare not only photovoltaic UV detectors, but also photoconductive detectors. When the light matches the resonance frequency of surface plasmon, the phenomenon of local field enhancement (scattering) occurs, so as to enhance the spectral response (Wu et al., 2018). Therefore, surface plasmon is an effective way to improve the sensitivity of semiconductor-based UV detector. Kunwar et al. (Kunwar et al., 2021) confirmed that plasmon could greatly enhance UV detection performance (Fig. 13c). The UV response of GQDs/TiO₂/plasma hybrid nanoparticles (HNPs) photoelectric UV detector was 95 times higher than that of TiO₂ alone. At the same time, with the increase of photocurrent, the optical response region could be extended to the visible and near-infrared regions.

GQDs/SCs can prepare semiconductor-based UV detectors (photovoltaic detectors or photoconductive detectors). And the prepared UV detectors have the advantages of low cost, high sensitivity and fast response. Moreover, combining some UV sensitive materials in a single nanostructure can greatly enhance the photoelectric detection performance. Therefore, the introduction of plasma nanostructures is the most effective means to improve the optical response rate, detection rate and quantum efficiency of photodetectors. However, UV detectors are only used in military. Therefore, expanding applications of GQDs/SCs in UV detection (industrial, commercial, etc.) is the focus in the future.

4.5. Antibiosis

The fields of antibiosis include disinfection and sterilization. And photocatalytic technology has been widely used in the field of antibacterial, which can remove microbial pollutants (pathogens and bacteria). These microorganisms endanger human health and effective remove them can prevent diseases and improve human immunity (McGuigan et al., 2012; Sajjad et al., 2017).

Disinfection has a certain effect on inhibiting microorganisms and it is an important step in sewage treatment. Traditional disinfection methods, including physical methods (radiation and heating) and chemical methods (chlorine (Cl), ultraviolet (UV) and ozone), have been widely used in the field of antibiosis (Miao et al., 2019). However, their energy consumption is high and their disinfection by-products are still toxic. Therefore, green photocatalytic disinfection technology has been effectively applied. And photocatalytic disinfection using the generated reactive oxygen species (ROS) is a common method, which can reduce the number of microorganisms to the appropriate level previously

specified (McDonnell and Burke, 2011). Xu et al. (Xu et al., 2020) synthesized graphene oxide quantum dots (ox-GQDs)/oxidized nanopore g-C₃N₄ (PCNO) for photocatalytic disinfection of pathogens. Then they used 5,5-dimethyl-1-pyrroline-n-oxide (DMPO) as free radical scavenger to analysis ROS by electron spin resonance (ESR), and it showed that H⁺, •O₂⁻, and •OH had high efficiency in inactivating pathogens, and could inactivate 99.6% of *Escherichia coli* (Fig. 14a).

Unlike disinfection, which only requires the inactivation of microorganisms, sterilization needs to kill bacteria (Panchal et al., 2020). There are many sterilization methods, physical methods (dry heat, damp heat, etc.) and chemical methods (hypochlorite solution, hydrogen peroxide steam, ethylene oxide gas, etc.) (Redigueri et al., 2016). Furthermore, GQDs/SCs have large specific surface area and good water solubility. They can be used as antibacterial material for sterilization. Teymourinia et al. (Teymourinia et al., 2019b) prepared Cu₂O/GQDs as a new antibacterial material, and studied its antibacterial activity against Gram-negative bacteria (such as *Escherichia coli*) and Gram-positive bacteria (such as *Staphylococcus aureus*). The result showed that the flower-like complex had the best antibacterial effect (Fig. 14b). At present, antibacterial materials are mainly copper and silver-based materials, which have great toxicity. Therefore, the use of non-toxic GQDs/SCs as antibacterial materials will be the main direction in the future research.

Most of GQDs/SCs used for antibiosis are toxic. At present, the research of non-toxic GQDs/SCs antibacterial materials is not perfect. Moreover, most studies on antibacterial activity use Gram-positive and Gram-negative bacteria, while there are few studies on viruses, fungi and even parasites. In the future, we can strengthen the research on the disinfection performance of non-toxic antibacterial materials against viruses, fungi and even parasites.

4.6. Biomedicine

At present, the researches of biosensor, biological imaging and drug delivery have always been hot spots in the field of biomedical diagnosis. Moreover, the crystalline or amorphous structure of nanocomposites can effectively improve the properties of biomaterials (Jian et al., 2020). GQDs/SCs are selective to molecules and can penetrate tissues or be cleared by cells. Therefore, they provide great opportunities in biomedical fields such as fluorescent biosensors, photobiological imaging, treatment and drug delivery.

The introduction of nano materials promotes the diversity of biosensors to a certain extent, such as electrochemical biosensors, fluorescent biosensors, electrochemiluminescence biosensors and colorimetric biosensors (Ge et al., 2019). Among them fluorescent biosensor can better express the signal, and quantitatively analyze the target according to the generated fluorescent signal (enhancement or quenching) (Jung and Chen, 2018). Besides, fluorescent biosensor can prevent the spread of diseases from the route of transmission. GQDs/SCs can be used as fluorescent biosensor for disease monitoring (Pang et al., 2017).

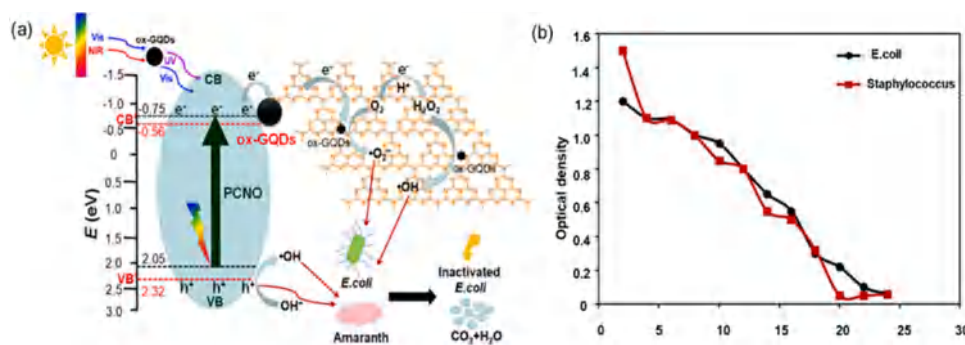


Fig. 14. (a) Mechanism diagram of active oxygen species for disinfection. Reprinted with permission (Xu et al., 2020). Copyright 2020 Elsevier B.V. (b) Optical density for growing *E. coli* and *Staphylococcus* for flower-like Cu₂O/GQDs. Reprinted with permission (Teymourinia et al., 2019b). Copyright 2019 Elsevier Ltd.

Ganganboina et al. (Ganganboina et al., 2018) studied N-QDs/ V_2O_5 as fluorescent biosensor probe, which had good sensitivity and specificity, and could be used to detect cysteine (fluorescence intensity recovery) (Fig. 15a). It was conducive to disease monitoring and diagnosis, and laid a foundation for the detection of organic compounds by sensor probe. Shi et al. (Shi et al., 2017) studied that GQDs/ MoS_2 could also be used as fluorescent biosensor to detect cancer cells.

Many imaging technologies, such as optical imaging, thermal imaging, photoacoustic imaging, magnetic resonance imaging and ultrasound imaging, have been successfully used in clinic (Ge et al., 2019). In addition, fluorescent probes of optical imaging have attracted much attention because of their superior performance, and replaced organic dyes or fluorescent proteins in intracellular sensors (Zrazhevskiy et al., 2010). Through surface functionalization, these 0D/2D materials can be transported to cancer cells, monitoring the internal and external physiological functions of organisms (Li et al., 2012) (Fig. 15b). Furthermore, up-conversion nanoparticles are often used in optical biological imaging, emitting higher energy detectable photons under infrared light. Therefore, the near infrared (GQDs/SCs) can be used as a biological imaging probe for disease monitoring. Song et al. (Song et al., 2018) found that the near-infrared MnO_2 /GQDs fluorescence system could be used for near-infrared fluorescence imaging of intracellular glutathione, targeted analysis *in vivo* and *in vitro*, which laid a foundation for the detection of tumor cells.

These studies confirmed that optical biosensors and biological imaging can be used for disease monitoring. Yao et al. (Yao et al., 2017b) found that GQDs/mesoporous silica nanoparticles (MSNs) could be used for disease treatment, having the potential of synergistic photothermal therapy. This research made biomedical researches from disease monitoring to disease treatment, and promoted biomedical development.

Drug delivery is an important step in the treatment of diseases. Drug carriers based on nano materials can deliver drugs and also can control space and time of delivery well. Moreover, some mechanical techniques

(such as microinjection, electroporation, chemical transfection and ligand mediated uptake) have been used to effectively transport macromolecules in cells (Zrazhevskiy et al., 2010). In recent years, non-mechanical methods have become more and more popular because of the minimum interference of high-throughput quantum dot intracellular drug delivery to cell physiology (Fig. 15c). Su et al. (Su et al., 2017) found GQDs/ $Fe_3O_4@SiO_2$ based opto-magnetic probe that could be used for drug delivery and dual-mode imaging, which was significant to tumor detection and treatment (Fig. 15d). In addition, the combination of biological monitoring and treatment makes GQDs/SCs have far-reaching practical significance in biomedicine.

Layered composites have large surface area, excellent physico-chemical properties and photoelectric properties. GQDs/(2D SCs) are the layered composite with biocompatibility and biological function, which are widely used in biomedicine. They can monitor human health status and find potential diseases in time, which are convenient for people to suit the remedy to the case. At the same time, they promote the development of biology and medicine, having broad prospects.

5. Summary and perspectives

In a word, the shape and edge states of GQDs depend on their size and affect electronic structure and optical properties. Excluding the effects of sp^2 structure and functional groups, the luminescence performance of GQDs is better expressed, bringing a new breakthrough in the field of catalysis. This work reviews the synthesis methods of GQDs/SCs, including bottom-up methods such as hydrothermal method, improved hydrothermal method, self-assembly method, top-down methods such as impregnation method, chemical vapor deposition method and freeze-drying method. Although the bottom-up is a common method for the synthesis of GQDs/SCs, the top-down is more convenient. GQDs can effectively improve photocatalytic performance, such as acting as electron acceptor/donor, photosensitizer, electron transfer accelerator,

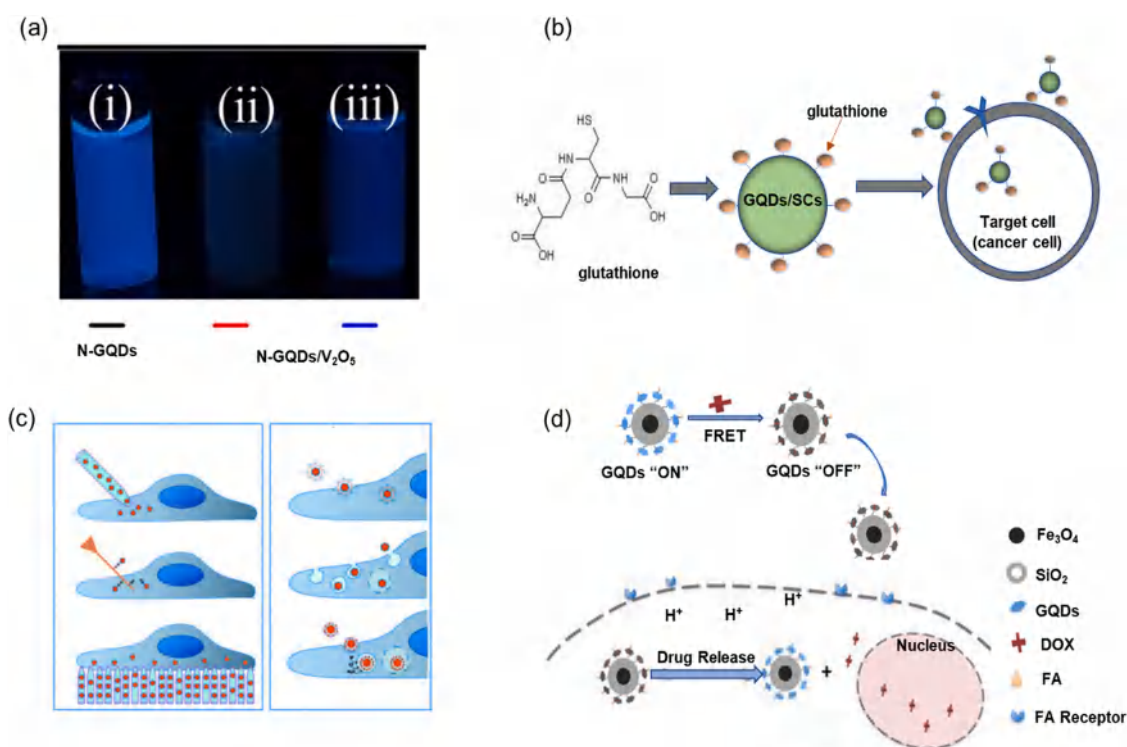


Fig. 15. (a) Fluorescence color under 365 nm UV. Reprinted with permission (Ganganboina et al., 2018). Copyright 2017 American Chemical Society. (b) the mechanism of biological imaging. (c) Mechanical (left) and non-mechanical (right) pathways for intracellular delivery of GQDs. Reprinted with permission (Zrazhevskiy et al., 2010). Copyright 2010 Royal Society of Chemistry. (d) GQDs is donor molecule and DOX is receptor molecule for drug delivery. Reprinted with permission (Su et al., 2017). Copyright 2016 Elsevier B.V.

synergistic effect, forming electric field or increasing contact area. Among them synergistic effect is the main mechanism to improve the photocatalytic activity, and most GQDs/SCs with heterojunction improve the photocatalytic activity by forming electric field. Due to their excellent photoelectric properties and biocompatibility, GQDs/SCs have potential applications in sewage treatment, energy storage, gas sensing, UV detection, antibiosis and biomedicine. And there are more researches on energy storage, antibacterial and biomedicine than other fields. In recent years, the researches have made some progress, but GQDs/SCs still face great challenges in industrial production and pollutant degradation, and further research is needed in the future.

1. Improve the synthesis method. The current synthesis method can't meet the large-scale production. Moreover, the shape of GQDs is difficult to accurately control, and the particle size is too large or too small can limit their applications in industry. Therefore, the synthesis route can be optimized and the cost can be controlled by controlling the factors affecting the synthetic strategy of GQDs/SCs (shape, size and surface effect). In addition, improving the operating conditions (temperature, pH and humidity) is also an effective method to make GQDs/SCs mass-produced and effectively applied in industry.
2. Rich the structure types. At present, the porous structure is the common structure of GQDs/SCs. And the porous structure can make GQDs and SCs contact closely and promote electron transfer. However, too much GQDs are combined with porous SCs can block the pores, reducing the contact area between them and affecting the improvement of photocatalytic efficiency. Therefore, the structural types (spherical, linear, janus) can be enriched by controlling the synthesis process to prepare small-size materials. Small size materials greatly increase the active center, effectively promote the photocatalytic activity and make the structure diversify.
3. Strengthen the van der Waals heterostructure construction. Most of van der Waals heterojunctions exist in 2D/2D materials. And van der Waals heterojunctions can exist in materials with low energy consumption and freedom. Strengthen the construction of non-2D heterostructures, such as GQDs/SCs (0D/2D), study whether van der Waals heterostructures can be formed, discover new functions of GQDs/SCs, and promote photocatalysis.
4. Reduce secondary pollution. When GQDs/SCs are used to remove pollutants, they may produce other toxic substances, such as thermoplastics and NO₂, harming to water. Furthermore, we can expand the photocatalysis method, using photocatalysis combined with Fenton method, or cooperative electrocatalysis method to reduce the generation of secondary pollutants. It is better to recycle the secondary pollutants and turn waste into treasure to meet the requirements of environmental protection.
5. Broaden the application scope of GQDs/SCs. In recent years, the research on the removal of pollutants by GQDs/SCs mainly exists in wastewater, which plays certain roles in solving environmental problems. However, the actual composition of wastewater is complex, and there are many kinds of pollutants, so we can increase the research on a variety of pollutants in wastewater, not just a single pollutant. In addition, there is no research on GQDs/SCs used to solve soil pollution, so it is necessary to expand the role of GQDs/SCs in soil remediation. Although GQDs/SCs can be used to prepare gas sensors, they only play role in detection, and there is no way to remove them. We should further increase the use of solar energy, explore GQDs/SCs photocatalytic CO₂ reduction, formaldehyde removal and so on.
6. Combine with theoretical calculation. Exchange correlation (XC) functional based on local density approximation (LDA) and generalized gradient approximation (GGA) are traditional DFT. DFT calculation can better study electron localization and improve the calculated energy band gap. Therefore, the conclusion is more reliable by the combination of experiment and calculation.

Declaration of Competing Interest

The authors declare that they have no known competing financial interests or personal relationships that could have appeared to influence the work reported in this paper.

Acknowledgements

The study was financially supported by the National Natural Science Foundation of China (51979103, 51909085, 51679085), the Program for Changjiang Scholars and Innovative Research Team in University (IRT-13R17), the Funds of Hunan Science and Technology Innovation Project (2018RS3115, 2020RC5012), the Key Research and Development Project of Hunan Province of China (2017SK2241), Natural Science Foundation of Hunan Province, China (2020JJ5069).

References

- Aguilera-Sigalat, J., Bradshaw, D., 2016. Synthesis and applications of metal-organic framework-quantum dot (QD at MOF) composites. *Coord. Chem. Rev.* 307, 267–291. <https://doi.org/10.1016/j.ccr.2015.08.004>.
- Al-Jalal, A.A., Al-Basheer, W., Gasmi, K., Romadhon, M.S., 2019. Measurement of low concentrations of NO₂ gas by differential optical absorption spectroscopy method. *Meas.: J. Int. Meas. Confed.* 146, 613–617. <https://doi.org/10.1016/j.measurement.2019.07.022>.
- Ambrosi, A., Chua, C.K., Bonanni, A., Pumera, M., 2014. Electrochemistry of graphene and related materials. *Chem. Rev.* 114, 7150–7188. <https://doi.org/10.1021/cr500023c>.
- Aneke, M., Wang, M., 2016. Energy storage technologies and real life applications – A state of the art review. *Appl. Energy* 179, 350–377. <https://doi.org/10.1016/j.apenergy.2016.06.097>.
- Aris, R., 1985. The distribution of active ingredients in supported catalysts prepared by impregnation. *Catal. Rev.* 27, 207–340. <https://doi.org/10.1080/01614948508064737>.
- Basavarajappa, P.S., Patil, S.B., Ganganagappa, N., Reddy, K.R., Raghu, A.V., Reddy, C. V., 2020. Recent progress in metal-doped TiO₂, non-metal doped/codoped TiO₂ and TiO₂ nanostructured hybrids for enhanced photocatalysis. *Int. J. Hydrog. Energy* 45, 7764–7778. <https://doi.org/10.1016/j.ijhydene.2019.07.241>.
- Beran, G.J.O., 2016. Modeling polymorphic molecular crystals with electronic structure theory. *Chem. Rev.* 116, 5567–5613. <https://doi.org/10.1021/acs.chemrev.5b00648>.
- Bokare, A., Chinnusamy, S., Erogbogbo, F., 2021. TiO₂-graphene quantum dots nanocomposites for photocatalysis in energy and biomedical applications. *Catalysts* 11, 1–51. <https://doi.org/10.3390/catal11030319>.
- Bonaccorso, F., Colombo, L., Yu, G., Stoller, M., Tozzini, V., Ferrari, A.C., Ruoff, R.S., Pellegrini, V., 2015. Graphene, related two-dimensional crystals, and hybrid systems for energy conversion and storage. *Science* 347, 1246501. <https://doi.org/10.1126/science.1246501>.
- Boyce, J.M., 2016. Modern technologies for improving cleaning and disinfection of environmental surfaces in hospitals. *Antimicrob. Resist. Infect. Control* 5. <https://doi.org/10.1186/s13756-016-0111-x>.
- Buchalska, M., Kunczewicz, J., Świątek, E., Labuz, P., Baran, T., Stochel, G., Macyk, W., 2013. Photoinduced hole injection in semiconductor-coordination compound systems. *Coord. Chem. Rev.* 257, 767–775. <https://doi.org/10.1016/j.ccr.2012.09.017>.
- Buckley, D.J., Black, N.C.G., Castanon, E.G., Melios, C., Hardman, M., Kazakova, O., 2020. Frontiers of graphene and 2D material-based gas sensors for environmental monitoring. *2D Mater.* 7, 032002. <https://doi.org/10.1088/2053-1583/ab7bc5>.
- Burnett, B.J., Choe, W., 2012. Sequential self-assembly in metal-organic frameworks. *Dalton Trans.* 41, 3889–3894. <https://doi.org/10.1039/c2dt12103d>.
- Buzzetti, L., Crisenza, G.E.M., Melchiorre, P., 2019. Mechanistic Studies in Photocatalysis. *Angew. Chem. - Int. Ed.* 58, 3730–3747. <https://doi.org/10.1002/anie.201809984>.
- Cao, S., Yu, J., 2016. Carbon-based H₂-production photocatalytic materials. *J. Photochem. Photobiol. C: Photochem. Rev.* 27, 72–99. <https://doi.org/10.1016/j.jphotochemrev.2016.04.002>.
- Chen, F., Liu, L.L., Zhang, Y.J., Wu, J.H., Huang, G.X., Yang, Q., Chen, J.J., Yu, H.Q., 2020. Enhanced full solar spectrum photocatalysis by nitrogen-doped graphene quantum dots decorated BiO_{2-x} nanosheets: Ultrafast charge transfer and molecular oxygen activation. *Appl. Catal. B: Environ.* 277, 119218. <https://doi.org/10.1016/j.apcatb.2020.119218>.
- Chen, W., Lv, G., Hu, W., Li, D., Chen, S., Dai, Z., 2018. Synthesis and applications of graphene quantum dots: A review. *Nanotechnol. Rev.* 7, 157–185. <https://doi.org/10.1515/ntrev-2017-0199>.
- Chen, Z., Wang, D., Wang, X., Yang, J., 2020. Preparation and formaldehyde sensitive properties of N-GQDs/SnO₂ nanocomposite. *Chin. Chem. Lett.* 31, 2063–2066. <https://doi.org/10.1016/j.ccllet.2019.11.043>.
- Cheng, F., Yin, H., Xiang, Q., 2017. Low-temperature solid-state preparation of ternary CdS/g-C₃N₄/CuS nanocomposites for enhanced visible-light photocatalytic H₂-production activity. *Appl. Surf. Sci.* 391, 432–439. <https://doi.org/10.1016/j.apsusc.2016.06.169>.

- Cheng, L., Dong, X., 2020. Carbonaceous 0D/2D composite photocatalyst for degradation of organic dyes. *Diam. Relat. Mater.* 109, 108096 <https://doi.org/10.1016/j.diamond.2020.108096>.
- Cheng, L., Zhang, H., Li, X., Fan, J., Xiang, Q., 2021. Carbon-graphitic carbon nitride hybrids for heterogeneous photocatalysis. *Small* 17, 2005231. <https://doi.org/10.1002/sml.202005231>.
- Cherevan, A.S., Deilmann, L., Weller, T., Eder, D., Marschall, R., 2018. Mesoporous Semiconductors: A New Model to Assess Accessible Surface Area and Increased Photocatalytic Activity? *ACS Appl. Energy Mater.* 1, 5787–5799. <https://doi.org/10.1021/acsaem.8b01123>.
- Cho, I., Koshika, M., Wagner, P., Koumura, N., Innis, P.C., Mori, S., Mozer, A.J., 2018. Exploiting Intermolecular Interactions between Alkyl-Functionalized Redox-Active Molecule Pairs to Enhance Interfacial Electron Transfer. *J. Am. Chem. Soc.* 140, 13935–13944. <https://doi.org/10.1021/jacs.8b09070>.
- Choi, S.H., 2017. Unique properties of graphene quantum dots and their applications in photonic/electronic devices. *J. Phys. D: Appl. Phys.* 50, 103002 <https://doi.org/10.1088/1361-6463/aa5244>.
- Chtouki, T., El Mrabet, M., Tarbi, A., Goncharova, I., Erguig, H., 2021. Comprehensive review of the morphological, linear and nonlinear optical characterization of spin-coated NiO thin films for optoelectronic applications. *Opt. Mater.* 118, 111294 <https://doi.org/10.1016/j.optmat.2021.111294>.
- Ciriminna, R., Fidalgo, A., Pandarus, V., Béland, F., Ilharco, L.M., Pagliaro, M., 2013. The sol-gel route to advanced silica-based materials and recent applications. *Chem. Rev.* 113, 6592–6620. <https://doi.org/10.1021/cr300399c>.
- Colherinhas, G., Fileti, E.E., Chaban, V.V., 2015. Can inorganic salts tune electronic properties of graphene quantum dots? *Phys. Chem. Chem. Phys.* 17, 17413–17420. <https://doi.org/10.1039/c5cp02083b>.
- Dawood, F., Anda, M., Shafiqullah, G.M., 2020. Hydrogen production for energy: An overview. *Int. J. Hydrog. Energy* 45, 3847–3869. <https://doi.org/10.1016/j.ijhydene.2019.12.059>.
- Di, T., Xu, Q., Ho, W.K., Tang, H., Xiang, Q., Yu, J., 2019. Review on metal sulphide-based Z-scheme photocatalysts. *ChemCatChem* 11, 1394–1411. <https://doi.org/10.1002/cctc.201802024>.
- Ding, Y., Yang, I.S., Li, Z., Xia, X., Lee, W.I., Dai, S., Bahnemann, D.W., Pan, J.H., 2020. Nanoporous TiO₂ spheres with tailored textural properties: Controllable synthesis, formation mechanism, and photochemical applications. *Prog. Mater. Sci.* 109 <https://doi.org/10.1016/j.pmatsci.2019.100620>.
- Du, Y., Guo, S., 2016. Chemically doped fluorescent carbon and graphene quantum dots for bioimaging, sensor, catalytic and photoelectronic applications. *Nanoscale* 8, 2532–2543. <https://doi.org/10.1039/c5nr07579c>.
- Ebrahimi, M., Samadi, M., Yousefzadeh, S., Soltani, M., Rahimi, A., Chou, T.C., Chen, L.C., Chen, K.H., Moshfegh, A.Z., 2017. Improved solar-driven photocatalytic activity of hybrid graphene quantum dots/ZnO nanowires: A direct z-scheme mechanism. *ACS Sustain. Chem. Eng.* 5, 367–375. <https://doi.org/10.1021/acscuschemeng.6b01738>.
- Fan, E., Li, L., Wang, Z., Lin, J., Huang, Y., Yao, Y., Chen, R., Wu, F., 2020. Sustainable Recycling Technology for Li-Ion Batteries and Beyond: Challenges and Future Prospects. *Chem. Rev.* 120, 7020–7063. <https://doi.org/10.1021/acs.chemrev.9b00535>.
- Fang, H., Battaglia, C., Carraro, C., Nemsak, S., Ozdol, B., Kang, J.S., Bechtel, H.A., Desai, S.B., Kronast, F., Unal, A.A., Conti, G., Conlon, C., Palsson, G.K., Martin, M.C., Minor, A.M., Fadley, C.S., Yablonovitch, E., Maboudian, R., Javey, A., 2014. Strong interlayer coupling in van der Waals heterostructures built from single-layer chalcogenides. *Proc. Natl. Acad. Sci. USA* 111, 6198–6202. <https://doi.org/10.1073/pnas.1405435111>.
- Fang, M.J., Tsao, C.W., Hsu, Y.J., 2020. Semiconductor nanoheterostructures for photoconversion applications. *J. Phys. D: Appl. Phys.* 53 <https://doi.org/10.1088/1361-6463/ab5f25>.
- Feng, C., Deng, Y., Tang, L., Zeng, G., Wang, J., Yu, J., Liu, Y., Peng, B., Feng, H., Wang, J., 2018. Core-shell Ag₂CrO₄/N-GQDs@g-C₃N₄ composites with anti-photocorrosion performance for enhanced full-spectrum-light photocatalytic activities. *Elsevier*. <https://doi.org/10.1016/j.apcatb.2018.08.049>.
- Feng, L., van Hullebusch, E.D., Rodrigo, M.A., Esposito, G., Oturan, M.A., 2013. Removal of residual anti-inflammatory and analgesic pharmaceuticals from aqueous systems by electrochemical advanced oxidation processes. A review. *Chem. Eng. J.* 228, 944–964. <https://doi.org/10.1016/j.cej.2013.05.061>.
- Fujishima, A., Honda, K., 1972. Electrochemical photolysis of water at a semiconductor electrode. *Nature* 238, 37–38. <https://doi.org/10.1038/238037a0>.
- Ganganboina, A.B., Dutta Chowdhury, A., Doong, R.A., 2018. N-Doped Graphene Quantum Dots-Decorated V₂O₅ Nanosheet for Fluorescence Turn Off-On Detection of Cysteine. *ACS Appl. Mater. Interfaces* 10, 614–624. <https://doi.org/10.1021/acsaami.7b15120>.
- Gao, Y., Hou, F., Hu, S., Wu, B., Wang, Y., Zhang, H., Jiang, B., Fu, H., 2018a. Graphene Quantum-Dot-Modified Hexagonal Tubular Carbon Nitride for Visible-Light Photocatalytic Hydrogen Evolution. *ChemCatChem* 10, 1330–1335. <https://doi.org/10.1002/cctc.201701823>.
- Gao, Y., Hou, F., Hu, S., Wu, B., Wang, Y., Zhang, H., Jiang, B., Fu, H., 2018b. Graphene Quantum-Dot-Modified Hexagonal Tubular Carbon Nitride for Visible-Light Photocatalytic Hydrogen Evolution. *ChemCatChem* 10, 1330–1335. <https://doi.org/10.1002/cctc.201701823>.
- Gawande, M.B., Goswami, A., Asefa, T., Guo, H., Biradar, A.V., Peng, D.L., Zboril, R., Varma, R.S., 2015. Core-shell nanoparticles: synthesis and applications in catalysis and electrocatalysis. *Chem. Soc. Rev.* 44, 7540–7590. <https://doi.org/10.1039/c5cs00343a>.
- Ge, X., Xia, Z., Guo, S., 2019. Recent Advances on Black Phosphorus for Biomedicine and Biosensing. *Adv. Funct. Mater.* 29 <https://doi.org/10.1002/adfm.201900318>.
- Ghosh, D., Kapri, S., Bhattacharyya, S., 2016. Phenomenal Ultraviolet Photoresponsivity and Detectivity of Graphene Dots Immobilized on Zinc Oxide Nanorods. *ACS Appl. Mater. Interfaces* 8, 35496–35504. <https://doi.org/10.1021/acsaami.6b13037>.
- Gordillo-Vázquez, F.J., Herrero, V.J., Tanarro, I., 2007. From carbon nanostructures to new photoluminescence sources: An overview of new perspectives and emerging applications of low-pressure PECVD. *Chem. Vap. Depos.* 13, 267–279. <https://doi.org/10.1002/cvde.200604034>.
- Guo, B., Yu, K., Li, H., Qi, R., Zhang, Y., Song, H., Tang, Z., Zhu, Z., Chen, M., 2017. Coral-shaped MoS₂ decorated with graphene quantum dots performing as a highly active electrocatalyst for hydrogen evolution reaction. *ACS Appl. Mater. Interfaces* 9, 3653–3660. <https://doi.org/10.1021/acsaami.6b14035>.
- Guo, Z., Ni, S., Wu, H., Wen, J., Li, X., Tang, T., Li, M., Liu, M., 2021. Designing nitrogen and phosphorus co-doped graphene quantum dots/g-C₃N₄ heterojunction composites to enhance visible and ultraviolet photocatalytic activity. *Appl. Surf. Sci.* 548, 149211 <https://doi.org/10.1016/j.apsusc.2021.149211>.
- Gupta, B.K., Kedawat, G., Agrawal, Y., Kumar, P., Dwivedi, J., Dhawan, S.K., 2015. A novel strategy to enhance ultraviolet light driven photocatalysis from graphene quantum dots infiltrated TiO₂ nanotube arrays. *RSC Adv.* 5, 10623–10631. <https://doi.org/10.1039/c4ra14039g>.
- Ham, S., Kim, Y., Park, M.J., Hong, B.H., Jang, D.J., 2016. Graphene quantum dots-decorated ZnS nanobelts with highly efficient photocatalytic performances. *RSC Adv.* 6, 24115–24120. <https://doi.org/10.1039/c5ra28026e>.
- Han, M., Zhu, S., Lu, S., Song, Y., Feng, T., Tao, S., Liu, J., Yang, B., 2018. Recent progress on the photocatalysis of carbon dots: Classification, mechanism and applications. *Nano Today* 19, 201–218. <https://doi.org/10.1016/j.nantod.2018.02.008>.
- Hao, Y., Dong, X., Wang, X., Zhai, S., Ma, H., Zhang, X., 2016. Controllable electrostatic self-assembly of sub-3 nm graphene quantum dots incorporated into mesoporous Bi₂MoO₆ frameworks: Efficient physical and chemical simultaneous co-catalysis for photocatalytic oxidation. *J. Mater. Chem. A* 4, 8298–8307. <https://doi.org/10.1039/c6ta02371a>.
- Hashemi, S.A., Ramakrishna, S., Aberle, A.G., 2020. Recent progress in flexible-wearable solar cells for self-powered electronic devices. *Energy Environ. Sci.* 13, 685–743. <https://doi.org/10.1039/c9ee03046h>.
- Hatefi, R., Younesi, H., Mashinchian-Moradi, A., Nojavan, S., 2021. A facile decoration of anatase Fe₃O₄/TiO₂ nanocomposite with graphene quantum dots: Synthesis, characterization, and photocatalytic activity. *Adv. Powder Technol.* 32, 2410–2422. <https://doi.org/10.1016/j.appt.2021.05.020>.
- He, H., Zhou, Z., 2017. Electro-fenton process for water and wastewater treatment. *Crit. Rev. Environ. Sci. Technol.* 47, 2100–2131. <https://doi.org/10.1080/10643389.2017.1405673>.
- Hernández-Carrillo, M.A., Torres-Ricárdez, R., García-Mendoza, M.F., Ramírez-Morales, E., Rojas-Blanco, L., Díaz-Flores, L.L., Sepúlveda-Palacios, G.E., Paraguayo-Delgado, F., Pérez-Hernández, G., 2020. Eu-modified ZnO nanoparticles for applications in photocatalysis. *Catal. Today* 349, 191–197. <https://doi.org/10.1016/j.cattod.2018.04.060>.
- Herrmann, J.M., 2010. Photocatalysis fundamentals revisited to avoid several misconceptions. *Appl. Catal. B: Environ.* 99, 461–468. <https://doi.org/10.1016/j.apcatb.2010.05.012>.
- Hisatomi, T., Domen, K., 2019. Reaction systems for solar hydrogen production via water splitting with particulate semiconductor photocatalysts. *Nat. Catal.* 2, 387–399. <https://doi.org/10.1038/s41929-019-0242-6>.
- Hu, C., Tu, S., Tian, N., Ma, T., Zhang, Y., Huang, H., 2021. Photocatalysis enhanced by external fields. *Angew. Chem. -Int. Ed.* 60, 16309–16328. <https://doi.org/10.1002/anie.202009518>.
- Hu, X., Li, G., Yu, J.C., 2010. Design, fabrication, and modification of nanostructured semiconductor materials for environmental and energy applications. *Langmuir* 26, 3031–3039. <https://doi.org/10.1021/la902142b>.
- Hu, Y., Chen, W., Lei, T., Jiao, Y., Wang, H., Wang, X., Rao, G., Wang, X., Chen, B., Xiong, J., 2020. Graphene quantum dots as the nucleation sites and interfacial regulator to suppress lithium dendrites for high-loading lithium-sulfur battery. *Nano Energy* 68, 104373. <https://doi.org/10.1016/j.nanoen.2019.104373>.
- Hu, Y., Zhou, C., Wang, H., Chen, M., Zeng, G., Liu, Z., Liu, Y., Wang, W., Wu, T., Shao, B., Liang, Q., 2021. Recent advance of graphene/semiconductor composite nanocatalysts: Synthesis, mechanism, applications and perspectives. *Chem. Eng. J.* 414, 128795 <https://doi.org/10.1016/j.cej.2021.128795>.
- Hu, Z., Cai, J., Song, G., Tian, Y., Zhou, M., 2021. Anodic oxidation of organic pollutants: Anode fabrication, process hybrid and environmental applications. *Curr. Opin. Electrochem.* 26, 100659 <https://doi.org/10.1016/j.coelec.2020.100659>.
- Huang, Y., Shi, T., Zhong, Y., Cheng, S., Jiang, S., Chen, C., Liao, G., Tang, Z., 2018. Graphene-quantum-dots induced NiCo₂S₄ with hierarchical-like hollow nanostructure for supercapacitors with enhanced electrochemical performance. *Electrochim. Acta* 269, 45–54. <https://doi.org/10.1016/j.electacta.2018.02.145>.
- Huo, P., Shi, X., Zhang, W., Kumar, P., Liu, B., 2021. An overview on the incorporation of graphene quantum dots on TiO₂ for enhanced performances. *J. Mater. Sci.* 56, 6031–6051. <https://doi.org/10.1007/s10853-020-05670-8>.
- Jamila, G.S., Sajjad, S., Leghari, S.A.K., Long, M., 2020a. Nitrogen doped carbon quantum dots and GO modified WO₃ nanosheets combination as an effective visible photo catalyst. *J. Hazard. Mater.* 382, 121087 <https://doi.org/10.1016/j.jhazmat.2019.121087>.
- Jamila, G.S., Sajjad, S., Leghari, S.A.K., Li, Y., 2020b. Pivotal role of N and Bi doping in CQD/Mn₃O₄ composite structure with outstanding visible photoactivity. *N. J. Chem.* 44, 11631–11642. <https://doi.org/10.1039/d0nj01457e>.
- Jamila, G.S., Sajjad, S., Leghari, S.A.K., Mahmood, T., 2020c. Role of nitrogen doped carbon quantum dots on CuO nano-leaves as solar induced photo catalyst. *J. Phys. Chem. Solids* 138, 109233. <https://doi.org/10.1016/j.jpcs.2019.109233>.

- Jegannathan, P., Termeh Yousefi, A., Karim, M.S.A., Kadri, N.A., 2018. Enhancement of graphene quantum dots-based applications via optimum physical chemistry: A review. *Biocybern. Biomed. Eng.* 38, 481–497. <https://doi.org/10.1016/j.bbe.2018.03.006>.
- Jia, H., Cai, Y., Lin, J., Liang, H., Qi, J., Cao, J., Feng, J., Fei, W.D., 2018a. Heterostructural graphene quantum Dot/MnO₂ nanosheets toward high-potential window electrodes for high-performance supercapacitors. *Adv. Sci.* 5 <https://doi.org/10.1002/adv.201700887>.
- Jia, H., Cai, Y., Lin, J., Liang, H., Qi, J., Cao, J., Feng, J., Fei, W.D., 2018b. Heterostructural Graphene Quantum Dot/MnO₂ Nanosheets toward High-Potential Window Electrodes for High-Performance Supercapacitors. *Adv. Sci.* 5 <https://doi.org/10.1002/adv.201700887>.
- Jia, H., Cai, Y., Lin, J., Liang, H., Qi, J., Cao, J., Feng, J., Fei, W.D., 2018c. Heterostructural graphene quantum Dot/MnO₂ nanosheets toward high-potential window electrodes for high-performance supercapacitors. *Adv. Sci.* 5 <https://doi.org/10.1002/adv.201700887>.
- Jian, W., Hui, D., Lau, D., 2020. Nanoengineering in biomedicine: Current development and future perspectives. *Nanotechnol. Rev.* 9, 700–715. <https://doi.org/10.1515/ntrv-2020-0053>.
- Jung, S., Chen, X., 2018. Quantum Dot–Dye Conjugates for Biosensing, Imaging, and Therapy. *Adv. Healthc. Mater.* 7 <https://doi.org/10.1002/adhm.201800252>.
- Kahrizi, P., Mohseni-Shahri, F.S., Moeinpour, F., 2018. Adsorptive removal of cadmium from aqueous solutions using NiFe₂O₄/hydroxyapatite/graphene quantum dots as a novel nano-adsorbent. *J. Nanostructure Chem.* 8, 441–452. <https://doi.org/10.1007/s40097-018-0284-3>.
- Karthikeyan, C., Arunachalam, P., Ramachandran, K., Al-Mayouf, A.M., Karuppuchamy, S., 2020. Recent advances in semiconductor metal oxides with enhanced methods for solar photocatalytic applications. *J. Alloy. Compd.* 828 <https://doi.org/10.1016/j.jallcom.2020.154281>.
- Kasper, J.C., Friess, W., 2011. The freezing step in lyophilization: Physico-chemical fundamentals, freezing methods and consequences on process performance and quality attributes of biopharmaceuticals. *Eur. J. Pharm. Biopharm.* 78, 248–263. <https://doi.org/10.1016/j.ejpb.2011.03.010>.
- Khaki, M.R.D., Shafeyyan, M.S., Raman, A.A.A., Daud, W.M.A.W., 2017. Application of doped photocatalysts for organic pollutant degradation - A review. *J. Environ. Manag.* 198, 78–94. <https://doi.org/10.1016/j.jenvman.2017.04.099>.
- Khreis, H., Kelly, C., Tate, J., Parslow, R., Lucas, K., Nieuwenhuijsen, M., 2017. Exposure to traffic-related air pollution and risk of development of childhood asthma: A systematic review and meta-analysis. *Environ. Int.* 100, 1–31. <https://doi.org/10.1016/j.envint.2016.11.012>.
- Kittiratanawasin, L., Hannongbua, S., 2016. The effect of edges and shapes on band gap energy in graphene quantum dots. *Integr. Ferroelectr.* 175, 211–219. <https://doi.org/10.1080/10584587.2016.1204893>.
- Kouskou, T., Bruel, P., Jamil, A., el Rhafiki, T., Zeraoui, Y., 2014. Energy storage: Applications and challenges. *Sol. Energy Mater. Sol. Cells* 120, 59–80. <https://doi.org/10.1016/j.solmat.2013.08.015>.
- Kubacka, A., Fernández-García, M., Colón, G., 2012. Advanced nanoarchitectures for solar photocatalytic applications. *Chem. Rev.* 112, 1555–1614. <https://doi.org/10.1021/cr100454n>.
- Kumar, D.K., Suazo-Davila, D., García-Torres, D., Cook, N.P., Ivaturi, A., Hsu, M.H., Martí, A.A., Cabrera, C.R., Chen, B., Bennett, N., Upadhyaya, H.M., 2019. Low-temperature titania-graphene quantum dots paste for flexible dye-sensitized solar cell applications. *Electrochim. Acta* 305, 278–284. <https://doi.org/10.1016/j.electacta.2019.03.040>.
- Kumar, S.G., Rao, K.S.R.K., 2017. Comparison of modification strategies towards enhanced charge carrier separation and photocatalytic degradation activity of metal oxide semiconductors (TiO₂, WO₃ and ZnO). *Appl. Surf. Sci.* 391, 124–148. <https://doi.org/10.1016/j.apsusc.2016.07.081>.
- Kunwar, S., Pandit, S., Kulkarni, R., Mandavkar, R., Lin, S., Li, M.Y., Lee, J., 2021. Hybrid device architecture using plasmonic nanoparticles, graphene quantum dots, and titanium dioxide for UV photodetectors. *ACS Appl. Mater. Interfaces* 13, 3408–3418. <https://doi.org/10.1021/acsmi.0c19058>.
- Lee, K.M., Lai, C.W., Ngai, K.S., Juan, J.C., 2016. Recent developments of zinc oxide based photocatalyst in water treatment technology: A review. *Water Res.* 88, 428–448. <https://doi.org/10.1016/j.watres.2015.09.045>.
- Lei, Y., Yang, C., Hou, J., Wang, F., Min, S., Ma, X., Jin, Z., Xu, J., Lu, G., Huang, K.W., 2017. Strongly coupled CdS/graphene quantum dots nanohybrids for highly efficient photocatalytic hydrogen evolution: Unraveling the essential roles of graphene quantum dots. *Appl. Catal. B: Environ.* 216, 59–69. <https://doi.org/10.1016/j.apcatb.2017.05.063>.
- Li, A., Zhu, W., Li, C., Wang, T., Gong, J., 2019. Rational design of yolk-shell nanostructures for photocatalysis. *Chem. Soc. Rev.* 48, 1874–1907. <https://doi.org/10.1039/c8cs00711j>.
- Li, J.L., Bao, H.C., Hou, X.L., Sun, L., Wang, X.G., Gu, M., 2012. Graphene oxide nanoparticles as a nonbleaching optical probe for two-photon luminescence imaging and cell therapy. *Angew. Chem. - Int. Ed.* 51, 1830–1834. <https://doi.org/10.1002/anie.201106102>.
- Li, N., Liu, Z., Hu, S., Chang, Q., Xue, C., Wang, H., 2019. Electronic and photocatalytic properties of modified MoS₂/graphene quantum dots heterostructures: A computational study. *Appl. Surf. Sci.* 473, 70–76. <https://doi.org/10.1016/j.apsusc.2018.12.122>.
- Li, X., Yu, J., Wageh, S., Al-Ghamdi, A.A., Xie, J., 2016. Graphene in Photocatalysis: A Review. *Small* 12, 6640–6696. <https://doi.org/10.1002/sml.201600382>.
- Li, X., Shen, R., Ma, S., Chen, X., Xie, J., 2018a. Graphene-based heterojunction photocatalysts. *Appl. Surf. Sci.* 430, 53–107. <https://doi.org/10.1016/j.apsusc.2017.08.194>.
- Li, X., Xie, J., Jiang, C., Yu, J., Zhang, P., 2018b. Review on design and evaluation of environmental photocatalysts. *Front. Environ. Sci. Eng.* 12 <https://doi.org/10.1007/s11783-018-1076-1>.
- Li, Z., Li, M., Bian, Z., Kathiraser, Y., Kawi, S., 2016. Design of highly stable and selective core/yolk-shell nanocatalysts-review. *Appl. Catal. B: Environ.* 188, 324–341. <https://doi.org/10.1016/j.apcatb.2016.01.067>.
- Liang, Q., Shao, B., Tong, S., Liu, Z., Tang, L., Liu, Y., Cheng, M., He, Q., Wu, T., Pan, Y., Huang, J., Peng, Z., 2021. Recent advances of melamine self-assembled graphitic carbon nitride-based materials: Design, synthesis and application in energy and environment. *Chem. Eng. J.* 405, 126951 <https://doi.org/10.1016/j.cej.2020.126951>.
- Liao, G., Gong, Y., Zhang, L., Gao, H., Yang, G.J., Fang, B., 2019. Semiconductor polymeric graphitic carbon nitride photocatalysts: The “holy grail” for the photocatalytic hydrogen evolution reaction under visible light. *Energy Environ. Sci.* 12, 2080–2147. <https://doi.org/10.1039/c9ee00717b>.
- Lin, J., Chen, X., Huang, P., 2016. Graphene-based nanomaterials for bioimaging. *Adv. Drug Deliv. Rev.* 105, 242–254. <https://doi.org/10.1016/j.addr.2016.05.013>.
- Lin, L., Ning, H., Song, S., Xu, C., Hu, N., 2020. Flexible electrochemical energy storage: The role of composite materials. *Compos. Sci. Technol.* 192 <https://doi.org/10.1016/j.compscitech.2020.108102>.
- Liu, J., Xu, H., Xu, Y., Song, Y., Lian, J., Zhao, Y., Wang, L., Huang, L., Ji, H., Li, H., 2017. Graphene quantum dots modified mesoporous graphite carbon nitride with significant enhancement of photocatalytic activity. *Appl. Catal. B: Environ.* 207, 429–437. <https://doi.org/10.1016/j.apcatb.2017.01.071>.
- Liu, N., Li, W., Pasta, M., Cui, Y., 2014. Nanomaterials for electrochemical energy storage. *Front. Phys.* 9, 323–350. <https://doi.org/10.1007/s11467-013-0408-7>.
- Liu, T., Yu, K., Gao, L., Chen, H., Wang, N., Hao, L., Li, T., He, H., Guo, Z., 2017. A graphene quantum dot decorated SrRuO₃ mesoporous film as an efficient counter electrode for high-performance dye-sensitized solar cells. *J. Mater. Chem. A* 5, 17848–17855. <https://doi.org/10.1039/c7ta05123a>.
- Liu, W., Zhou, X., Xu, L., Zhu, S., Yang, S., Chen, X., Dong, B., Bai, X., Lu, G., Song, H., 2019a. Graphene quantum dot-functionalized three-dimensional ordered mesoporous ZnO for acetone detection toward diagnosis of diabetes. *Nanoscale* 11, 11496–11504. <https://doi.org/10.1039/c9nr00942f>.
- Liu, W., Ren, B., Zhang, W., Zhang, M., Li, G., Xiao, M., Zhu, J., Yu, A., Ricardez-Sandoval, L., Chen, Z., 2019b. Defect-enriched nitrogen doped-graphene quantum dots engineered NiCo₂S₄ nanoarray as high-efficiency bifunctional catalyst for flexible Zn-air battery. *Small* 15, 1–11. <https://doi.org/10.1002/sml.201903610>.
- Liu, X., Yang, H., Jian, X., Dai, H., Song, X., Liang, Z., 2017. Constructing a novel GQDs/PANI/g-C₃N₄ ternary heterostructure with enhanced photoelectrocatalytic performance. *Mater. Lett.* 209, 247–250. <https://doi.org/10.1016/j.matlet.2017.08.022>.
- Liu, X., Zhou, Y., Zhang, J., Luo, L., Yang, Y., Huang, H., Peng, H., Tang, L., Mu, Y., 2018. Insight into electro-Fenton and photo-Fenton for the degradation of antibiotics: Mechanism study and research gaps. *Chem. Eng. J.* 347, 379–397. <https://doi.org/10.1016/j.cej.2018.04.142>.
- Liu, X., Xu, J., Ni, Z., Wang, R., You, J., Guo, R., 2019. Adsorption and visible-light-driven photocatalytic properties of Ag₃PO₄/WO₃ composites: A discussion of the mechanism. *Chem. Eng. J.* 356, 22–33. <https://doi.org/10.1016/j.cej.2018.09.001>.
- Liu, Y., Yu, S., Zhao, Z., Dong, F., Dong, X.A., Zhou, Y., 2017. N-Doped Bi₂O₂CO₃/Graphene Quantum Dot Composite Photocatalyst: Enhanced Visible-Light Photocatalytic NO Oxidation and in Situ DRIFTS Studies. *J. Phys. Chem. C* 121, 12168–12177. <https://doi.org/10.1021/acs.jpcc.7b02285>.
- Liu, Y., Cheng, M., Liu, Z., Zeng, G., Zhong, H., Chen, M., Zhou, C., Xiong, W., Shao, B., Song, B., 2019. Heterogeneous Fenton-like catalyst for treatment of rhamnolipid-solubilized hexadecane wastewater. *Chemosphere* 236. <https://doi.org/10.1016/j.chemosphere.2019.124387>.
- Liu, Y., Huang, D., Cheng, M., Liu, Z., Lai, C., Zhang, C., Zhou, C., Xiong, W., Qin, L., Shao, B., Liang, Q., 2020. Metal sulfide/MOF-based composites as visible-light-driven photocatalysts for enhanced hydrogen production from water splitting. *Coord. Chem. Rev.* 409 <https://doi.org/10.1016/j.ccr.2020.213220>.
- Liu, Z., Yu, X., Li, L., 2020. Piezopotential augmented photo- and photoelectro-catalysis with a built-in electric field. *Chin. J. Catal.* 41, 534–549. [https://doi.org/10.1016/S1872-2067\(19\)63431-5](https://doi.org/10.1016/S1872-2067(19)63431-5).
- Long, R., Casanova, D., Fang, W.H., Prezhdo, O.V., 2017. Donor-acceptor interaction determines the mechanism of photoinduced electron injection from graphene quantum dots into TiO₂: π -stacking supersedes covalent bonding. *J. Am. Chem. Soc.* 139, 2619–2629. <https://doi.org/10.1021/jacs.6b09598>.
- Low, J., Yu, J., Jaroniec, M., Wageh, S., Al-Ghamdi, A.A., 2017a. Heterojunction photocatalysts. *Adv. Mater.* 29 <https://doi.org/10.1002/adma.201601694>.
- Low, J., Jiang, C., Cheng, B., Wageh, S., Al-Ghamdi, A.A., Yu, J., 2017b. A review of direct Z-scheme photocatalysts. *Small Methods* 1, 1700080. <https://doi.org/10.1002/smt.201700080>.
- Lu, F., Astruc, D., 2020. Nanocatalysts and other nanomaterials for water remediation from organic pollutants. *Coord. Chem. Rev.* 408, 213180 <https://doi.org/10.1016/j.ccr.2020.213180>.
- Lu, H., Huang, Z., Martinez, M.S., Johnson, J.C., Luther, J.M., Beard, M.C., 2020. Transforming energy using quantum dots. *Energy Environ. Sci.* 13, 1347–1376. <https://doi.org/10.1039/c9ee03930a>.
- Luo, J., Wang, J., Liu, S., Wu, W., Jia, T., Yang, Z., Mu, S., Huang, Y., 2019. Graphene quantum dots encapsulated tremella-like NiCo₂O₄ for advanced asymmetric supercapacitors. *Carbon* 146, 1–8. <https://doi.org/10.1016/j.carbon.2019.01.078>.
- Lv, Y.K., Li, Y.Y., Zhou, R.H., Pan, Y.P., Yao, H.C., Li, Z.J., 2020. N-Doped Graphene Quantum Dot-Decorated Three-Dimensional Ordered Macroporous In₂O₃ for NO₂ Sensing at Low Temperatures. *ACS Appl. Mater. Interfaces* 12, 34245–34253. <https://doi.org/10.1021/acsmi.0c03369>.

- McDonnell, G., Burke, P., 2011. Disinfection: Is it time to reconsider Spaulding? *J. Hosp. Infect.* 78, 163–170. <https://doi.org/10.1016/j.jhin.2011.05.002>.
- McGuigan, K.G., Conroy, R.M., Mosler, H.J., du Preez, M., Ubomba-Jaswa, E., Fernandez-Ibanez, P., 2012. Solar water disinfection (SODIS): A review from bench-top to rooftop. *J. Hazard. Mater.* 235–236, 29–46. <https://doi.org/10.1016/j.jhazmat.2012.07.053>.
- Meng, A., Zhang, L., Cheng, B., Yu, J., 2019. TiO₂-MnO_x-Pt Hybrid Multiheterojunction Film Photocatalyst with Enhanced Photocatalytic CO₂-Reduction Activity. *ACS Appl. Mater. Interfaces* 11, 5581–5589. <https://doi.org/10.1021/acsami.8b02552>.
- Miao, H., Teng, Z., Wang, S., Xu, L., Wang, C., Chong, H., 2019. Recent advances in the disinfection of water using nanoscale antimicrobial materials. *Adv. Mater. Technol.* 4. <https://doi.org/10.1002/admt.201800213>.
- Min, S., Hou, J., Lei, Y., Ma, X., Lu, G., 2017. Facile one-step hydrothermal synthesis toward strongly coupled TiO₂/graphene quantum dots photocatalysts for efficient hydrogen evolution. *Appl. Surf. Sci.* 396, 1375–1382. <https://doi.org/10.1016/j.apsusc.2016.11.169>.
- Mo, F., Liang, G., Huang, Z., Li, H., Wang, D., Zhi, C., 2020. An Overview of Fiber-Shaped Batteries with a Focus on Multifunctionality, Scalability, and Technical Difficulties. *Adv. Mater.* 32. <https://doi.org/10.1002/adma.201902151>.
- Mou, Z., Lu, C., Yu, K., Wu, H., Zhang, H., Sun, J., Zhu, M., Cynthia Goh, M., 2019. Chemical interaction in nitrogen-doped graphene quantum dots/graphitic carbon nitride heterostructures with enhanced photocatalytic H₂ evolution. *Energy Technol.* 7. <https://doi.org/10.1002/ente.201800589>.
- Moxon, S., Cooke, M., Cox, S., Smow, M., Jeys, L., Jones, S., Grover, L., Smith, A., 2017. Suspended manufacture of biological structures. *Adv. Mater.* 29. [https://doi.org/10.1002/\(ISSN\)1521-4095](https://doi.org/10.1002/(ISSN)1521-4095).
- Munnik, P., De Jongh, P.E., Jong, K.P.De, 2015. Recent developments in the synthesis of supported catalysts. *Chem. Rev.* 115, 6687–6718. <https://doi.org/10.1021/cr500486u>.
- Muthosamy, K., Manickam, S., 2017. State of the art and recent advances in the ultrasound-assisted synthesis, exfoliation and functionalization of graphene derivatives. *Ultrason. Sonochem.* 39, 478–493. <https://doi.org/10.1016/j.ultsonch.2017.05.019>.
- Nandiyanto, A.B.D., Zaen, R., Oktiani, R., 2020. Correlation between crystallite size and photocatalytic performance of micrometer-sized monoclinic WO₃ particles. *Arab. J. Chem.* 13, 1283–1296. <https://doi.org/10.1016/j.arabjc.2017.10.010>.
- Natarajan, T.S., Thampi, K.R., Tayade, R.J., 2018. Visible light driven redox-mediator-free dual semiconductor photocatalytic systems for pollutant degradation and the ambiguity in applying Z-scheme concept. *Appl. Catal. B: Environ.* 227, 296–311. <https://doi.org/10.1016/j.apcatb.2018.01.015>.
- Nie, Y.C., Yu, F., Wang, L.C., Xing, Q.J., Liu, X., Pei, Y., Zou, J.P., Dai, W.L., Li, Y., Suib, S.L., 2018. Photocatalytic degradation of organic pollutants coupled with simultaneous photocatalytic H₂ evolution over graphene quantum dots/Mn-N-TiO₂/g-C₃N₄ composite catalysts: Performance and mechanism. *Appl. Catal. B: Environ.* 227, 312–321. <https://doi.org/10.1016/j.apcatb.2018.01.033>.
- Nielsen, G.D., Larsen, S.T., Wolkoff, P., 2017. Re-evaluation of the WHO (2010) formaldehyde indoor air quality guideline for cancer risk assessment. *Arch. Toxicol.* 91, 35–61. <https://doi.org/10.1007/s00204-016-1733-8>.
- Nisticò, R., Scalarone, D., Magnacca, G., 2017. Sol-gel chemistry, templating and spin-coating deposition: A combined approach to control in a simple way the porosity of inorganic thin films/coatings. *Microporous Mesoporous Mater.* 248, 18–29. <https://doi.org/10.1016/j.micromeso.2017.04.017>.
- Noman, M.T., Ashraf, M.A., Ali, A., 2019. Synthesis and applications of nano-TiO₂: a review. *Environ. Sci. Pollut. Res.* 26, 3262–3291. <https://doi.org/10.1007/s11356-018-3884-z>.
- Noor, S., Sajjad, S., Leghari, S.A.K., Flox, C., Kallio, T., Kauppinen, E.I., Ahmad, S., 2021. Electronic transitions of SWCNTs in comparison to GO on Mn₃O₄/TiO₂ nanocomposites for hydrogen energy generation and solar photocatalysis. *N. J. Chem.* 45, 2431–2442. <https://doi.org/10.1039/d0nj05120a>.
- Obot, I.B., Macdonald, D.D., Gasem, Z.M., 2015. Density functional theory (DFT) as a powerful tool for designing new organic corrosion inhibitors: Part 1: An overview. *Corros. Sci.* 99, 1–30. <https://doi.org/10.1016/j.corsci.2015.01.037>.
- Olabi, A.G., Onumaegbu, C., Wilberforce, T., Ramadan, M., Abdelkareem, M.A., al -Alami, A.H., 2021. Critical review of energy storage systems. *Energy* 214, 118987. <https://doi.org/10.1016/j.energy.2020.118987>.
- Orooji, Y., Ghanbari, M., Amiri, O., Salavati-Niasari, M., 2020. Facile fabrication of silver iodide/graphitic carbon nitride nanocomposites by notable photo-catalytic performance through sunlight and antimicrobial activity. *J. Hazard. Mater.* 389. <https://doi.org/10.1016/j.jhazmat.2020.122079>.
- Osterloh, F.E., 2015. Nanoscale effects in water splitting photocatalysis. In: *Topics in Current Chemistry*. Springer Verlag, pp. 105–142. https://doi.org/10.1007/128_2015_633.
- Ou, H., Chen, X., Lin, L., Fang, Y., Wang, X., 2018. Biomimetic donor-acceptor motifs in conjugated polymers for promoting exciton splitting and charge separation. *Angew. Chem. - Int. Ed.* 57, 8729–8733. <https://doi.org/10.1002/anie.201803863>.
- Pan, D., Zhang, J., Li, Z., Wu, M., 2010. Hydrothermal route for cutting graphene sheets into blue-luminescent graphene quantum dots. *Adv. Mater.* 22, 734–738. <https://doi.org/10.1002/adma.200902825>.
- Pan, D., Jiao, J., Li, Z., Guo, Y., Feng, C., Liu, Y., Wang, L., Wu, M., 2015. Efficient separation of electron-hole pairs in graphene quantum dots by TiO₂ heterojunctions for dye degradation. *ACS Sustain. Chem. Eng.* 3, 2405–2413. <https://doi.org/10.1021/acssuschemeng.5b00771>.
- Pan, Y., Liu, X., Zhang, W., Liu, Z., Zeng, G., Shao, B., Liang, Q., He, Q., Yuan, X., Huang, D., Chen, M., 2020. Advances in photocatalysis based on fullerene C₆₀ and its derivatives: Properties, mechanism, synthesis, and applications. *Appl. Catal. B: Environ.* 265, 118579. <https://doi.org/10.1016/j.apcatb.2019.118579>.
- Panchal, P., Paul, D.R., Sharma, A., Choudhary, P., Meena, P., Nehra, S.P., 2020. Biogenic mediated Ag/ZnO nanocomposites for photocatalytic and antibacterial activities towards disinfection of water. *J. Colloid Interface Sci.* 563, 370–380. <https://doi.org/10.1016/j.jcis.2019.12.079>.
- Pang, X., Bian, H., Wang, W., Liu, C., Khan, M.S., Wang, Q., Qi, J., Wei, Q., Du, B., 2017. A bio-chemical application of N-GQDs and g-C₃N₄ QDs sensitized TiO₂ nanopillars for the quantitative detection of pCDNA3-HBV. *Biosens. Bioelectron.* 91, 456–464. <https://doi.org/10.1016/j.bios.2016.12.059>.
- Papageorgiou, D.G., Kinloch, I.A., Young, R.J., 2017. Mechanical properties of graphene and graphene-based nanocomposites. *Prog. Mater. Sci.* 90, 75–127. <https://doi.org/10.1016/j.pmatsci.2017.07.004>.
- Parr, R.G., Pearson, R.G., 1983. Absolute hardness: Companion parameter to absolute electronegativity. *J. Am. Chem. Soc.* 105, 7512–7516. <https://doi.org/10.1021/ja00364a005>.
- Peng, Z., Liu, X., Zhang, W., Zeng, Z., Liu, Z., Zhang, C., Liu, Y., Shao, B., Liang, Q., Tang, W., Yuan, X., 2020. Advances in the application, toxicity and degradation of carbon nanomaterials in environment: A review. *Environ. Int.* 134. <https://doi.org/10.1016/j.envint.2019.105298>.
- Qian, J., Shen, C., Yan, J., Xi, F., Dong, X., Liu, J., 2018a. Tailoring the Electronic Properties of Graphene Quantum Dots by P Doping and Their Enhanced Performance in Metal-Free Composite Photocatalyst. *J. Phys. Chem. C* 122, 349–358. <https://doi.org/10.1021/acs.jpcc.7b08702>.
- Qian, J., Shen, C., Yan, J., Xi, F., Dong, X., Liu, J., 2018b. Tailoring the Electronic Properties of Graphene Quantum Dots by P Doping and Their Enhanced Performance in Metal-Free Composite Photocatalyst. *J. Phys. Chem. C* 122, 349–358. <https://doi.org/10.1021/acs.jpcc.7b08702>.
- Qin, T., Xu, X., Pačáková, V., Štulík, K., Jech, L., 1997. A simple method for the trace determination of methanol, ethanol, acetone and pentane in human breath and in the ambient air by preconcentration on solid sorbents followed by gas chromatography. *Talanta* 44, 1683–1690. [https://doi.org/10.1016/S0039-9140\(97\)00073-8](https://doi.org/10.1016/S0039-9140(97)00073-8).
- Rajender, G., Kumar, J., Giri, P.K., 2018. Interfacial charge transfer in oxygen deficient TiO₂-graphene quantum dot hybrid and its influence on the enhanced visible light photocatalysis. *Appl. Catal. B: Environ.* 224, 960–972. <https://doi.org/10.1016/j.apcatb.2017.11.042>.
- Raziq, F., Qu, Y., Humayun, M., Zada, A., Yu, H., Jing, L., 2017. Synthesis of SnO₂/B-P codoped g-C₃N₄ nanocomposites as efficient cocatalyst-free visible-light photocatalysts for CO₂ conversion and pollutant degradation. *Appl. Catal. B: Environ.* 201, 486–494. <https://doi.org/10.1016/j.apcatb.2016.08.057>.
- Redigueri, C.F., Sassonia, R.C., Dua, K., Kikuchi, I.S., de Jesus Andreoli Pinto, T., 2016. Impact of sterilization methods on electrospon scaffolds for tissue engineering. *Eur. Polym. J.* 82, 181–195. <https://doi.org/10.1016/j.eurpolymj.2016.07.016>.
- Safardoust-Hojaghan, H., Salavati-Niasari, M., 2017a. Degradation of methylene blue as a pollutant with N-doped graphene quantum dot/titanium dioxide nanocomposite. *J. Clean. Prod.* 148, 31–36. <https://doi.org/10.1016/j.jclepro.2017.01.169>.
- Safardoust-Hojaghan, H., Salavati-Niasari, M., 2017b. Degradation of methylene blue as a pollutant with N-doped graphene quantum dot/titanium dioxide nanocomposite. *J. Clean. Prod.* 148, 31–36. <https://doi.org/10.1016/j.jclepro.2017.01.169>.
- Sajjad, S., Khan Leghari, S.A., Iqbal, A., 2017. Study of Graphene Oxide Structural Features for Catalytic, Antibacterial, Gas Sensing, and Metals Decontamination Environmental Applications. *ACS Appl. Mater. Interfaces* 9, 43393–43414. <https://doi.org/10.1021/acsami.7b08232>.
- Shamaila, S., Sajjad, A.K.L., Iqbal, A., 2016. Modifications in development of graphene oxide synthetic routes. *Chem. Eng. J.* 294, 458–477. <https://doi.org/10.1016/j.cej.2016.02.109>.
- Shao, B., Liu, Z., Zeng, G., Liu, Y., Liang, Q., He, Q., Wu, T., Pan, Y., Huang, J., Peng, Z., Luo, S., Liang, C., Liu, X., Tong, S., Liang, J., 2021. Synthesis of 2D/2D CoAl-LDHs/Ti₃C₂T_x Schottky-junction with enhanced interfacial charge transfer and visible-light photocatalytic performance. *Appl. Catal. B: Environ.* 286, 119867. <https://doi.org/10.1016/j.apcatb.2020.119867>.
- Sharma, K., Sharma, V., Sharma, S.S., 2018. Dye-Sensitized Solar Cells: Fundamentals and Current Status. *Nanoscale Res. Lett.* 13. <https://doi.org/10.1186/s11671-018-2760-6>.
- Sharma, V., Som, N.N., Pillai, S.B., Jha, P.K., 2020. Utilization of doped GQDs for ultrasensitive detection of catastrophic melamine: A new SERS platform. *Spectrochim. Acta - Part A: Mol. Biomol. Spectrosc.* 224. <https://doi.org/10.1016/j.saa.2019.117352>.
- Shen, R., Jiang, C., Xiang, Q., Xie, J., Li, X., 2019. Surface and interface engineering of hierarchical photocatalysts. *Appl. Surf. Sci.* 471, 43–87. <https://doi.org/10.1016/j.apsusc.2018.11.205>.
- Sheng, Z.-Q., Xing, Y.-Q., Chen, Y., Zhang, G., Liu, S.-Y., Chen, L., 2021. Nanoporous and nonporous conjugated donor-acceptor polymer semiconductors for photocatalytic hydrogen production. *Beilstein J. Nanotechnol.* 12, 607–623. <https://doi.org/10.3762/bjnano.12.50>.
- Shi, J., Lyu, J., Tian, F., Yang, M., 2017. A fluorescence turn-on biosensor based on graphene quantum dots (GQDs) and molybdenum disulfide (MoS₂) nanosheets for epithelial cell adhesion molecule (EPCAM) detection. *Biosens. Bioelectron.* 93, 182–188. <https://doi.org/10.1016/j.bios.2016.09.012>.
- Song, Z.L., Dai, X., Li, M., Teng, H., Song, Z., Xie, D., Luo, X., 2018. Biodegradable nanoprobe based on MnO₂ nanoflowers and graphene quantum dots for near infrared fluorescence imaging of glutathione in living cells. *Microchim. Acta* 185. <https://doi.org/10.1007/s00604-018-3024-y>.
- Stergiou, A., Pagona, G., Tagmatarchis, N., 2014. Donor-acceptor graphene-based hybrid materials facilitating photo-induced electron-transfer reactions. *Beilstein J. Nanotechnol.* 5, 1580–1589. <https://doi.org/10.3762/bjnano.5.170>.

- Su, J., Li, G., Li, X., Chen, J., 2019a. 2D/2D Heterojunctions for Catalysis. *Adv. Sci.* 6, 1801702 <https://doi.org/10.1002/advs.201801702>.
- Su, J., Li, G.D., Li, X.H., Chen, J.S., 2019b. 2D/2D Heterojunctions for Catalysis. *Adv. Sci.* 6, 1801702 <https://doi.org/10.1002/advs.201801702>.
- Su, X., Chan, C., Shi, J., Tsang, M.K., Pan, Y., Cheng, C., Gerile, O., Yang, M., 2017. A graphene quantum dot@Fe₃O₄@SiO₂ based nanoprobe for drug delivery sensing and dual-modal fluorescence and MRI imaging in cancer cells. *Biosens. Bioelectron.* 92, 489–495. <https://doi.org/10.1016/j.bios.2016.10.076>.
- Su, Y., Yang, T., Zhao, X., Cai, Z., Chen, G., Yao, M., Chen, K., Bick, M., Wang, J., Li, S., Xie, G., Tai, H., Du, X., Jiang, Y., Chen, J., 2020. A wireless energy transmission enabled wearable active acetone biosensor for non-invasive prediabetes diagnosis. *Nano Energy* 74. <https://doi.org/10.1016/j.nanoen.2020.104941>.
- Tang, L., Ji, R., Cao, X., Lin, J., Jiang, H., Li, X., Teng, K.S., Luk, C.M., Zeng, S., Hao, J., Lau, S.P., 2012. Deep ultraviolet photoluminescence of water-soluble self-passivated graphene quantum dots. *ACS Nano* 6, 5102–5110. <https://doi.org/10.1021/nl300760g>.
- Tang, L., Wang, J. jun, Jia, C. tao, Lv, G. xin, Xu, G., Li, W. tao, Wang, L., Zhang, J. ye, Wu, M. hong, 2017. Simulated solar driven catalytic degradation of psychiatric drug carbamazepine with binary BiVO₄ heterostructures sensitized by graphene quantum dots. *Appl. Catal. B: Environ.* 205, 587–596. <https://doi.org/10.1016/j.apcatb.2016.10.067>.
- Tang, X., Pikal, M.J., 2004. Design of Freeze-Drying Processes for Pharmaceuticals: Practical Advice. *Pharm. Res.* 21, 191–200. <https://doi.org/10.1023/B:PHAM.0000016234.73023.75>.
- Teh, C.Y., Wu, T.Y., Juan, J.C., 2017. An application of ultrasound technology in synthesis of titania-based photocatalyst for degrading pollutant. *Chem. Eng. J.* 317, 586–612. <https://doi.org/10.1016/j.cej.2017.01.001>.
- Teymourinia, H., Salavati-Niasari, M., Amiri, O., Yazdian, F., 2019a. Application of green synthesized TiO₂/Sb₂S₃/GQDs nanocomposite as high efficient antibacterial agent against E. coli and Staphylococcus aureus. *Mater. Sci. Eng. C* 99, 296–303. <https://doi.org/10.1016/j.msec.2019.01.094>.
- Teymourinia, H., Salavati-Niasari, M., Amiri, O., 2019b. Simple synthesis of Cu₂O/GQDs nanocomposite with different morphologies fabricated by tuning the synthesis parameters as novel antibacterial material. *Compos. Part B: Eng.* 172, 785–794. <https://doi.org/10.1016/j.compositesb.2019.05.047>.
- Theerthagiri, J., Salla, S., Senthil, R.A., Nithyadharseni, P., Madankumar, A., Arunachalam, P., Maiyalagan, T., Kim, H.S., 2019. A review on ZnO nanostructured materials: Energy, environmental and biological applications. *Nanotechnology* . 30. <https://doi.org/10.1088/1361-6528/ab268a>.
- Tian, H., Shen, K., Hu, X., Qiao, L., Zheng, W., 2017. N, S co-doped graphene quantum dots-graphene-TiO₂ nanotubes composite with enhanced photocatalytic activity. *J. Alloy. Compd.* 691, 369–377. <https://doi.org/10.1016/j.jallcom.2016.08.261>.
- Tsang, C.H.A., Huang, H., Xuan, J., Wang, H., Leung, D.Y.C., 2020. Graphene materials in green energy applications: Recent development and future perspective. *Renew. Sustain. Energy Rev.* 120 <https://doi.org/10.1016/j.rser.2019.109656>.
- Tuteja, S.K., Chen, R., Kukkar, M., Song, C.K., Mutreja, R., Singh, S., Paul, A.K., Lee, H., Kim, K.H., Deep, A., Suri, C.R., 2016. A label-free electrochemical immunosensor for the detection of cardiac marker using graphene quantum dots (GQDs). *Biosens. Bioelectron.* 86, 548–556. <https://doi.org/10.1016/j.bios.2016.07.052>.
- Wan, Y., Yang, H., Zhao, D., 2006. “Host-guest” chemistry in the synthesis of ordered nonilicaceous mesoporous materials. *Acc. Chem. Res.* 39, 423–432. <https://doi.org/10.1021/ar050091a>.
- Wang, B., Ruan, T., Chen, Y., Jin, F., Peng, L., Zhou, Y., Wang, D., Dou, S., 2020. Graphene-based composites for electrochemical energy storage. *Energy Storage Mater.* 24, 22–51. <https://doi.org/10.1016/j.ensm.2019.08.004>.
- Wang, H., Sun, Y., Jiang, G., Zhang, Y., Huang, H., Wu, Z., Lee, S.C., Dong, F., 2018a. Unraveling the mechanisms of visible light photocatalytic NO purification on earth-abundant insulator-based core-shell heterojunctions. *Environ. Sci. Technol.* 52, 1479–1487. <https://doi.org/10.1021/acs.est.7b05457>.
- Wang, H., Zhang, B., Zhao, F., Zeng, B., 2018b. One-Pot Synthesis of N-Graphene Quantum Dot-Functionalized I-BiOCl Z-Scheme Cathodic Materials for “signal-Off” Photoelectrochemical Sensing of Chlorpyrifos. *ACS Appl. Mater. Interfaces* 10, 35281–35288. <https://doi.org/10.1021/acsami.8b12979>.
- Wang, Q., Domen, K., 2020. Particulate photocatalysts for light-driven water splitting: Mechanisms, challenges, and design strategies. *Chem. Rev.* 120, 919–985. <https://doi.org/10.1021/acs.chemrev.9b00201>.
- Wang, Q., Zhu, N., Liu, E., Zhang, C., Crittenden, J.C., Zhang, Y., Cong, Y., 2017. Fabrication of visible-light active Fe₂O₃-GQDs/NF-TiO₂ composite film with highly enhanced photoelectrocatalytic performance. *Appl. Catal. B: Environ.* 205, 347–356. <https://doi.org/10.1016/j.apcatb.2016.11.046>.
- Wang, R., Ma, N., Yan, Y., Wang, Z., 2018. Ultrasonic-assisted fabrication of high flux T-type zeolite membranes on alumina hollow fibers. *J. Membr. Sci.* 548, 676–684. <https://doi.org/10.1016/j.memsci.2017.10.047>.
- Wang, T., Quan, W., Jiang, D., Chen, L., Li, D., Meng, S., Chen, M., 2016. Synthesis of redox-mediator-free direct Z-scheme AgI/WO₃ nanocomposite photocatalysts for the degradation of tetracycline with enhanced photocatalytic activity. *Chem. Eng. J.* 300, 280–290. <https://doi.org/10.1016/j.cej.2016.04.128>.
- Wang, X., Sun, G., Li, N., Chen, P., 2016. Quantum dots derived from two-dimensional materials and their applications for catalysis and energy. *Chem. Soc. Rev.* 45, 2239–2262. <https://doi.org/10.1039/c5cs00811e>.
- Wang, X., Yuan, W., Yu, Y., Li, C.M., 2017. Synthesis of cobalt phosphide nanoparticles supported on pristine graphene by dynamically self-assembled graphene quantum dots for hydrogen evolution. *ChemSusChem* 10, 1014–1021. <https://doi.org/10.1002/cssc.201601761>.
- Wang, Z.L., 2010. Piezopotential gated nanowire devices: Piezotronics and piezophotonics. *Nano Today* 5, 540–552. <https://doi.org/10.1016/j.nantod.2010.10.008>.
- Wen, J., Xie, J., Chen, X., Li, X., 2017. A review on g-C₃N₄-based photocatalysts. *Appl. Surf. Sci.* 391, 72–123. <https://doi.org/10.1016/j.apsusc.2016.07.030>.
- Wu, H., Ding, J., Yang, D., Li, J., Shi, Y., Zhou, Y., 2020. Graphene quantum dots doped ZnO superstructure (ZnO superstructure/GQDs) for weak UV intensity photodetector application. *Ceram. Int.* 46, 17800–17808. <https://doi.org/10.1016/j.ceramint.2020.04.086>.
- Wu, K., Lian, T., 2016. Quantum confined colloidal nanorod heterostructures for solar-to-fuel conversion. *Chem. Soc. Rev.* 45, 3781–3810. <https://doi.org/10.1039/c5cs00472a>.
- Wu, T., Liu, X., Liu, Y., Cheng, M., Liu, Z., Zeng, G., Shao, B., Liang, Q., Zhang, W., He, Q., 2020. Application of QD-MOF composites for photocatalysis: Energy production and environmental remediation. *Coord. Chem. Rev.* 403 <https://doi.org/10.1016/j.ccr.2019.213097>.
- Wu, Y., Sun, X.J., Jia, Y.P., Li, D.B., 2018. Review of improved spectral response of ultraviolet photodetectors by surface plasmon. *Chin. Phys. B* 27, 126101. <https://doi.org/10.1088/1674-1056/27/12/126101>.
- Xiang, Q., Cheng, F., Lang, D., 2016. Hierarchical layered WS₂/Graphene-Modified CdS nanorods for efficient photocatalytic hydrogen evolution. *ChemSusChem* 9, 996–1002. <https://doi.org/10.1002/cssc.201501702>.
- Xie, H., Hou, C., Wang, H., Zhang, Q., Li, Y., 2017. S, N Co-Doped Graphene Quantum Dot/TiO₂ Composites for Efficient Photocatalytic Hydrogen Generation. *Nanoscale Res. Lett.* 12 <https://doi.org/10.1186/s11671-017-2101-1>.
- Xie, J., Huang, K., Yu, X., Yang, Z., Xiao, K., Qiang, Y., Zhu, X., Xu, L., Wang, P., Cui, C., Yang, D., 2017. Enhanced Electronic Properties of SnO₂ via Electron Transfer from Graphene Quantum Dots for Efficient Perovskite Solar Cells. *ACS Nano* 11, 9176–9182. <https://doi.org/10.1021/acsnano.7b04070>.
- Xie, M., Yang, J., Liang, J., Guo, X., Ding, W., 2014. In situ hydrothermal deposition as an efficient catalyst supporting method towards low-temperature graphitization of amorphous carbon. *Carbon* 77, 215–225. <https://doi.org/10.1016/j.carbon.2014.05.024>.
- Xie, Y., Yu, S., Zhong, Y., Zhang, Q., Zhou, Y., 2018. SnO₂/graphene quantum dots composited photocatalyst for efficient nitric oxide oxidation under visible light. *Appl. Surf. Sci.* 448, 655–661. <https://doi.org/10.1016/j.apsusc.2018.04.145>.
- Xu, C., Ravi Anusuyadevi, P., Aymonier, C., Luque, R., Marre, S., 2019. Nanostructured materials for photocatalysis. *Chem. Soc. Rev.* 48, 3868–3902. <https://doi.org/10.1039/c9cs00102f>.
- Xu, J., Huang, J., Wang, Z., Zhu, Y., 2020. Enhanced visible-light photocatalytic degradation and disinfection performance of oxidized nanoporous g-C₃N₄ via decoration with graphene oxide quantum dots. *Chin. J. Catal.* 41, 474–484. [https://doi.org/10.1016/S1872-2067\(19\)63501-1](https://doi.org/10.1016/S1872-2067(19)63501-1).
- Xu, K., Fu, C., Gao, Z., Wei, F., Ying, Y., Xu, C., Fu, G., 2018. Nanomaterial-based gas sensors: A review. *Instrum. Sci. Technol.* 46, 115–145. <https://doi.org/10.1080/10739149.2017.1340896>.
- Xu, T., Wang, D., Dong, L., Shen, H., Lu, W., Chen, W., 2019. Graphitic carbon nitride modified by zinc phthalocyanine and graphene quantum dots for the efficient photocatalytic degradation of refractory contaminants. *Appl. Catal. B: Environ.* 244, 96–106. <https://doi.org/10.1016/j.apcatb.2018.11.049>.
- Xu, Y., Li, Y., Wang, P., Wang, X., Yu, H., 2018. Highly efficient dual cocatalyst-modified TiO₂ photocatalyst: RGO as electron-transfer mediator and MoS_x as H₂-evolution active site. *Appl. Surf. Sci.* 430, 176–183. <https://doi.org/10.1016/j.apsusc.2017.07.188>.
- Yan, X., Song, Y., Zhu, C., Song, J., Du, D., Su, X., Lin, Y., 2016. Graphene quantum dot-MnO₂ nanosheet based optical sensing platform: a sensitive fluorescence “turn Off-On” nanosensor for glutathione detection and intracellular imaging. *ACS Appl. Mater. Interfaces* 8, 21990–21996. <https://doi.org/10.1021/acsmi.6b05465>.
- Yan, Y., Chen, J., Li, N., Tian, J., Li, K., Jiang, J., Liu, J., Tian, Q., Chen, P., 2018. Systematic Bandgap Engineering of Graphene Quantum Dots and Applications for Photocatalytic Water Splitting and CO₂ Reduction. *ACS Nano* 12, 3523–3532. <https://doi.org/10.1021/acsnano.8b00498>.
- Yan, Y., Gong, J., Chen, J., Zeng, Z., Huang, W., Pu, K., Liu, J., Chen, P., 2019a. Recent Advances on Graphene Quantum Dots: From Chemistry and Physics to Applications. *Adv. Mater.* 31 <https://doi.org/10.1002/adma.201808283>.
- Yan, Y., Gong, J., Chen, J., Zeng, Z., Huang, W., Pu, K., Liu, J., Chen, P., 2019b. Recent advances on graphene quantum dots: from chemistry and physics to applications. *Adv. Mater.* 31 <https://doi.org/10.1002/adma.201808283>.
- Yang, Y., Rodríguez-Córdoba, W., Xiang, X., Lian, T., 2012. Strong electronic coupling and ultrafast electron transfer between PbS quantum dots and TiO₂ nanocrystalline films. *Nano Lett.* 12, 303–309. <https://doi.org/10.1021/nl2035783>.
- Yang, Y., Bremner, S., Menictas, C., Kay, M., 2018. Battery energy storage system size determination in renewable energy systems: A review. *Renew. Sustain. Energy Rev.* 91, 109–125. <https://doi.org/10.1016/j.rser.2018.03.047>.
- Yang, Z., Zhang, J., Kintner-Meyer, M.C.W., Lu, X., Choi, D., Lemmon, J.P., Liu, J., 2011. Electrochemical energy storage for green grid. *Chem. Rev.* 111, 3577–3613. <https://doi.org/10.1021/cr100290v>.
- Yao, X., Niu, X., Ma, K., Huang, P., Grothe, J., Kaskel, S., Zhu, Y., 2017a. Graphene Quantum Dots-Capped Magnetic Mesoporous Silica Nanoparticles as a Multifunctional Platform for Controlled Drug Delivery, Magnetic Hyperthermia, and Photothermal Therapy. *Small* 13. <https://doi.org/10.1002/sml.201602225>.
- Yao, X., Tian, Z., Liu, J., Zhu, Y., Hanagata, N., 2017b. Mesoporous silica nanoparticles capped with graphene quantum dots for potential chemo-photothermal synergistic cancer therapy. *Langmuir* 33, 591–599. <https://doi.org/10.1021/acs.langmuir.6b04189>.

- Yin, X., Chen, H., Zhi, C., Sun, W., Lv, L., Wang, Y., 2018. Functionalized graphene quantum dot modification of yolk-shell NiO Microspheres for superior lithium storage. *Small* 1800589, 1–10. <https://doi.org/10.1002/smll.201800589>.
- Yin, Y., Liu, Q., Jiang, D., Du, X., Qian, J., Mao, H., Wang, K., 2016. Atmospheric pressure synthesis of nitrogen doped graphene quantum dots for fabrication of BiOBr nanohybrids with enhanced visible-light photoactivity and photostability. *Carbon* 96, 1157–1165. <https://doi.org/10.1016/j.carbon.2015.10.068>.
- Younis, M.R., He, G., Lin, J., Huang, P., 2020. Recent advances on graphene quantum dots for bioimaging applications. *Front. Chem.* 8, 424. <https://doi.org/10.3389/fchem.2020.00424>.
- Yu, Y., Wu, L., Gao, S., Jia, K., Zeng, W., Liao, B., Pang, H., 2021. Fabrication of multi-nanocavity and multi-reflection interface in rGO for enhanced EMI absorption and reduced EMI reflection. *Appl. Surf. Sci.* 562, 150034 <https://doi.org/10.1016/j.apsusc.2021.150034>.
- Yuan, A., Lei, H., Xi, F., Liu, J., Qin, L., Chen, Z., Dong, X., 2019a. Graphene quantum dots decorated graphitic carbon nitride nanorods for photocatalytic removal of antibiotics. *J. Colloid Interface Sci.* 548, 56–65. <https://doi.org/10.1016/j.jcis.2019.04.027>.
- Yuan, A., Lei, H., Xi, F., Liu, J., Qin, L., Chen, Z., Dong, X., 2019b. Graphene quantum dots decorated graphitic carbon nitride nanorods for photocatalytic removal of antibiotics. *J. Colloid Interface Sci.* 548, 56–65. <https://doi.org/10.1016/j.jcis.2019.04.027>.
- Yue, D., Qian, X., Zhao, Y., 2015. Photocatalytic remediation of ionic pollutant. *Sci. Bull.* 60, 1791–1806. <https://doi.org/10.1007/s11434-015-0918-5>.
- Zamiri, G., Bagheri, S., 2018. Fabrication of green dye-sensitized solar cell based on ZnO nanoparticles as a photoanode and graphene quantum dots as a photo-sensitizer. *J. Colloid Interface Sci.* 511, 318–324. <https://doi.org/10.1016/j.jcis.2017.10.026>.
- Zarezadeh, S., Habibi-Yangjeh, A., Mousavi, M., 2019. BiOBr and AgBr co-modified ZnO photocatalyst: A novel nanocomposite with p-n-n heterojunctions for highly effective photocatalytic removal of organic contaminants. *J. Photochem. Photobiol. A: Chem.* 379, 11–23. <https://doi.org/10.1016/j.jphotochem.2019.05.013>.
- Zeng, Z., Chen, S., Tan, T.T.Y., Xiao, F.X., 2018. Graphene quantum dots (GQDs) and its derivatives for multifarious photocatalysis and photoelectrocatalysis. *Catal. Today* 315, 171–183. <https://doi.org/10.1016/j.cattod.2018.01.005>.
- Zhang, D., Wu, Z., Zong, X., 2019. Metal-organic frameworks-derived zinc oxide nanopolyhedra/S, N: graphene quantum dots/polyaniline ternary nanohybrid for high-performance acetone sensing. *Sens. Actuators, B: Chem.* 288, 232–242. <https://doi.org/10.1016/j.snb.2019.02.093>.
- Zhang, W., Zou, L., Wang, L., 2009. Photocatalytic TiO₂/adsorbent nanocomposites prepared via wet chemical impregnation for wastewater treatment: A review. *Appl. Catal. A: Gen.* 371, 1–9. <https://doi.org/10.1016/j.apcata.2009.09.038>.
- bin Zhang, W., Yu, X., Wang, C.L., Sun, H.J., Hsieh, I.F., Li, Y., Dong, X.H., Yue, K., van Horn, R., Cheng, S.Z.D., 2014. Molecular nanoparticles are unique elements for macromolecular science: From “nanoatoms” to giant molecules. *Macromolecules* 47, 1221–1239. <https://doi.org/10.1021/ma401724p>.
- Zhang, W., Mohamed, A.R., Ong, W.J., 2020. Z-scheme photocatalytic systems for carbon dioxide reduction: Where are we now? *Angew. Chem. - Int. Ed.* 59, 22894–22915. <https://doi.org/10.1002/anie.201914925>.
- Zhang, X., Shen, J., 2001. Self-assembled ultrathin films: from layered nanoarchitectures to functional assemblies. *Adv. Mater.* 22, 1057–1065. [https://doi.org/10.1002/\(SICI\)1521-4095\(199909\)11:13<1139::AID-ADMA1139>3.0.CO;2-7](https://doi.org/10.1002/(SICI)1521-4095(199909)11:13<1139::AID-ADMA1139>3.0.CO;2-7).
- Zhang, Z., Zhang, J., Chen, N., Qu, L., 2012. Graphene quantum dots: An emerging material for energy-related applications and beyond. *Energy Environ. Sci.* 5, 8869–8890. <https://doi.org/10.1039/c2ee22982j>.
- Zhao, C., Chen, Z., Shi, R., Yang, X., Zhang, T., 2020. Recent advances in conjugated polymers for visible-light-driven water splitting. *Adv. Mater.* 32 <https://doi.org/10.1002/adma.201907296>.
- Zhao, C., Shao, B., Yan, M., Liu, Z., Liang, Q., He, Q., Wu, T., Liu, Y., Pan, Y., Huang, J., Wang, J., Liang, J., Tang, L., 2021. Activation of peroxymonosulfate by biochar-based catalysts and applications in the degradation of organic contaminants: A review. *Chem. Eng. J.* 416, 128829 <https://doi.org/10.1016/j.cej.2021.128829>.
- Zhao, Y., Huang, X., Gao, F., Zhang, L., Tian, Q., bin Fang, Z., Liu, P., 2019. Study on water splitting characteristics of CdS nanosheets driven by the coupling effect between photocatalysis and piezoelectricity. *Nanoscale* 11, 9085–9090. <https://doi.org/10.1039/c9nr01676g>.
- Zheng, H., Li, Y., Liu, H., Yin, X., Li, Y., 2011. Construction of heterostructure materials toward functionality. *Chem. Soc. Rev.* 40, 4506–4524. <https://doi.org/10.1039/c0cs00222d>.
- Zheng, L., Su, H., Zhang, J., Walekar, L.S., Vafaei Molamahmood, H., Zhou, B., Long, M., Hu, Y.H., 2018. Highly selective photocatalytic production of H₂O₂ on sulfur and nitrogen co-doped graphene quantum dots tuned TiO₂. *Appl. Catal. B: Environ.* 239, 475–484. <https://doi.org/10.1016/j.apcatb.2018.08.031>.
- Zheng, X.T., Ananthanarayanan, A., Luo, K.Q., Chen, P., 2015. Glowing graphene quantum dots and carbon dots: Properties, syntheses, and biological applications. *Small* 11, 1620–1636. <https://doi.org/10.1002/smll.201402648>.
- Zhou, X., Zhang, X., Wang, Y., Wu, Z., 2021. 2D Graphene-TiO₂ Composite and Its Photocatalytic Application in Water Pollutants. *Front. Energy Res.* 8, 400. <https://doi.org/10.3389/fenrg.2020.612512>.
- Zhu, L., Yue, Q., Jiang, D., Chen, H., Irfan, R.M., Du, P., 2018. Metal-free graphene quantum dots photosensitizer coupled with nickel phosphide cocatalyst for enhanced photocatalytic hydrogen production in water under visible light, Cuihua Xuebao/. *Chin. J. Catal.* 39, 1753–1761. [https://doi.org/10.1016/S1872-2067\(18\)63135-3](https://doi.org/10.1016/S1872-2067(18)63135-3).
- Zhu, M., Liu, Q., Chen, W., Yin, Y., Ge, L., Li, H., Wang, K., 2017. Boosting the Visible-Light Photoactivity of BiOCl/BiVO₄/N-GQD Ternary Heterojunctions Based on Internal Z-Scheme Charge Transfer of N-GQDs: Simultaneous Band Gap Narrowing and Carrier Lifetime Prolonging. *ACS Appl. Mater. Interfaces* 9, 38832–38841. <https://doi.org/10.1021/acsami.7b14412>.
- Zhu, S., Song, Y., Wang, J., Wan, H., Zhang, Y., Ning, Y., Yang, B., 2017. Photoluminescence mechanism in graphene quantum dots: Quantum confinement effect and surface/edge state. *Nano Today* 13, 10–14. <https://doi.org/10.1016/j.nantod.2016.12.006>.
- Zou, J.P., Wang, L.C., Luo, J., Nie, Y.C., Xing, Q.J., Luo, X.B., Du, H.M., Luo, S.L., Suib, S. L., 2016. Synthesis and efficient visible light photocatalytic H₂ evolution of a metal-free g-C₃N₄/graphene quantum dots hybrid photocatalyst. *Appl. Catal. B: Environ.* 193, 103–109. <https://doi.org/10.1016/j.apcatb.2016.04.017>.
- Zou, Y., Zhang, Y., Hu, Y., Gu, H., 2018. Ultraviolet detectors based on wide bandgap semiconductor nanowire: A review. *Sens. (Switz.)* 18, 2072. <https://doi.org/10.3390/s18072072>.
- Zrazhevskiy, P., Sena, M., Gao, X., 2010. Designing multifunctional quantum dots for bioimaging, detection, and drug delivery. *Chem. Soc. Rev.* 39, 4326–4354. <https://doi.org/10.1039/b915139g>.
- Zubair, M., Kim, H., Razaq, A., Grimes, C.A., In, S.II, 2018. Solar spectrum photocatalytic conversion of CO₂ to CH₄ utilizing TiO₂ nanotube arrays embedded with graphene quantum dots. *J. CO₂ Util.* 26, 70–79. <https://doi.org/10.1016/j.jcou.2018.04.004>.
- Züttel, A., Remhof, A., Borgschulte, A., Friedrichs, O., 2010. Hydrogen: The future energy carrier. *Philos. Trans. R. Soc. A: Math., Phys. Eng. Sci.* 368, 3329–3342. <https://doi.org/10.1098/rsta.2010.0113>.